Multiple Testing of Local Maxima for Detection of Peaks and Change Points with Non-stationary Noise

by

Shuang Gu

A Dissertation Presented in Partial Fulfillment
of the Requirements for the Degree
Doctor of Philosophy

Approved July 2023 by the
Graduate Supervisory Committee:

Dan Cheng, Chair
Hedibert Lopes
John Fricks
Shiwei Lan
Yi Zheng

ARIZONA STATE UNIVERSITY

August 2023

ABSTRACT

This dissertation comprises two projects: (i) Multiple testing of local maxima for detection of peaks and change points with non-stationary noise, and (ii) Height distributions of critical points of smooth isotropic Gaussian fields: computations, simulations and asymptotics.

The first project introduces a topological multiple testing method for one-dimensional domains to detect signals in the presence of non-stationary Gaussian noise. The approach involves conducting tests at local maxima based on two observation conditions: (i) the noise is smooth with unit variance and (ii) the noise is not smooth where kernel smoothing is applied to increase the signal-to-noise ratio (SNR). The smoothed signals are then standardized, which ensures that the variance of the new sequence's noise becomes one, making it possible to calculate p-values for all local maxima using random field theory. Assuming unimodal true signals with finite support and non-stationary Gaussian noise that can be repeatedly observed. The algorithm introduced in this work, demonstrates asymptotic strong control of the False Discovery Rate (FDR) and power consistency as the number of sequence repetitions and signal strength increase. Simulations indicate that FDR levels can also be controlled under non-asymptotic conditions with finite repetitions. The application of this algorithm to change point detection also guarantees FDR control and power consistency.

The second project focuses on investigating the explicit and asymptotic height densities of critical points of smooth isotropic Gaussian random fields on both Euclidean space and spheres. The formulae are based on characterizing the distribution of the Hessian of the Gaussian field using the Gaussian orthogonally invariant (GOI) matrices and the Gaussian orthogonal ensemble (GOE) matrices, which are special cases of GOI matrices. However, as the dimension increases, calculating explicit formulae becomes computationally challenging.The project includes two simulation methods for these distributions. Additionally, asymptotic distributions are obtained by utilizing the asymptotic distribution of

the eigenvalues (excluding the maximum eigenvalues) of the GOE matrix for large dimensions. However, when it comes to the maximum eigenvalue, the Tracy-Widom distribution is utilized. Simulation results demonstrate the close approximation between the asymptotic distribution and the real distribution when N is sufficiently large.

ACKNOWLEDGMENTS

I would like to express my deepest gratitude and appreciation to all those who have supported and guided me throughout this journey of completing my PhD dissertation.

First and foremost, I am immensely grateful to my advisor, Dr. Dan Cheng, for his unwavering support, invaluable guidance, and expert knowledge. His mentorship and encouragement have been instrumental in shaping the direction of my research and fostering my academic growth. I am truly fortunate to have had the opportunity to work under his supervision.

I am deeply grateful to Dr. Yun Kang for providing me with the first student job during my Ph.D., which set the foundation for my research and academic growth.

I extend my heartfelt thanks to the members of my dissertation committee: Dr. Hedibert Lopes, Dr. John Fricks, Dr. Ming-Hung Kao, Dr. Shiwei Lan and Dr. Yi Zheng for their valuable insights, critical feedback, and thoughtful suggestions. Their expertise and scholarly input have significantly enriched the quality of my research. I am grateful for their time, dedication, and commitment.

I would like to acknowledge the support and assistance provided by School of Mathematical and Statistical Sciences, Arizona State University. The resources, facilities, and collaborative environment they offered have been instrumental in carrying out my research effectively. I am grateful to all the individuals who contributed to my project, whether directly or indirectly.

I would also like to express my deep gratitude to my friends, Zhong Zhuang, Weixi Liu and Haoran Shi, for their constant friendship and support throughout my academic journey. I am truly thankful for their unwavering presence in my life.

Lastly, I would like to express my heartfelt gratitude to my parents, Shifang Huang and Zhongliang Gu, for their unwavering trust and unstoppable support since my childhood. Their belief in me and constant encouragement have been the driving force behind my

achievements. I am forever grateful for their unwavering presence and dedication in my life.

In conclusion, this dissertation would not have been possible without the support and contributions of the aforementioned individuals and institutions. I am truly grateful for their unwavering support, guidance, and belief in my abilities.

TABLE OF CONTENTS

CHAPTER Page

CHAPTER Page

LIST OF TABLES

Table Page

LIST OF FIGURES

Chapter 1

INTRODUCTION

This dissertation contains two different research projects: Multiple Testing of Local Maxima for Detection of Peaks and Change Points with Non-stationary Noise and Height Distributions of Critical Points of Smooth Isotropic Gaussian Fields: Computations, Simulations and Asymptotics.

1.1 Multiple Testing of Local Maxima for Detection of Peaks and Change Points with Non-stationary Noise

Peak detection is a crucial task in various fields, including medical condition monitoring [20, 21, 7], image analysis [22, 24], and statistics. Accurate and efficient peak detection provides valuable information for decision-making, such as identifying the presence or absence of specific components in a chemical mixture or detecting abnormal changes in physiological signals.

Different methods for peak detection have been developed, including threshold-based methods, template-based methods, and wavelet-based methods. However, peak detection can be challenging due to factors such as noise, baseline variation, and artifacts.

Threshold-based methods involve setting a threshold level to identify peaks in a signal. The method defines a threshold, above which the signal is considered a peak. Peaks are identified as points in the signal where the value exceeds the threshold. Threshold-based methods are simple and computationally efficient, making them popular in many applications. However, they can be sensitive to noise and baseline variations, leading to false positives or false negatives. Various modifications, such as adaptive or multiscale thresholds, have been developed to enhance the performance of threshold-based methods.

Template-based methods utilize a pre-defined waveform or template to detect peaks in a signal. The template is derived from a representative waveform of the signal of interest. The method aligns the template with the signal at different positions and scales, measuring similarity using metrics such as cross-correlation or Euclidean distance. Positions where the similarity exceeds a threshold are identified as peaks. Template-based methods are effective when peaks have similar shapes to the template but may struggle with different peak shapes or situations requiring template updates.

Wavelet-based methods use wavelet transforms to analyze and detect peaks in a signal. Wavelet transforms decompose a signal into frequency components, enabling the identification of peaks at different scales. Wavelet-based methods apply wavelet transforms to the signal and detect peaks in the resulting coefficients or subbands. These methods are suitable for noisy or non-stationary signals but require more computational resources and depend on the choice of wavelet function and decomposition level. Enhancements, such as multiscale or adaptive thresholding, have been developed to improve wavelet-based methods.

In this dissertation, a threshold-based method is applied, where the core idea is finding an appropriate threshold to determine the significance of observations. Previous papers assume stationary and ergodic Gaussian noise. However, in this project, the noise is non-stationary. And the thresholding problem can be treated as a multiple testing problem, that is, tests at local maxima of the observed signals will be performed. This approach allows error rates (FDR) and peak detection power to be defined topologically based on the detected peaks, offering computational efficiency compared to pointwise testing.

Keith Worsley [33, 36, 37] is a pioneer in the use of random field theory, and his work, particularly the Euler characteristic heuristic, has proven to be a valuable approach for approximating the null distribution of the global maximum of observed signals. In this paper, we apply BH procedure for controlling the false discovery rate (FDR) to obtain less

conservative results.

Schwartzman, Gavrilov, and Adler [31] structured peak detection by introducing a multiple testing paradigm that involves testing the significance of local maxima in smoothed data. However, their work was limited to stationary noise, because closed-form expressions for the distribution and properties of the height of local maxima, which are essential for calculating the p-values and controlling the FDR, are only known for stationary Gaussian processes.

Recently, Cheng, D. and A. Schwartzman [12, 14] made significant progress by obtaining implicit expressions for the height distribution of local maxima of one-dimensional Gaussian fields with constant variance. And Cheng [9] obtained the explicit expression for 1D. He achieved this by using random matrix theory and the property of Gaussian process. These developments are so important because they allow us to extend the multiple testing method proposed in [13, 31] to handle non-stationary noise.

Our algorithm comprises the following steps:

1.**Kernel smoothing**: If the noise is smooth, go to step 3. If the noise is not smooth, do the kernel smoothing to increase the signal-to-noise ratio (SNR) [32].

2.**Standardizing**: Transfer the variance of noise to one.

3.**Candidate peaks**: Find local maxima of the smoothed and standardized sequence.

4.**P-values**: Compute the p-values at each local maximum under the null hypothesis of no signal on the local maximum.

5.**Multiple testing**: Apply a multiple testing procedure to get a threshold. Then mark the detected local maxima as signals if their p-values are below the threshold.

In this paper, the p-values in step 4 can be computed by using the Gaussian processes theory of Cheng [9]. For step 5, we use the Benjamini-Hochberg (BH) procedure to control the FDR. The algorithm is illustrated by a simulated example in Figure 1.1.

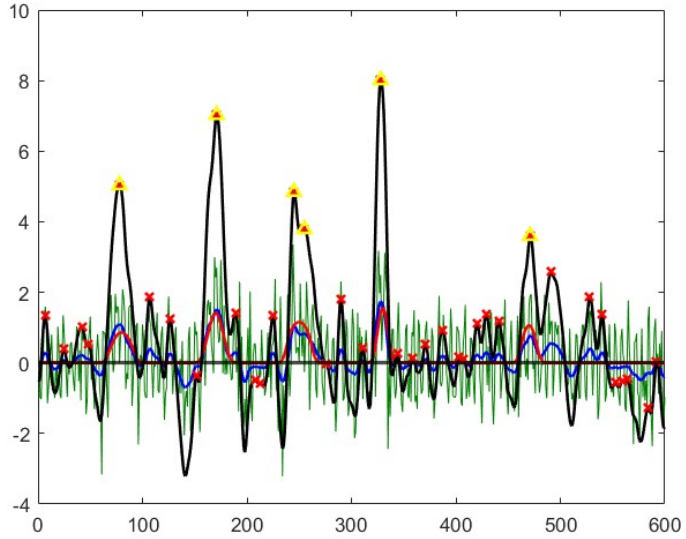

Figure 1.1: The green line is observed sequence $y(t)$, the red line is the original signal $\mu(t)$, the blue line is smoothed sequence $y_\gamma(t)$, the black line is smoothed and standardized sequence $X_\gamma(t)$. Out of 38 local maxima of $X_\gamma(t)$(red cross), 6 of them are marked as significant(yellow triangle), where 5 of 5 peaks are detected.

1.2 Height Distributions of Critical Points of Smooth Isotropic Gaussian Fields: Computations, Simulations and Asymptotics

1.2.1 Motivations

Computing the expected number of critical points of smooth Gaussian random fields is a significant problem in probability theory because of its broad applications in various fields, such as physics [3, 8, 17, 19], statistics [1, 10, 6, 16, 25], neuroimaging [28, 33, 34, 35], oceanography [26, 27], astronomy [5, 23], engineering, environmental science, and geophysics. Numerous researchers from diverse disciplines have dedicated their efforts to this problem and have developed many powerful tools, notably the renowned Kac-Rice formula. While the Kac-Rice formula [2, 30] allows us to derive an implicit formula for the expected number of critical points, evaluating the explicit formula proves challenging for most smooth Gaussian random fields defined on Euclidean space $\mathbb{R}^N$ or the N-dimensional

unit sphere $\mathbb{S}^N$ when $N > 1$. However, Fyodorov [18] made a breakthrough which enables the explicit evaluation available for a large class of isotropic Gaussian random fields. The main novel idea is writing the Hessian of the Gaussian field as a Gaussian random matrix involving the Gaussian Orthogonal Ensemble (GOE).

The project is divided into three main components: computations, simulations, and asymptotics.

In the computations part, building upon the work of Cheng [12, 14], the explicit form of the peak height density of critical points in smooth isotropic Gaussian random fields can be calculated when the dimension N is small (3 and 4).

However, as the dimension N increases, obtaining the explicit form of the peak height density becomes increasingly challenging. In such cases, simulation approaches for both the GOE and the GOI matrices are provided, based on the implicit form of the height density.

When the dimension N becomes sufficiently large, the asymptotic distributions of the height density can be determined. By the work of O'Rourke, S.[29] and the Tracy-Widom distribution. The algorithms for simulating the height density can be provided.

Overall, this project combines computations, simulations, and asymptotic analysis to explore the height distributions of critical points in smooth isotropic Gaussian fields.

1.2.2 Definitions and Notations

For simplicity, the notations are all from the work of Cheng and Schwartzman [14].

GOE matrix: An $N \times N$ random matrix $H = (H_{ij})_{1 \le i,j \le N}$ is said to have the Gaussian Orthogonal Ensemble (GOE) distribution if it is symmetric and all entries are centered Gaussian variables Critical points of isotropic Gaussian fields such that:

$$\mathbb{E}[H_{ij}H_{kl}] = \frac{1}{2}(\delta_{ik}\delta_{jl} + \delta_{il}\delta_{jk})$$

where δ_{ij} is the Kronecker delta function.

GOI matrix: An $N \times N$ random matrix $M = (M_{ij})_{1\le i,j\le N}$ is said to have the Gaussian Orthogonal Invariant (GOI) distribution with covariance parameter c, denoted by $\mathrm{GOI}_{(c)}$ if it is symmetric and all entries are centered Gaussian variables such that:

$$\mathbb{E}[M_{ij}M_{kl}] = \frac{1}{2}(\delta_{ik}\delta_{jl} + \delta_{il}\delta_{jk}) + c\delta_{ij}\delta_{kl}$$

where δ_{ij} is the Kronecker delta function. Let $X = \{X(t), t \in T\}$ be a smooth isotropic Gaussian random field whose mean is 0 and variance is 1, where T is $\mathbb{R}^N$ or $\mathbb{S}^N$. For $i = 0, \dots, N$, let:

$$\mu_i(X,u) = \#\{t \in D : X(t) \le u, \nabla X(t) = 0, \mathrm{index}(\nabla^2 X(t)) = i\}, \tag{1.1}$$

where D is an N-dimensional unit-area disc on T, $\nabla X(t)$ and $\nabla^2 X(t)$ are respectively the gradient and Hessian matrix of X, and $\mathrm{index}(\nabla^2 X(t))$ denotes the number of negative eigenvalues of $\nabla^2 X(t)$. Then, $\mu_i(X,u)$ is the number of critical points of index i of X exceeding u over D.

We Define the height density of a critical value of index i of X at some point t_0, as:

$$F_i(u) := \lim_{\varepsilon\to 0} \mathbb{P}\{X(t_0) > u | \exists \text{ a critical point of index } i \text{ of } X(t) \text{ in } B(t_0,\varepsilon))\} \tag{1.2}$$

For non-boundary case: $0 < \kappa^2 < (N+2)/N$

$$F_i(u) = \frac{\int_u^\infty \phi(x)\mathbb{E}^N_{\mathrm{GOI}((1-\kappa^2)/2)}[\prod_{j=1}^N |\lambda_j - \kappa x/\sqrt{2}| \mathbb{1}_{\{\lambda_i < \kappa x/\sqrt{2} < \lambda_{i+1}\}} dx}{\mathbb{E}^N_{\mathrm{GOI}(1/2)}[\prod_{j=1}^N |\lambda_j| \mathbb{1}_{\{\lambda_i<0<\lambda_{i+1}\}}]}$$

For boundary case: $\kappa^2 = (N+2)/N$

$$F_i(u) = \frac{\mathbb{E}^N_{\mathrm{GOI}(1/2)}[\prod_{j=1}^N |\lambda_j| \mathbb{1}_{\{\lambda_i<0<\lambda_{i+1}\}} \mathbb{1}_{\{\sum_{j=1}^N \lambda_j/N \le -\sqrt{(N+2)/(2N)}u\}}]}{\mathbb{E}^N_{\mathrm{GOI}(1/2)}[\prod_{j=1}^N |\lambda_j| \mathbb{1}_{\{\lambda_i<0<\lambda_{i+1}\}}]}$$

From the definition givn before, when $0 < \kappa^2 < (N+2)/N$, the height density of critical points can be written as:

$$f_i(x) = \frac{\phi(x)\mathbb{E}^N_{\mathrm{GOI}((1-\kappa^2)/2)}[\prod_{j=1}^N |\lambda_j - \kappa x/\sqrt{2}|\mathbb{1}_{\{\lambda_i<\kappa x/\sqrt{2}<\lambda_{i+1}\}}}{\mathbb{E}^N_{\mathrm{GOI}(1/2)}[\prod_{j=1}^N |\lambda_j|\mathbb{1}_{\{\lambda_i<0<\lambda_{i+1}\}}]} \tag{1.3}$$

Where $f_i(x)$ represents the density of critical points of index i, the two implicit forms of height density are lemmas from Cheng[14, 12]

Chapter 2

MULTIPLE TESTING OF LOCAL MAXIMA FOR DETECTION OF PEAKS AND CHANGE POINTS WITH NON-STATIONARY NOISE

2.1 The Model

Consider the signal-plus-noise model:

$$y(t) = \mu(t) + z(t), \qquad t \in [0, L] \subset R \tag{2.1}$$

Where the signal $\mu(t)$ is a train of unimodal positive peaks of the form:

$$\mu(t) = \sum_{j=-\infty}^{\infty} a_j h_j(t), \qquad a_j > 0, \tag{2.2}$$

And the peak shape, denoted by $h_j(t) \leq 0$, has a compact connected support $S_j = \{t : h_j(t) > 0\}$ and unit action $\int_{s_j} h_j(t)dt = 1$ for each j. The noise $z(t)$ is a non-stationary Gaussian process. In this paper, we discuss two conditions for the noise. The first condition assumes smooth noise, where $z(t)$ has unit variance and is smooth. Under this condition, Gaussian process theory from Cheng [9] can be directly applied, eliminating the need for kernel smoothing or other transformations. p-values can be calculated, and multiple testing can be conducted directly.

The second condition considers unsmooth noise, which is the main focus of this dissertation. We assume $z(t)$ is not smooth, and to increase the signal-to-noise ratio (SNR) [31], kernel smoothing is essential. Gaussian process theory can still be applied in this case, but standardization is necessary. Further details will be provided in the following algorithm section.

Let $w_\gamma(t) \geq 0$ be a unimodal kernel with a compact connected support and unit area, where $\gamma > 0$ is the bandwidth. Convolving the process 2.1 with the kernel $w_\gamma(t)$ can

generate the smoothed process.

$$y_\gamma(t) = w_\gamma(t) * y(t) = \int_{-\infty}^{\infty} w_\gamma(t-s)y(s)ds = \mu_\gamma(t) + z_\gamma(t), \tag{2.3}$$

where the smoothed signal and smoothed noise are defined as

$$\mu_\gamma(t) = w_\gamma(t) * \mu(t) = \sum_{j=-\infty}^{\infty} a_j h_{j,\gamma}(t), \qquad z_\gamma(t) = w_\gamma(t) * z(t) \tag{2.4}$$

For each peak j, the smoothed peak shape function is defined as $h_{j,\gamma}(t) = w_\gamma(t) * h_j(t) \geq 0$. It is unimodal and possesses a compact connected support, denoted as $S_{j,\gamma}$. The smoothed peak shape $h_{j,\gamma}(t)$ is required to be twice differentiable in the $S_{j,\gamma}$ and has only one critical point in its support. For simplicity, this work assumes that the supports $S_{j,\gamma}$ do not overlap each other.

The smoothed noise is defined as $z_\gamma(t)$, which is obtained through convolution as described in equations 2.3 and 2.4. We assume that $z_\gamma(t)$'s mean is zero and is a thrice differentiable non-stationary Gaussian process. However, after the convolution, the variance of the noise cannot be guaranteed to be 1. To apply the theory of random fields, an additional step of standardization is performed. This involves dividing the entire observation $y_\gamma(t)$ by the standard deviation of $z_\gamma(t)$. By doing this, the new model has a noise component with unit variance, allowing us to apply the theory described subsequently.

Let X be a standard Gaussian process, X' be its first derivative, and X'' be its second derivative.

2.2 Difference Between Stationary Process and Non-stationary Process

The previous research of Schwartzman, Gavrilov and Adler[31] primarily focused on the scenario where the noise $z(t)$ is a stationary ergodic Gaussian process. However, in this project, we will address the condition when $z(t)$ is non-stationary. The key distinction between these two conditions is that in the case of stationary noise, the parameter ρ remains

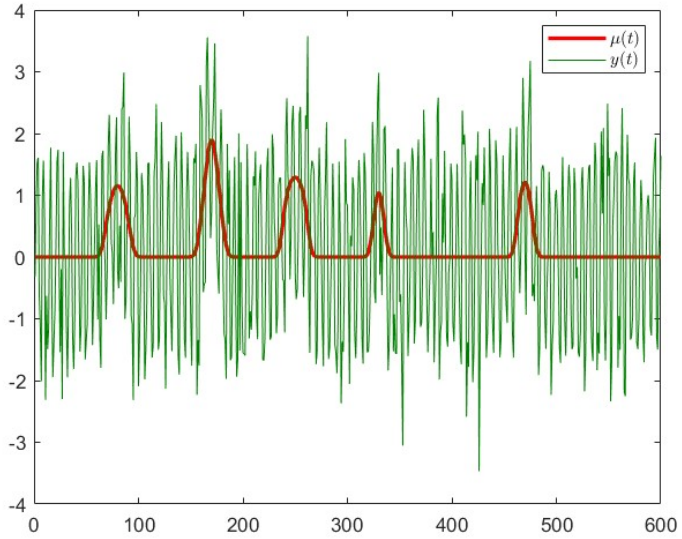

Figure 2.1: The green line is observed sequence $y(t)$, the red line is the original signal $\mu(t)$

constant across the entire support $[0, L]$. This allows us to establish a global threshold for observations to determine the significance of each local maximum.

On the other hand, when $z(t)$ is non-stationary, the parameter ρ varies for different values of t. In other words, $\rho(t)$ differs for each point t, indicating that we cannot obtain a global threshold for the observations. Consequently, proving results under this condition becomes challenging, necessitating the introduction of new theories and approaches.

2.3 Unsmooth Noise

We will first discuss the condition where the observed noise is not smooth. Smooth noise can be considered a special case within the broader category of unsmooth noise. As we will perform kernel smoothing in the initial step, certain transformations need to be applied to make our theory applicable. Subsequently, the following sections will outline the steps of our algorithms.

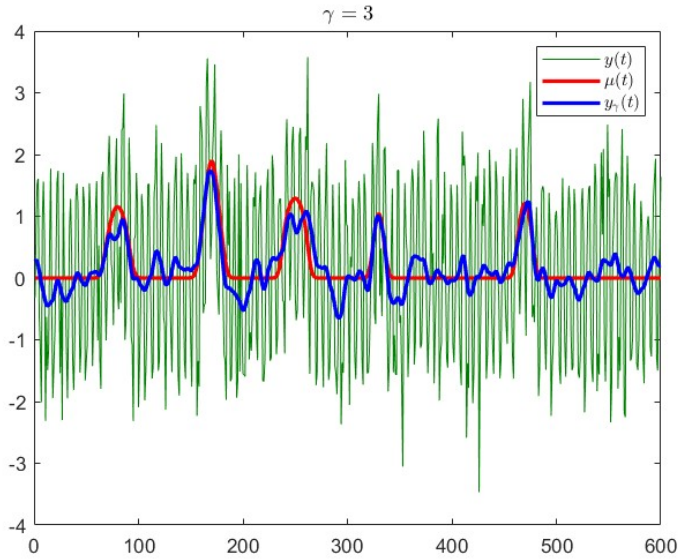

Figure 2.2: The green line is observed sequence $y(t)$, the red line is the original signal $\mu(t)$, the blue line is smoothed sequence $y_\gamma(t)$.

2.3.1 Kernel Smoothing

This part is described in the section 2.1, we can construct the smoothed process $y_\gamma(t)$ by (2.3) and (2.4). And the figure 2.2 displays the process of kernel smoothing.

2.3.2 Standardization

This step constitutes the core idea of the project. Its objective is to transform the variance of the smoothed noise to one, thereby facilitating the application of Gaussian process theory for calculating p-values. This is accomplished by standardizing the sequence, which involves dividing the entire smoothed sequence by the estimated standard deviation of the smoothed noise. As a result of this process, the variance of the new noise becomes one. Standardizing the process 2.3 yields the smoothed and standardized process.

$$f_\gamma(t) = \frac{\mu_\gamma(t)}{\sqrt{var(z_\gamma(t))}} + \frac{z_\gamma(t)}{\sqrt{var(z_\gamma(t))}} \tag{2.5}$$

For this sequence, we define $X_\gamma(t) = \frac{z_\gamma(t)}{\sqrt{var(z_\gamma(t))}}$ as the smoothed and standardized noise.

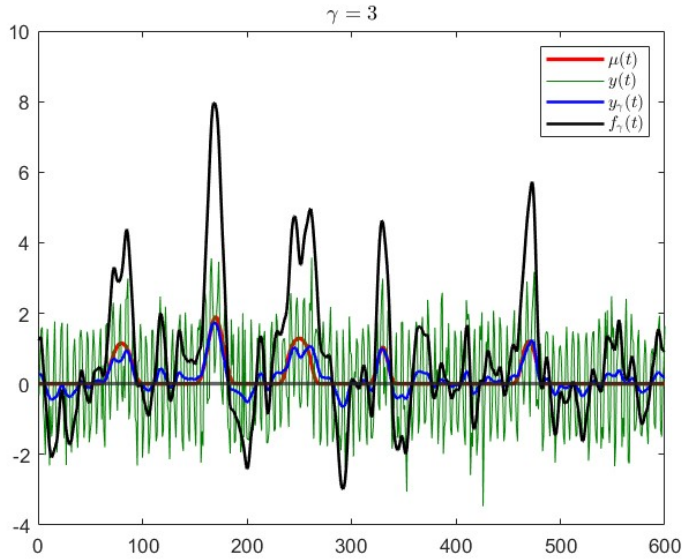

Figure 2.3: The green line is observed sequence $y(t)$, the red line is the original signal $\mu(t)$, the blue line is smoothed sequence $y_\gamma(t)$, the black line is smoothed and standardized sequence $X_\gamma(t)$.

2.3.3 Candidate Peaks

The objective of this step is to identify the peaks for the subsequent calculation of p-values in the context of multiple testing. While many studies focus on pointwise testing, which involves calculating p-values for individual points in a sequence, Schwartzman, A. and Y. Gavrilov and R. J. Adler [31] proposes an alternative approach. In their research, local maxima are considered representative of underlying signal peak regions. By calculating p-values and conducting multiple testing on the local maxima, the efficiency can be significantly improved.

In the process described by equation 2.5, with the sequence $f_\gamma(t)$, we define the set of local maxima of $f_\gamma(t)$ within the interval $[0, L]$ as

$$\tilde{T} = \left\{ t \in [0, L] : f'_\gamma(t) = \frac{df_\gamma(t)}{dt} = 0, f''_\gamma(t) = \frac{d^2 f_\gamma(t)}{dt^2} < 0 \right\} \tag{2.6}$$

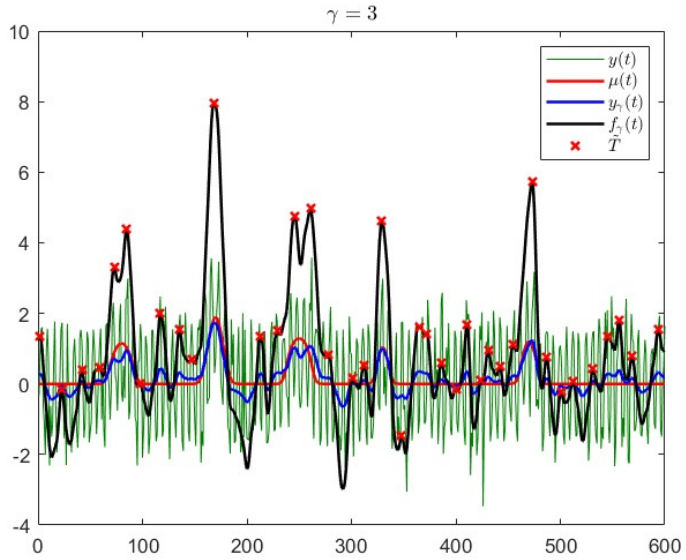

Figure 2.4: The green line is observed sequence $y(t)$, the red line is the original signal $\mu(t)$, the blue line is smoothed sequence $y_\gamma(t)$, the black line is smoothed and standardized sequence $f_\gamma(t)$, the red crosses are the detected local maxima

2.3.4 P-values

This part focuses on calculating the p-values which will be used to do multiple testing in next step.

Calculation of P-values

For each $t \in \tilde{T}$, compute the p-values $p_\gamma(t)$ for testing the hypothesis

$$H_0(t) : \mu(t) = 0 \quad vs \quad H_A(t) : \mu(t) > 0, \qquad t \in \tilde{T} \tag{2.7}$$

Given the observation heights $f_\gamma(t)$ at the local maxima $t \in \tilde{T}$, the p-values are computed as

$$P_\gamma(t) = F_\gamma[f_\gamma(t)], \qquad t \in \tilde{T} \tag{2.8}$$

where

$$F_\gamma(u) = P[f_\gamma(t) > u | t \in \tilde{T}] \tag{2.9}$$

represents the right cumulative distribution function (cdf) of $X_\gamma(t)$ at the local maxima $t \in \tilde{T}$, which can be calculated under the null hypothesis $\mu(t) = 0, \forall t$. From the work of Cheng, D. and A. Schwartzman[12], the formula to calculate the $F_\gamma(u)$ is:

Lemma 2.3.1. *Let $X(t) : t \in T$ be a Gaussian random field with dimension one, then for each $t \in T$ and $u \in R$.*

$$F_\gamma(u) = \frac{E\{|X''(t)|\mathbb{1}_{\{X(t)>u\}}\mathbb{1}_{\{X''(t)<0)\}}|X'(t) = 0\}}{E\{|X''(t)|\mathbb{1}_{\{X''(t)<0)\}}|X'(t) = 0\}} \tag{2.10}$$

From the lemma above, we can see that it is an implicit form of distribution, to calculate the explicit form of $F_\gamma(u)$, we need the joint distribution of $(X(t), X'(t), X''(t))$. And from the pre-print work of Cheng, suppose X is a standard Gaussian. The joint distribution of $(X(t), X'(t), X''(t))$ is:

$$(X(t), X'(t), X''(t)) \sim N(0, \Sigma)$$

where:

$$\Sigma = \begin{pmatrix} var(X(t)) & E(X(t)X'(t)) & E(X(t)X''(t)) \\ E(X'(t)X(t)) & var(X'(t)) & E(X'(t)X''(t)) \\ E(X''(t)X(t)) & E(X''(t)X'(t)) & var(X''(t)) \end{pmatrix}$$

With the covariance matrix, we assume that $X(t)$ has unit variance, and with the following definitions:

$$var(X(t)) = 1,\ var(X'(t)) = \lambda_1(t),\ var(X''(t)) = \lambda_2(t)$$

After some calculation, we can get the following elements:

$$E(X(t)X'(t)) = 0,$$
$$E(X(t)X''(t)) = -\lambda_1(t),$$
$$E(X'(t)X''(t)) = \frac{\lambda_1'(t)}{2}.$$

With all the elements, we can get the covariance matrix:

$$\Sigma = \begin{pmatrix} 1 & 0 & -\lambda_1(t) \\ 0 & \lambda_1(t) & \frac{\lambda_1'(t)}{2} \\ -\lambda_1(t) & \frac{\lambda_1'(t)}{2} & \lambda_2(t) \end{pmatrix} \tag{2.11}$$

With the joint distribution, we can calculate the explicit form of $F_\gamma(u)$ in lemma 2.3.1

Theorem 2.3.2. *Suppose X is a standard Gaussian process with unit variance, the notations are defined in 2.11, the explicit form of $F_\gamma(u)$ in lemma 2.3.1 is:*

$$F_\gamma(u) = 1 - \Phi(\frac{u}{\sqrt{1-\rho^2(t)}}) + \rho(t)\sqrt{2\pi}\phi(u)\Phi(\frac{\rho(t)u}{\sqrt{1-\rho(t)^2}}) \tag{2.12}$$

where $\rho(t) = \frac{\lambda_1(t)\sqrt{\lambda_1(t)}}{\sqrt{\lambda_1(t)\lambda_2(t)-\lambda_1'^2(t)/4}}$.

Proof. Assume λ_1, λ_2 are defined before, from the property of normal distribution, we can get the following conditional covariance:

$$var(X(t)|X'(t)=0) = 1 - \frac{[E(X(t)X'(t))]^2}{var(X'(t))} = 1$$

$$var(X''(t)|X'(t)=0) = var(X''(t)) - \frac{[E(X''(t)X'(t))]^2}{var(X'(t))} = \lambda_2(t) - \frac{\lambda_1'(t)^2}{4\lambda_1(t)}$$

$$cov(X(t), X''(t)|X'(t)=0)$$
$$= E(X(t)X''(t)) - \frac{E(X(t)X'(t))E(X''(t)X'(t))}{var(X'(t))} = -\lambda_1(t)$$

Then, from the implicit form of lemma 2.3.1, we can calculate the distribution of the height of the local maxima. The denominator is:

$$E[|X''(t)|\mathbb{1}_{\{X''(t)<0\}}|X'(t)=0]$$

where:

$$X''(t)|X'(t)=0 \sim N(0, \lambda_2(t) - \frac{\lambda_1'(t)^2}{4\lambda_1(t)})$$

Let $x = (X''(t)|X'(t) = 0)$ and $\delta = \sqrt{\lambda_2(t) - \frac{\lambda_1'(t)^2}{4\lambda_1(t)}}$:

$$\begin{aligned} & E\{|X''(t)|\mathbb{1}_{\{X''(t)<0\}}|X'(t) = 0\} \\ &= \int_{-\infty}^{0} -\frac{x}{\sqrt{2\pi}\delta} e^{-\frac{x^2}{2\delta^2}} dx \end{aligned}$$

Then, let $t = \frac{x}{\delta}$:

$$\begin{aligned} &= -\int_{-\infty}^{0} \frac{t}{\sqrt{2\pi}} e^{-\frac{t^2}{2}} \delta dt \\ &= -\delta[-\phi(t)]|_{-\infty}^{0} \\ &= \frac{\delta}{\sqrt{2\pi}} \end{aligned}$$

From lemma 2.3.1, the numerator is:

$$\begin{aligned} & E\{|X''(t)|\mathbb{1}_{\{X(t)>u\}}\mathbb{1}_{\{X''(t)<0)\}}|X'(t) = 0\} \\ &= -E\{X''(t)\mathbb{1}_{\{X(t)>u\}}\mathbb{1}_{\{X''(t)<0)\}}|X'(t) = 0\} \end{aligned} \tag{2.13}$$

where:

$$X(t), X''(t)|X'(t) = 0 \sim N(0, \begin{pmatrix} 1 & -\lambda_1(t) \\ -\lambda_1(t) & \lambda_2(t) - \frac{\lambda_1'(t)^2}{4\lambda_1(t)} \end{pmatrix})$$

That is, let $x = X(t)$, $y = X''(t)$ and $z = X'(t)$:

$$\begin{aligned} & -E\{X''(t)\mathbb{1}_{\{X(t)>u\}}\mathbb{1}_{\{X''(t)<0)\}}|X'(t) = 0\} \\ &= -\int_{u}^{\infty}\int_{-\infty}^{0} y f(x, y|z = 0) dy dx \end{aligned}$$

where:

$$f(x, y|z = 0) \sim N(0, \begin{pmatrix} \delta_x^2 & \rho\delta_x\delta_y \\ \rho\delta_x\delta_y & \delta_y^2 \end{pmatrix})$$

where:

$$\begin{aligned} \delta_x &= 1, \\ \delta_y &= \sqrt{\lambda_2(t) - \frac{\lambda_1'^2(t)}{4\lambda_1(t)}}, \\ \rho &= -\frac{\lambda_1(t)\sqrt{\lambda_1(t)}}{\sqrt{\lambda_1(t)\lambda_2(t) - \frac{\lambda_1'^2(t)}{4}}} \end{aligned}$$

Then, plug in, we can get:

$$
\begin{aligned}
&- E\{X''(t)\mathbb{1}_{\{X(t)>u\}}\mathbb{1}_{\{X''(t)<0)\}}|X'(t)=0\} \\
&= -\int_u^\infty \int_{-\infty}^0 y\frac{1}{2\pi\delta_y\sqrt{1-\rho^2}}\exp\{-\frac{1}{2(1-\rho^2)}[x^2-2\rho x\frac{y}{\delta_y}+\frac{y^2}{\delta_y^2}]\}dydx
\end{aligned}
$$

let $t = \frac{y}{\sqrt{1-\rho^2}\delta_y}$ and $k = \frac{x}{\sqrt{1-\rho^2}}$, then, we have:

$$
\begin{aligned}
&= -(1-\rho^2)\delta_y \int_{\frac{u}{\sqrt{1-\rho^2}}}^\infty e^{-\frac{k^2}{2}} \int_{-\infty}^0 \frac{t}{2\pi} e^{\rho kt} e^{-\frac{t^2}{2}} dtdk \\
&= -(1-\rho^2)\delta_y \int_{\frac{u}{\sqrt{1-\rho^2}}}^\infty \frac{1}{\sqrt{2\pi}} e^{-\frac{k^2}{2}} e^{\frac{\rho^2k^2}{2}} [-\phi(-\rho k)+\rho k\Phi(-\rho k)]dk \\
&= (1-\rho^2)\delta_y \int_{\frac{u}{\sqrt{1-\rho^2}}}^\infty \frac{\phi(-\rho k)}{\sqrt{2\pi}} e^{-\frac{k^2}{2}} e^{\frac{\rho^2k^2}{2}} dk - (1-\rho^2)\delta_y \int_{\frac{u}{\sqrt{1-\rho^2}}}^\infty \frac{\rho}{\sqrt{2\pi}} k e^{-\frac{k^2}{2}} e^{\frac{\rho^2k^2}{2}} \Phi(-\rho k)dk \\
&= \frac{(1-\rho^2)\delta_y}{\sqrt{2\pi}}[1-\Phi(\frac{u}{\sqrt{1-\rho^2}})] + \frac{\rho^2\delta_y}{\sqrt{2\pi}} - \rho\delta_y\phi(u)\Phi(-\frac{\rho u}{\sqrt{1-\rho^2}}) - \frac{\rho^2\delta_y}{\sqrt{2\pi}}\Phi(\frac{u}{\sqrt{1-\rho^2}}) \\
&= \frac{\delta_y}{\sqrt{2\pi}}\{1-\Phi(\frac{u}{\sqrt{1-\rho^2}}) - \rho\sqrt{2\pi}\phi(u)\Phi(-\frac{\rho u}{\sqrt{1-\rho^2}})\}
\end{aligned}
$$

so, the cdf is:

$$
F_\gamma(u) = 1-\Phi(\frac{u}{\sqrt{1-\rho^2(t)}}) - \rho(t)\sqrt{2\pi}\phi(u)\Phi(-\frac{\rho(t)u}{\sqrt{1-\rho^2(t)}})
$$

If we take $\rho(t) = \frac{\lambda_1(t)\sqrt{\lambda_1(t)}}{\sqrt{\lambda_1(t)\lambda_2(t)-\frac{\lambda_1'^2(t)}{4}}}$, the cdf is:

$$
F_\gamma(u) = 1-\Phi(\frac{u}{\sqrt{1-\rho^2(t)}}) + \rho(t)\sqrt{2\pi}\phi(u)\Phi(\frac{\rho(t)u}{\sqrt{1-\rho^2(t)}})
$$

□

One thing to notice is that because $\rho(t)$ is a function of t which takes different values for different t. $F_\gamma(u)$ may also be different for different t, which means there is no global threshold for the next step multiple testing. As a result, the FDR control and power consistency are so hard to prove.

Regional Peak Height Density

We introduce regional peak height density from the preprint work of Cheng, Schwartzman and Zhao[15].This density function allows us to determine the height distribution of peaks of $X(t)$ over the entire domain $D = [0, L]$, enabling us to establish the proof.

Let $\{X(t), t \in D\}$ be a smooth random field. We are interested in finding the height distribution of X over the entire domain D.

We define $M(D)$ and $M(u, D)$ as the number of local maxima and the number of local maxima above u of the random field X over D. Define the regional peak height distribution of X over D as:

$$F_D(u) = \frac{E[M(u, D)]}{E[M(D)]} \tag{2.14}$$

Plug in the explicit formula of $F_\gamma(u)$ and use the Kac-Rice formula, the explicit form of regional peak height density can be calculated as:

$$F_D(u) = \frac{\int_D \frac{\sqrt{\lambda_1(t)}}{\rho(t)}\{1 - \Phi(\frac{u}{\sqrt{1-\rho^2(t)}}) + \rho(t)\sqrt{2\pi}\phi(u)\Phi(\frac{\rho(t)u}{\sqrt{1-\rho^2(t)}})\}dt}{\int_D \frac{\sqrt{\lambda_1(t)}}{\rho(t)}dt} \tag{2.15}$$

We can see the whole support of the process as a region, that is $D = [0, L]$, by calculation:

$$F_\gamma(u) = \frac{\int_0^L \frac{\sqrt{\lambda_1(t)}}{\rho(t)}\{1 - \Phi(\frac{u}{\sqrt{1-\rho^2(t)}}) + \rho(t)\sqrt{2\pi}\phi(u)\Phi(\frac{\rho(t)u}{\sqrt{1-\rho^2(t)}})\}dt}{\int_0^L \frac{\sqrt{\lambda_1(t)}}{\rho(t)}dt} \tag{2.16}$$

From 2.16, a global threshold can be calculated for peak detection.

Example

One example is provided to show the calculation of density.

Example 2.3.1. Consider the following non-stationary Gaussian process as our noise $z(t)$:

$$z(t) = cos(t) \cdot \xi + sin(t) \cdot dB(t) \tag{2.17}$$

where ξ is a standard Gaussian random variable, $dB(t)$ is white noise which is independent of ξ. Do the convolution with a Gaussian kernel $w_\gamma(t) = (1/\gamma)\phi(t/\gamma)$ with $\gamma > 0$ as in (2.4) produces a non-stationary Gaussian process that has a zero mean and can be infinitely differentiated:

$$z_\gamma(t) = N(0,1)\int_{-\infty}^{\infty}\frac{cos(s)}{\gamma}\phi(\frac{t-s}{\gamma})ds + \int_{-\infty}^{\infty}\frac{sin(s)}{\gamma}\phi(\frac{s-t}{\gamma})dB(s) \tag{2.18}$$

From some basic calculation, we can get:

$$var(z_\gamma(t)) = (\int_{-\infty}^{\infty}\frac{cos(s)}{\gamma}\phi(\frac{t-s}{\gamma})ds)^2 + \int_{-\infty}^{\infty}\frac{sin^2(s)}{\gamma^2}\phi^2(\frac{s-t}{\gamma})ds \tag{2.19}$$

Then do more calculation to get $\lambda_1(t)$, $\lambda_2(t)$.

$$z'_\gamma(t) = N(0,1)\int_{-\infty}^{\infty}\frac{cos(s)(s-t)}{\gamma^3}\phi(\frac{t-s}{\gamma})ds + \int_{-\infty}^{\infty}\frac{sin(s)(s-t)}{\gamma^3}\phi(\frac{t-s}{\gamma})dB(s) \tag{2.20}$$

$$var(z'_\gamma(t)) = (\int_{-\infty}^{\infty}\frac{cos(s)(s-t)}{\gamma^3}\phi(\frac{t-s}{\gamma})ds)^2 + \int_{-\infty}^{\infty}\frac{sin^2(s)(s-t)^2}{\gamma^6}\phi^2(\frac{s-t}{\gamma})ds \tag{2.21}$$

$$\begin{aligned} z''_\gamma(t) = N(0,1)&\int_{-\infty}^{\infty}\frac{cos(s)[(s-t)^2-\gamma^2]}{\gamma^5}\phi(\frac{t-s}{\gamma})ds \\ &+ \int_{-\infty}^{\infty}\frac{sin(s)[(s-t)^2-\gamma^2]}{\gamma^5}\phi(\frac{t-s}{\gamma})dB(s) \end{aligned} \tag{2.22}$$

$$\begin{aligned} var(z''_\gamma(t)) = (&\int_{-\infty}^{\infty}\frac{cos(s)[(s-t)^2-\gamma^2]}{\gamma^5}\phi(\frac{t-s}{\gamma})ds)^2 \\ &+ \int_{-\infty}^{\infty}\frac{sin^2(s)[(s-t)^2-\gamma^2]^2}{\gamma^{10}}\phi^2(\frac{s-t}{\gamma})ds \end{aligned} \tag{2.23}$$

$$\begin{aligned} z'''_\gamma(t) =N(0,1)&\int_{-\infty}^{\infty}\frac{cos(s)(s-t)[(s-t)^2-3\gamma^2]}{\gamma^7}\phi(\frac{t-s}{\gamma})ds \\ &+ \int_{-\infty}^{\infty}\frac{sin(s)(s-t)[(s-t)^2-3\gamma^2]}{\gamma^7}\phi(\frac{t-s}{\gamma})dB(s) \end{aligned} \tag{2.24}$$

$$\begin{aligned} var(z'''_\gamma(t)) =(&\int_{-\infty}^{\infty}\frac{cos(s)(s-t)[(s-t)^2-3\gamma^2]}{\gamma^7}\phi(\frac{t-s}{\gamma})ds)^2 \\ &+ \int_{-\infty}^{\infty}\frac{sin^2(s)(s-t)^2[(s-t)^2-3\gamma^2]^2}{\gamma^{14}}\phi^2(\frac{t-s}{\gamma})ds \end{aligned} \tag{2.25}$$

$$
\begin{aligned}
[var(z_\gamma(t))]' =& 2\int_{-\infty}^{\infty}\frac{cos(s)}{\gamma}\phi(\frac{t-s}{\gamma})ds\int_{-\infty}^{\infty}\frac{cos(s)(s-t)}{\gamma^3}\phi(\frac{t-s}{\gamma})ds \\
&+\int_{-\infty}^{\infty}\frac{2sin^2(s)(s-t)}{\gamma^4}\phi^2(\frac{t-s}{\gamma})ds
\end{aligned}
\tag{2.26}
$$

$$
\begin{aligned}
[var(z_\gamma(t))]'' =& 2(\int_{-\infty}^{\infty}\frac{cos(s)(s-t)}{\gamma^3}\phi(\frac{t-s}{\gamma})ds)^2 \\
&+2\int_{-\infty}^{\infty}\frac{cos(s)}{\gamma}\phi(\frac{t-s}{\gamma})ds\int_{-\infty}^{\infty}\frac{cos(s)[(s-t)^2-\gamma^2]}{\gamma^5}\phi(\frac{t-s}{\gamma})ds \\
&+\int_{-\infty}^{\infty}\frac{2sin^2(s)[2(s-t)^2-\gamma^2]}{\gamma^6}\phi^2(\frac{t-s}{\gamma})ds
\end{aligned}
\tag{2.27}
$$

$$
\begin{aligned}
[var(z_\gamma(t))]''' =& 4\int_{-\infty}^{\infty}\frac{cos(s)(s-t)}{\gamma^3}\phi(\frac{t-s}{\gamma})ds\int_{-\infty}^{\infty}\frac{cos(s)[(s-t)^2-\gamma^2]}{\gamma^5}\phi(\frac{t-s}{\gamma})ds \\
&+2\int_{-\infty}^{\infty}\frac{cos(s)(s-t)}{\gamma^3}\phi(\frac{t-s}{\gamma})ds\int_{-\infty}^{\infty}\frac{cos(s)[(s-t)^2-\gamma^2]}{\gamma^5}\phi(\frac{t-s}{\gamma})ds \\
&+2\int_{-\infty}^{\infty}\frac{cos(s)}{\gamma}\phi(\frac{t-s}{\gamma})ds \\
&\times\int_{-\infty}^{\infty}\frac{cos(s)(s-t)[(s-t)^2-3\gamma^2]}{\gamma^7}\phi(\frac{t-s}{\gamma})ds \\
&+\int_{-\infty}^{\infty}\frac{4sin^2(s)(s-t)[2(s-t)^2-3\gamma^2]}{\gamma^8}\phi^2(\frac{t-s}{\gamma})ds
\end{aligned}
\tag{2.28}
$$

Let:

$$
\begin{aligned}
X_\gamma(t) &= \frac{z_\gamma(t)}{\sqrt{var(z_\gamma(t))}} \\
&= \frac{N(0,1)\int_{-\infty}^{\infty}\frac{cos(s)}{\gamma}\phi(\frac{t-s}{\gamma})ds+\int_{-\infty}^{\infty}\frac{sin(s)}{\gamma}\phi(\frac{s-t}{\gamma})dB(s)}{\sqrt{(\int_{-\infty}^{\infty}\frac{cos(s)}{\gamma}\phi(\frac{t-s}{\gamma})ds)^2+\int_{-\infty}^{\infty}\frac{sin^2(s)}{\gamma^2}\phi^2(\frac{s-t}{\gamma})ds}}
\end{aligned}
\tag{2.29}
$$

Then:

$$
\begin{aligned}
X'_\gamma(t) &= \frac{z'_\gamma(t)\sqrt{var(z_\gamma(t))}-(\sqrt{var(z_\gamma(t))})'z_\gamma(t)}{var(z_\gamma(t))} \\
&= \frac{z'_\gamma(t)}{\sqrt{var(z_\gamma(t))}}-\frac{z_\gamma(t)[var(z_\gamma(t))]'}{2[var(z_\gamma(t))]^{\frac{3}{2}}}
\end{aligned}
\tag{2.30}
$$

And:

$$
\begin{aligned}
X''_\gamma(t) = & \frac{z''_\gamma(t)}{\sqrt{var(z_\gamma(t))}} - \frac{z'_\gamma(t)[var(z_\gamma(t))]'}{2(var(z_\gamma(t)))^{\frac{3}{2}}} \\
& - \frac{2\{z'_\gamma(t)[var(z_\gamma(t))]' + z_\gamma(t)[var(z_\gamma(t))]''\}[var(z_\gamma(t))]^{\frac{3}{2}}}{4[var(z_\gamma(t))]^3} \\
& + \frac{3z_\gamma(t)var(z_\gamma(t))^{\frac{1}{2}}\{[var(z_\gamma(t))]'\}^2}{4[var(z_\gamma(t))]^3}
\end{aligned}
\tag{2.31}
$$

Then calculate the $\lambda_1(t)$, $\lambda_2(t)$, let:

$$
X'_\gamma(t) = a(t)z_\gamma(t) + b(t)z'_\gamma(t) \tag{2.32}
$$

Where $a(t) = -\frac{[var(z_\gamma(t))]'}{2[var(z_\gamma(t))]^{\frac{3}{2}}}$ and $b(t) = \frac{1}{\sqrt{var(z_\gamma(t))}}$, which are constants when t is fixed, then $var(X'_\gamma(t))$ can be calculated as:

$$
\begin{aligned}
var(X'_\gamma(t)) &= E[(a(t)z_\gamma(t) + b(t)z'_\gamma(t))(a(t)z_\gamma(t) + b(t)z'_\gamma(t))] \\
&= a^2(t)var(z_\gamma(t)) + b^2(t)var(z'_\gamma(t)) + 2a(t)b(t)E(z_\gamma(t)z'_\gamma(t))
\end{aligned}
\tag{2.33}
$$

where we can calculate:

$$
\begin{aligned}
var(z_\gamma(t)) =& (\int_{-\infty}^{\infty} \frac{cos(s)}{\gamma}\phi(\frac{t-s}{\gamma})ds)^2 + \int_{-\infty}^{\infty} \frac{sin^2(s)}{\gamma^2}\phi^2(\frac{s-t}{\gamma})ds \\
var(z'_\gamma(t)) =& (\int_{-\infty}^{\infty} \frac{cos(s)(s-t)}{\gamma^3}\phi(\frac{t-s}{\gamma})ds)^2 + \int_{-\infty}^{\infty} \frac{sin^2(s)(s-t)^2}{\gamma^6}\phi^2(\frac{s-t}{\gamma})ds \\
E(z_\gamma(t)z'_\gamma(t)) =& (\int_{-\infty}^{\infty} \frac{cos(s)}{\gamma}\phi(\frac{t-s}{\gamma})ds)(\int_{-\infty}^{\infty} \frac{cos(s)(s-t)}{\gamma^3}\phi(\frac{t-s}{\gamma})ds) \\
& + \int_{-\infty}^{\infty} \frac{sin^2(s)(s-t)}{\gamma^4}\phi^2(\frac{s-t}{\gamma})ds
\end{aligned}
\tag{2.34}
$$

They are all constants when t is fixed. So we can calculate $var(X'_\gamma(t))$ when t is fixed.

Let

$$
X''_\gamma(t) = c(t)z_\gamma(t) + d(t)z'_\gamma(t) + g(t)z''_\gamma(t) \tag{2.35}
$$

where $c(t) = \frac{-2[var(z_\gamma(t))''][var(z_\gamma(t))]^{\frac{3}{2}} + 3var(z_\gamma(t))^{\frac{1}{2}}[var(z_\gamma(t))]'^2}{4[var(z_\gamma(t))]^3}$,
$d(t) = -\frac{[var(z_\gamma(t))]'}{2[var(z_\gamma(t))]^{\frac{3}{2}}} - \frac{[var(z_\gamma(t))]'}{2[var(z_\gamma(t))]^3}$ and $g(t) = \frac{1}{\sqrt{var(z_\gamma(t))}}$, which are constants when t is

fixed, then $var(X''_\gamma(t))$ can be calculated as:

$$\begin{aligned} var(X''_\gamma(t)) &= E[(c(t)z_\gamma(t) + d(t)z'_\gamma(t) + g(t)z''_\gamma(t)) \\ &\quad \times (c(t)z_\gamma(t) + d(t)z'_\gamma(t) + g(t)z''_\gamma(t))] \\ &= c^2(t)var(z_\gamma(t)) + d^2(t)var(z'_\gamma(t)) + g^2(t)var(z''_\gamma(t)) \\ &\quad + 2c(t)d(t)E(z_\gamma(t)z'_\gamma(t)) + 2c(t)g(t)E(z_\gamma(t)z''_\gamma(t)) \\ &\quad + 2d(t)g(t)E(z'_\gamma(t)z''_\gamma(t)) \end{aligned} \tag{2.36}$$

where we can calculate:

$$\begin{aligned} var(z''_\gamma(t)) =& (\int_{-\infty}^{\infty} \frac{cos(s)[(s-t)^2-\gamma^2]}{\gamma^5}\phi(\frac{t-s}{\gamma})ds)^2 \\ &+ \int_{-\infty}^{\infty} \frac{sin^2(s)[(s-t)^2-\gamma^2]^2}{\gamma^{10}}\phi^2(\frac{s-t}{\gamma})ds \\ E(z_\gamma(t)z''_\gamma(t)) =& (\int_{-\infty}^{\infty} \frac{cos(s)}{\gamma}\phi(\frac{t-s}{\gamma})ds)(\int_{-\infty}^{\infty} \frac{cos(s)[(s-t)^2-\gamma^2]}{\gamma^5}\phi(\frac{t-s}{\gamma})ds) \\ &+ \int_{-\infty}^{\infty} \frac{sin^2(s)[(s-t)^2-\gamma^2]}{\gamma^6}\phi^2(\frac{s-t}{\gamma})ds \\ E(z'_\gamma(t)z''_\gamma(t)) =& (\int_{-\infty}^{\infty} \frac{cos(s)(s-t)}{\gamma^3}\phi(\frac{t-s}{\gamma})ds)(\int_{-\infty}^{\infty} \frac{cos(s)[(s-t)^2-\gamma^2]}{\gamma^5}\phi(\frac{t-s}{\gamma})ds) \\ &+ \int_{-\infty}^{\infty} \frac{sin^2(s)(s-t)[(s-t)^2-\gamma^2]}{\gamma^8}\phi^2(\frac{s-t}{\gamma})ds \end{aligned}$$

They are all constants when t is fixed. So we can calculate $var(X''_\gamma(t))$ when t is fixed. Now we calculate $E(X'_\gamma(t)X''_\gamma(t))$, from the definitions given before, we can get:

$$\begin{aligned} E(X'_\gamma(t)X''_\gamma(t)) &= E[(a(t)z_\gamma(t) + b(t)z'_\gamma(t))(c(t)z_\gamma(t) + d(t)z'_\gamma(t) + g(t)z''_\gamma(t))] \\ &= a(t)c(t)var(z_\gamma(t)) + b(t)d(t)var(z'_\gamma(t)) \\ &\quad + [a(t)d(t) + b(t)c(t)]E(z_\gamma(t)z'_\gamma(t)) + a(t)g(t)E(z_\gamma(t)z''_\gamma(t)) \\ &\quad + b(t)g(t)E(z'_\gamma(t)z''_\gamma(t)) \end{aligned} \tag{2.37}$$

All the terms mentioned in this context are expressions that are related to the variable t. Therefore, $\lambda_1(t)$, $\lambda_2(t)$, and $\lambda'_1(t)$ can be expressed as functions of t. With the regional

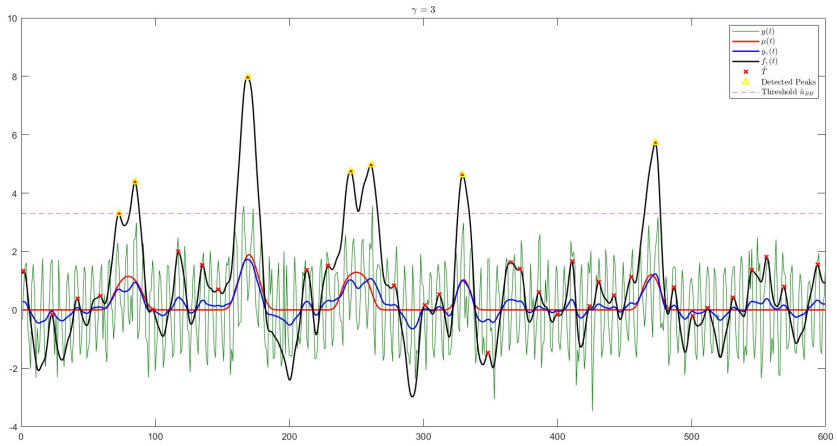

Figure 2.5: The green line is observed sequence $y(t)$, the red line is the original signal $\mu(t)$, the blue line is smoothed sequence $y_\gamma(t)$, the black line is smoothed and standardized sequence $f_\gamma(t)$. The red crosses are candidate peaks. The yellow triangles are detected signals, the magenta dotted line is the global threshold for multiple testing

peak height density described by equation 2.16, the p-values can be calculated using the observations u.

2.3.5 Multiple Testing

In this step, we define $\tilde{m}$ which denotes the number of local maxima in $\tilde{T}$. Employing a multiple testing procedure, we evaluate the $\tilde{m}$ p-values and identify the peaks as significant if their p-values are below the threshold we calculated in this step.

In this project, we utilize the Benjamini-Hochberg (BH) procedure. For a fixed significance level $\alpha \in (0, 1)$, given the $\tilde{m}$ p-values $(p_1, p_2, \cdots, p_{\tilde{m}})$ calculated previously, we determine the largest index k for which the ith smallest p-value is less than $i\alpha/\tilde{m}$. Thus, the null hypothesis $H_0(t)$ at $t \in \tilde{T}$ is rejected if:

$$p_\gamma(t) < \frac{k\alpha}{\tilde{m}} \iff f_\gamma(t) > \tilde{u}_{\text{BH}} = F_\gamma^{-1}(\frac{k\alpha}{\tilde{m}}) \tag{2.38}$$

2.3.6 Error Definitions

Due to the influence of noise, detected peaks may be shifted out of the true signal region. In order to evaluate the accuracy of peak detection, we categorize a significant local maximum as true positive if it is in the signal region. If the detected peak is outside the signal region, it is considered as false positive. The definition of signal region will be given in the next part.

With the model described in section 2.1, we define the signal region $\mathbb{S}_1$ and the null region $\mathbb{S}_0$ as follows:

$$\mathbb{S}_1 = \bigcup_{j=1}^{J} S_j \quad \text{and} \quad \mathbb{S}_0 = [0, L] \setminus \left(\bigcup_{j=1}^{J} S_j \right) \tag{2.39}$$

For a given threshold u, the number of all detected peaks and the number of all falsely detected peaks are:

$$R(u) = \# \left\{ t \in \tilde{T} : f_\gamma(t) > u \right\} \quad \text{and} \quad V(u) = \# \left\{ t \in \tilde{T} \cap \mathbb{S}_0 : f_\gamma(t) > u \right\} \tag{2.40}$$

Both of $R(u)$ and $V(u)$ are defined as 0 if $\tilde{T}$ has no elements. The FDR is defined as the expected proportion of falsely detected peaks

$$\text{FDR}(u) = \mathbb{E} \left\{ \frac{V(u)}{R(u) \vee 1} \right\} \tag{2.41}$$

If $R(u) = 0$, FDR is defined as 0.

2.3.7 Control of FDR

In this step, we use the BH procedure to perform the multiple testing: for a fixed $\alpha \in (0, 1)$, with the $\tilde{m}$ p-values $(p_1, p_2, \cdots, p_{\tilde{m}})$ calculated before, let k be the largest index for which the ith smallest p-values is less than $i\alpha/\tilde{m}$. Then the null hypothesis $H_0(t)$ at $t \in \tilde{T}$ is rejected if:

$$p_\gamma(t) < \frac{k\alpha}{\tilde{m}} \iff f_\gamma(t) > \tilde{u}_{\text{BH}} = F_\gamma^{-1}(\frac{k\alpha}{\tilde{m}}) \tag{2.42}$$

We get the threshold $\tilde{u}_{\text{BH}}$.

Define the following conditions:

(C1) The assumptions of Section 2.1 hold.

(C2) The number of trials $N \to \infty$ and $a = \inf_j a_j \to \infty$.

Theorem 2.3.3. *Suppose that the algorithm of this work is applied with the BH threshold* $\tilde{u}_{\text{BH}}$. *Then under conditions* (C1) *and* (C2).

$$\limsup \text{FDR}(\tilde{u}_{\text{BH}}) \leq \alpha \tag{2.43}$$

The proof of theorem 2.3.3 is given in chapter 4.

2.3.8 Power Consistency

A significant local maximum is defined as true positive if it is in the signal region $\mathbb{S}_1$. The power of this algorithm is defined as the expected fraction of true discovered peaks:

$$\begin{aligned} \text{Power}(\tilde{u}_{\text{BH}}) &= \mathbb{E}\left[\frac{1}{J}\sum_{j=1}^{J} 1(\tilde{T} \cap S_j \neq \varnothing \quad \text{and} \quad \max_{\tilde{t}\in\tilde{T}\cap S_j} f_\gamma(t) > \tilde{u}_{\text{BH}}\right] \\ &= \frac{1}{J}\sum_{j=1}^{J} \text{Power}_j(\tilde{u}_{\text{BH}}) \end{aligned} \tag{2.44}$$

where $\text{Power}_j(\tilde{u}_{\text{BH}})$ is the probability of detecting peak j

$$\text{Power}_j(\tilde{u}_{\text{BH}}) = \text{P}\left\{\tilde{T} \cap S_j \neq \varnothing \quad \text{and} \quad \max_{\tilde{t}\in\tilde{T}\cap S_j} f_\gamma(t) > \tilde{u}_{\text{BH}}\right\} \tag{2.45}$$

The inclusion of the maximum operator ensures that if multiple significant local maxima fall within the same peak support, only one of them is considered, thereby preventing an inflation of power.

When only kernel smoothing is applied, the local maxima are not expected to shift outside the signal region. However, in this project, standardization is also applied to the

kernel-smoothed sequence. Therefore, it is important to ensure that the local maximum of $f_\gamma(t)$ asymptotically falls within the support of the signal with probability 1. This is crucial to maintain the accuracy and reliability of the peak detection method.

Lemma 2.3.4. *If the noise satisfies* $\sup_{t\in S_0\cap S_{1,\gamma}}[\frac{\mu_\gamma(t)}{\sqrt{\mathrm{var}(z_\gamma(t))}}] < \sup_{t\in S_1}[\frac{\mu_\gamma(t)}{\sqrt{\mathrm{var}(z_\gamma(t))}}]$*, the local maxima of* $f_\gamma(t)$ *will asymptotically locates in the support of signal with probability 1.*

If the noise satisfies lemma 2.3.4, then we have the following theorem:

Theorem 2.3.5. *Suppose that noise satisfies theorem 2.3.4 Then, under conditions* $(\mathrm{C1})$ *and* $(\mathrm{C2})$*,*

$$\mathrm{Power}(\tilde{u}_{BH}) \to 1$$

The proof of this theorem is provided in the chapter 4.

2.3.9 SNR

If the smoothed and standardized process is smooth enough and conditions $(\mathrm{C1})$ and $(\mathrm{C2})$ are met. By the FDR control discussed before. To choose the best smoothing kernel $w_\gamma(t)$. We can try to maximize the power under the model. This maximization is very difficult to analyze, we can relax some requirement to a less formal argument here. The original true signal S_j can be detected within a small interval which contains the peak mode τ_j with probability tending to 1. Then the power for peak j may be approximated as:

$$\mathrm{Power}_j(u(\tau_j)) \approx \mathbb{P}\{f_\gamma(\tau_j) > u(\tau_j)\} = \Phi\left[\frac{a_j h_{\gamma,j}(\tau_j)}{\sqrt{var(z_\gamma(\tau_j))}} - u(\tau_j)\right] \tag{2.46}$$

because $f_\gamma(\tau_j) \sim N(\frac{a_j h_{\gamma,j}(\tau_j)}{\sqrt{var(z_\gamma(\tau_j))}}, 1)$

The power can be approximated maximized by maximizing the SNR_γ.

$$\mathrm{SNR}_\gamma = \frac{a_j h_{\gamma,j}(\tau_j)}{\sqrt{var(z_\gamma(\tau_j))}} = \frac{a_j \int_{-\infty}^{\infty} w_\gamma(s) h_j(s) ds}{\sqrt{var(z_\gamma(\tau_j))}}$$

Where $\sqrt{var(z_\gamma(\tau_j))}$ is the standard deviation of the kernel smoothed process $z_\gamma(t)$ when $t = \tau_j$.

2.4 Smooth Noise

2.4.1 The Algorithm

When the noise is smooth with unit variance and non-stationary, algorithm is as follows:

1.**Candidate peaks**: Find the set of local maxima of the observed sequence $y(t)$ in $[0, L]$.

$$\tilde{T} = \left\{ t \in [0, L] : y'(t) = \frac{dy(t)}{dt} = 0, y''(t) = \frac{d^2y(t)}{dt^2} < 0 \right\} \tag{2.47}$$

2.**P-values**: For each $t \in \tilde{T}$ compute the p-value for the test:

$$\mathcal{H}_0(t) : \mu(t) = 0 \quad vs \quad \mathcal{H}_A(t) : \mu(t) > 0, \qquad t \in \tilde{T} \tag{2.48}$$

The distribution of the noise is the same as the formula 2.16.

3.**Multiple testing**: Let $\tilde{m}$ represents the number of tested hypotheses, which is equal to the number of local maxima in $\tilde{T}$. Then apply the BH procedure to the $\tilde{m}$ p-values $(p_1, \cdots, p_{\tilde{m}})$ associated with the local maxima at $t \in \tilde{T}$. We declare a peak as significant if its corresponding p-value is smaller than the chosen significance threshold.

The error definition, FDR, and power consistency aspects remain the same as in the case of unsmooth noise. The key differences between smooth noise and unsmooth noise lie in the first two steps of the procedure: kernel smoothing and standardization. These steps are specific to handling unsmooth noise, allowing for accurate peak detection and subsequent analysis.

Chapter 3

NUMERICAL STUDIES

3.1 Simulation Studies

3.1.1 Simulation Settings

Simulations were performed to assess the performance of the algorithm under moderate signal strength a and finite repetitions. In the simulation, the range of support $L = 600$, the simulations involved $J = 5$ truncated Gaussian peaks with equal heights, denoted as $a_j h_j(t)$, where $a_j h_j(t) = a/b\phi[(t-\tau_j)/b]\mathbf{1}[-cb, cb]$ and $j = 1, \ldots, J$. Here, $b = 3$ and $c = 3$, and a varied to represent different signal strengths.

The noise component was constructed as follows:

$$z(t) = \cos(t) \cdot \xi + \sin(t) \cdot dB(t) \tag{3.1}$$

where ξ is a standard Gaussian random variable, $dB(t)$ is a sequence of white noise which is independent of ξ. The simulation process is repeated $N = 1000$ times to obtain estimates of the FDR and the corresponding power. It is important to note that the FDR is calculated by summing the number of falsely detected signals across all $N = 1000$ trials as the numerator, and summing all the detected signals as the denominator. This approach allows for obtaining the expectation of the FDR through the law of large numbers.

By conducting a large number of simulations, the estimated FDR and power provide valuable insights into the performance and characteristics of the algorithm under different scenarios, including various signal strengths and finite range conditions.

The algorithm was executed using a truncated Gaussian density as the smoothing ker-

nel.:

$$w_\gamma(t) = (1/\gamma)\phi(t/\gamma)\mathbf{1}[-c\gamma, c\gamma]$$

Which has the same definition as 2.17. With $c = 3$ and varying γ. We can estimate the noise parameter of $z(t)$ by calculating its first and second-order differences to approximate the corresponding first and second derivatives. With the same smoothing kernel, the level α of BH procedures is 0.05 in this simulation.

3.1.2 Nonasymptotic Performance

Figure 3.1 presents the observed levels of the false discovery rate (FDR) for the BH procedure. The FDR is evaluated using equation (2.41), with the expectation replaced by the ensemble average over 1000 replications. It is worth noting that I calculated the FDR by summing the denominator and numerator separately and then dividing them. By the law of large numbers, this calculation guarantees an asymptotic estimate of the FDR. The error rates are controlled under the level $\alpha = 0.05$ for bandwidths larger than 2 and for sufficiently large signal strengths a. When γ is small, i.e., $\gamma < 2$, the FDR exceeds the nominal level. This is because a small γ leads to a process which is not smooth enough to apply our algorithm.

When the bandwidth γ is larger than the bandwidth of signal peak $b = 3$, the error rates also do not exceed the nominal level. As γ increases, the value of $\sqrt{\text{var}(z_\gamma(t))}$ decreases, amplifying the difference between the noise and peak heights.

Figure 3.2 illustrates the observed power of the BH procedure, evaluated using the definition in equation 2.3.5, with the expectations replaced by the ensemble average over the 1000 replications. When the kernel bandwidth is small, increasing the bandwidth leads to an increase in power. This is also because a small bandwidth results in unsmooth process, leading to low power. As the bandwidth increases, the plot becomes smoother, resulting in a decrease in candidate peaks and, consequently, a decrease in power.

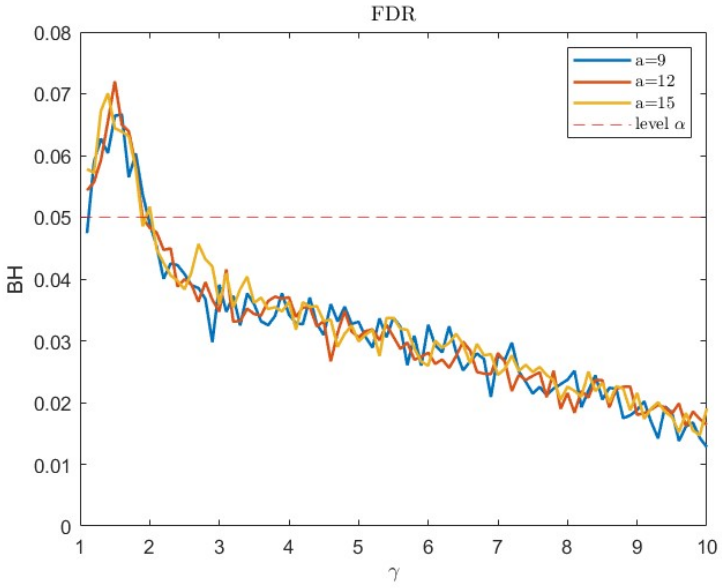

Figure 3.1: FDR of the BH procedure for a = 9, a = 12 and a = 15

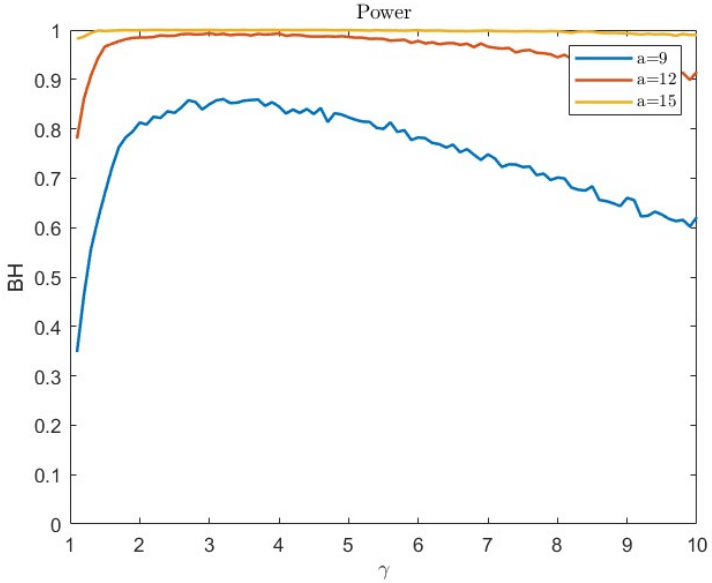

Figure 3.2: Power of the BH procedure for a = 9, a = 12 and a = 15

3.2 Discussion of Non-stationary Noise's Variance

The simulations assume that the variance of the non-stationary noise is one. However, even if the variance of the noise is not one, the standardization step in the algorithm guarantees that the standardized and smoothed noise will have unit variance. As a result, the formula to calculate the p-values can still be applied under this condition.

It is important to note that when the variance of the noise increases, it can have a substantial impact on the signal, especially if the signal strength is not sufficiently strong. This means that the noise can overshadow or obscure the signal, making it more challenging to detect peaks accurately. The influence of the noise variance on peak detection is an essential consideration in understanding the limitations and performance of the algorithm.

Further analysis and investigations can explore the specific effects of varying noise variances on peak detection performance, allowing for a better understanding of the algorithm's behavior under different noise conditions.

Consider the following non-stationary Gaussian process as our noise $z(t)$:

$$z(t) = 2 \cdot \sin(t) dB(t) \tag{3.2}$$

The variance of the noise, $z(t)$, does not remain constant across the entire support.

From the two plots, figure 3.3 shows the FDR of the BH procedure for $a = 9$, $a = 12$, $a = 15$ and $a = 21$, which shows little difference from the first FDR plot, however, figure 3.4 shows the power, one thing to notice is that, when the signal strength is small, the power is low, which may caused by the bigger variance of the noise. When the variance of the noise is big, the signal will be absolutely effected, signals may be buried within noise that exhibits higher variance. However, when the signal strength increases, the problem will be solved.

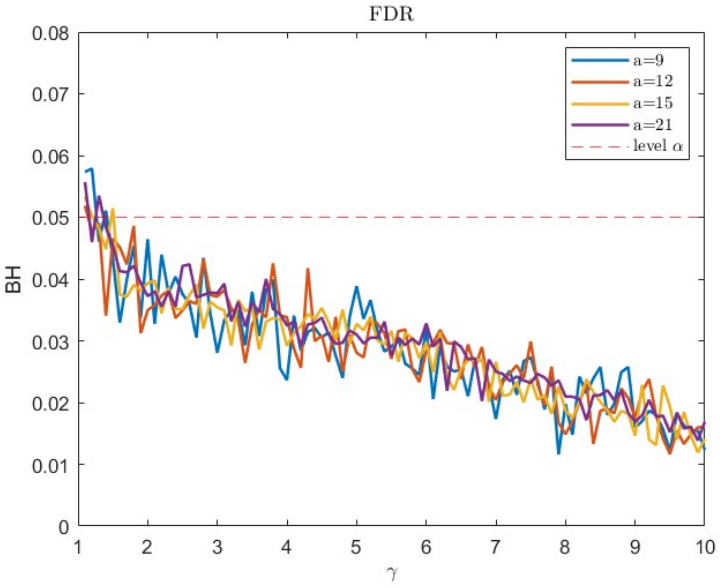

Figure 3.3: FDR of the BH procedure for a = 9, a = 12, a = 15 and a = 21

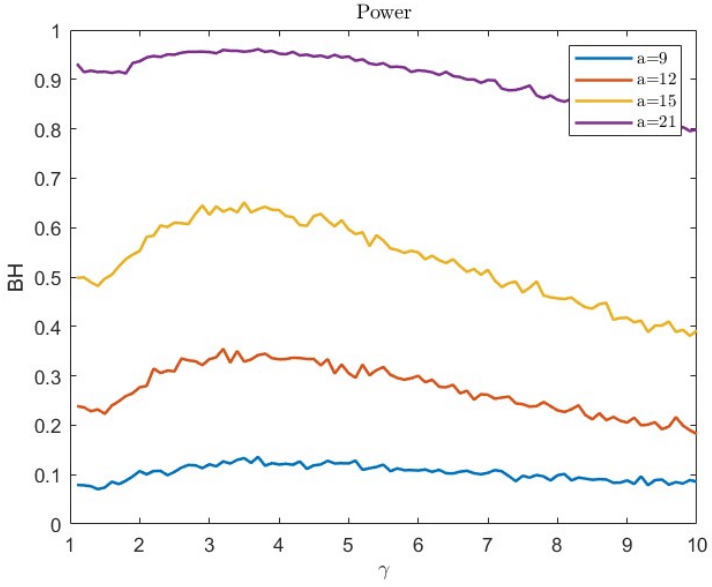

Figure 3.4: Power of the BH procedure for a = 9, a = 12 a = 15 and a = 21

3.3 Data Example

In this section, we aim to apply our method to real-world applications. Finding repeatable processes with non-stationary noise can be challenging in everyday life due to the fast-changing nature of the world. Even if observations of a certain process are obtained multiple times, it is likely to undergo significant changes, and the assumption that $\mu(t)$ does not change substantially may not hold. Sunspot data from the World Data Center SILSO, Royal Observatory of Belgium, Brussels.

However, when it comes to the Sun, observing it over a ten-year period does not result in substantial alterations. In this project, we will utilize the number of sunspots from 1749 to 2013 as our data set. This data set comprises nearly 3400 data points, representing the average number of sunspots observed each month. Based on the work of Balogh, A., Hudson, H., Petrovay, K. and von Steiger, R. [4], the first solar cycle begins in 1755, and the duration of a solar cycle is approximately 11 years. Therefore, we have 24 independent solar cycles since 1755. In our models, we set $L = 132$ and $N = 24$.

To begin, let's plot all the data starting from 1755. Figure 3.5 displays the entire process of the average number of sunspots for each month from 1755 to 2018.

There are 24 solar cycles included, from the plot, it is easy to find that in some solar cycles, the number is small, in other cycles, the number is medium and the other cycles, the number is large. Then I divide the 24 cycles into three groups: inactive, normal and active solar cycle. I decided to use the method to detect the peaks of active solar cycles.

Figure 3.6 presents the combination of 11 active solar cycles. From the plot, it is evident that these 11 solar cycles exhibit a similar signal pattern. To further analyze these cycles, I will calculate the mean of these 11 solar cycles. By calculating the mean, we can obtain an estimate of the underlying signal, while the variability across the cycles contributes to the estimation of the noise component. With these parameters determined, we can proceed to

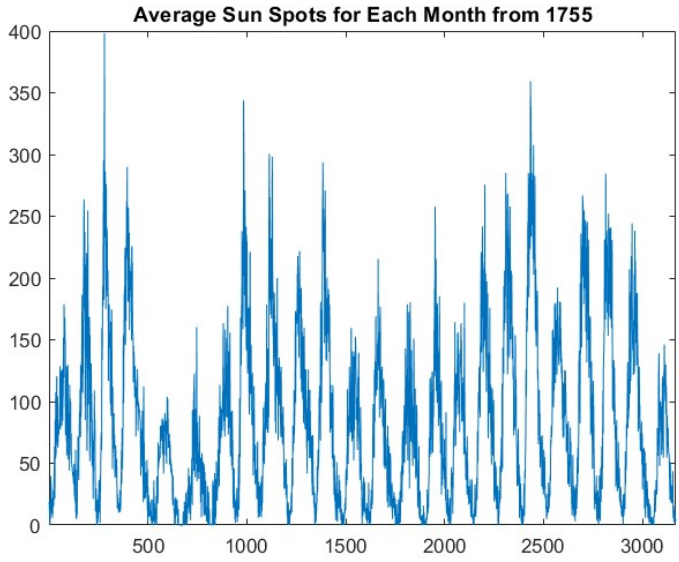

Figure 3.5: The average number of sun spots from 1755 to 2018

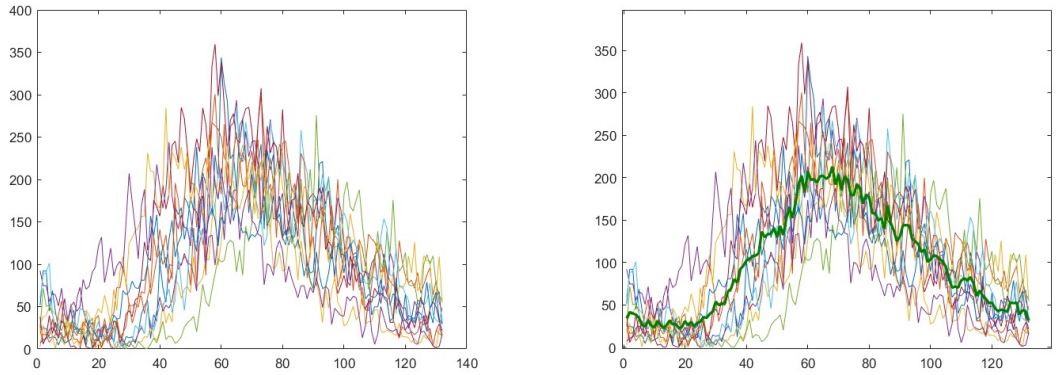

Figure 3.6: The left plot is a combination of 11 active solar cycles, the green line in the right plot is the mean of the 11 solar cycles, which can be seen as $\mu(t)$

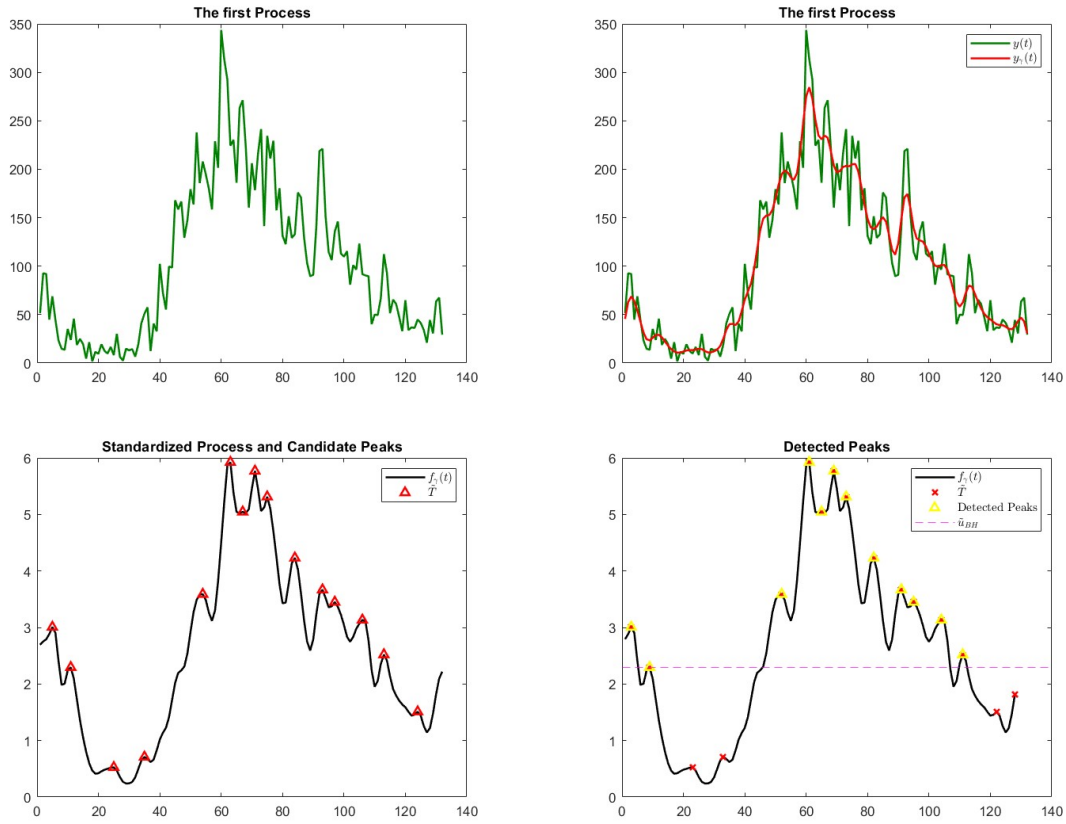

Figure 3.7: The top left plot shows the first process of 11 active solar cycles $y(t)$. The red line in the top right plot is the smoothed process $y_\gamma(t)$. The bottom left plot is the standardized and smoothed process $f_\gamma(t)$, the red triangles are candidate peaks and the yellow triangles in the bottom right plot are detected signals, the pink dotted line is the threshold.

apply the algorithm and detect the signal for each individual solar cycle.

By applying the algorithm to the data, we can detect the signal within each process and analyze the characteristics and patterns of the solar cycles.

The figure 3.7 shows the result of our algorithm on one process. After applying the 11 processes, I can achieve 11 different data sets. The following table shows the results. From the table 3.1, the sun spots activity can be detected as the same location for the 11 processes, for example, location 61, 81 and so on.

1	2	3	4	5	6	7	8	9	10	11
3	25	8	5	61	2	53	48	6	25	8
9	56	55	11	70	8	61	52	49	34	14
52	61	61	52	77	53	69	61	54	40	21
61	69	68	62	80	68	73	69	61	43	28
65	81	73	69	88	75	81	73	69	48	39
69	96	76	73	94	82	101	81	73	53	54
73	106	81	81	102	94		101	81	61	61
82	117	95	87	110	106			94	69	68
91	122	101	95	114	111			100	81	77
95	128	106	102	126				109		80
104		122	106							
111		128	113							

Table 3.1: Each column represents the number of process, the data indicates the location of the detected signals

Chapter 4

TECHNICAL DETAILS FOR MULTIPLE TESTING

4.1 Unsmooth Noise

This part is the proof for the unsmooth noise, the smooth part is the same as the unsmooth part.

4.1.1 FDR Control and Power Consistency

Lemma 4.1.1. *Let* $L_k = (\frac{L(k-1)}{K}, \frac{Lk}{K})$ *be a partition of support L, where* $k = 1, 2, \ldots, K$, $\tilde{m}_{0,n,\gamma,k} = \#\{t \in \tilde{T}_n \cap \mathbb{S}_{0,\gamma} \cap L_k\}$ *be the number of* t *which is the local maxima of* $f_\gamma(t)$*[or* $X_\gamma(t)$*] in the intersection of* $\mathbb{S}_{0,\gamma}$ *and* L_k *on trial* n*, where* $\mathbb{S}_{0,\gamma}$ *is the transition region of the process. Let* $V_{n,\gamma,k}(u) = \#\{t \in \tilde{T}_n \cap \mathbb{S}_{0,\gamma} \cap L_k : f_\gamma(t) > u\}$ *be the number of* t *which is the local maxima of* $f_\gamma(t)$*[or* $X_\gamma(t)$*] in the intersection of* $\mathbb{S}_{0,\gamma}$ *and* L_k*, whose heights are above the level* u *on trial* n*. Then*

$$\frac{\sum_{n=1}^{N} V_{n,\gamma,k}(u)}{\sum_{n=1}^{N} \tilde{m}_{0,n,\gamma,k}} \to \frac{\mathbb{E}[V_{n,\gamma,k}(u)]}{\mathbb{E}[\tilde{m}_{0,n,\gamma,k}]} = F_{\gamma,k}(u) \tag{4.1}$$

in probability as $N \to \infty$*, where* $F_{\gamma,k}(t) = \mathbb{P}[X_\gamma(t) > u | t \in \tilde{T} \cap \mathbb{S}_{0,\gamma} \cap L_k]$ *is the conditional distribution and* N *is the number of trials.*

Proof. :Notice that $f_\gamma(t) = X_\gamma(t)$ for all $t \in \mathbb{S}_{0,\gamma}$, so the process $f_\gamma(t)$ has the same properties as the process $X_\gamma(t)$ on the set $\mathbb{S}_{0,\gamma}$. And notice that for each $n = 1, 2, ..., N$, $X_\gamma(t)$ has the same distribution. Applying the weak law of large number can give that:

$$\frac{\sum_{n=1}^{N} V_{n,\gamma,k}(u)}{\sum_{n=1}^{N} \tilde{m}_{0,n,\gamma,k}} = \frac{\sum_{n=1}^{N} V_{n,\gamma,k}(u)/N}{\sum_{n=1}^{N} \tilde{m}_{0,n,\gamma,k}/N} \to \frac{\mathbb{E}[V_{n,\gamma,k}(u)]}{\mathbb{E}[\tilde{m}_{0,n,\gamma,k}]} \tag{4.2}$$

By the definition of $F_{\gamma,k}(t)$, the right hand of ratio (4.2) equals the conditional probability.

□

From the definition of regional peak height density, let $K = 1$, that is, we see the whole support L as the region. Then we have that:

$$\frac{\sum_{n=1}^{N} V_{n,\gamma}(u)}{\sum_{n=1}^{N} \tilde{m}_{0,n,\gamma}} \to \frac{\mathbb{E}[V_{n,\gamma}(u)]}{\mathbb{E}[\tilde{m}_{0,n,\gamma}]} = F_{\gamma}(u) \tag{4.3}$$

Where $\tilde{m}_{0,n,\gamma} = \#\{t \in \tilde{T}_n \cap \mathbb{S}_{0,\gamma}\}$ be the number of t which is the local maxima of $f_{\gamma}(t)$[or $X_{\gamma}(t)$] in the $\mathbb{S}_{0,\gamma}$on trial n, where $\mathbb{S}_{0,\gamma}$ is the transition region of the process. $V_{n,\gamma}(u) = \#\{t \in \tilde{T}_n \cap \mathbb{S}_{0,\gamma} : f_{\gamma}(t) > u\}$ be the number of t which is the local maxima of $f_{\gamma}(t)$[or $X_{\gamma}(t)$] in the $\mathbb{S}_{0,\gamma}$, whose heights are above the level u on trial n.

For simplicity, we introduce a new notation: $\eta_{j,\gamma}(t) = \frac{h_{j,\gamma}(t)}{\sqrt{\mathrm{var}(\mathrm{z}_{\gamma}(\mathrm{t}))}}$. The original support of the whole process is divided into two parts $\mathbb{S}_1$ and $\mathbb{S}_0$. After the step of kernel smoothing, the signal region is enlarged [32] to $\mathbb{S}_{1,\gamma}$ and the null region is transferred into $\mathbb{S}_{0,\gamma}$. However, after the step of standardization, the two regions $\mathbb{S}_{1,\gamma}$ and $\mathbb{S}_{0,\gamma}$ remain the same.

Lemma 4.1.2. *Assume the model of section 2.1 hold and there exist a universal $\delta > 0$ such that $I_{j,\gamma}^{\mathrm{mode}} := \{t \in L : |t - \tau_{j,\gamma}| \leq \delta\}$ and $I_{j,\gamma}^{\mathrm{side}} = S_{j,\gamma} \backslash I_{j,\gamma}^{\mathrm{mode}}$. Let $S_{j,\gamma} = I_{j,\gamma}^{\mathrm{side}} \bigcup I_{j,\gamma}^{\mathrm{mode}}$ be a partition, where $\tau_{j,\gamma} \in S_{j,\gamma}$ be the mode where peak shape $\eta_{j,\gamma}(t)$ reaches its maximum value. Then we define $I_{j,\gamma}^{\mathrm{side}} = I_{j,\gamma}^{\mathrm{left}} \bigcup I_{j,\gamma}^{\mathrm{right}}$, where $I_{j,\gamma}^{\mathrm{left}}$ is the left part of $I_{j,\gamma}^{\mathrm{side}}$ and $I_{j,\gamma}^{\mathrm{right}}$ is the right part of $I_{j,\gamma}^{\mathrm{side}}$. Let:*

- M_j *be the largest value of* $|\eta_{j,\gamma}(t)|$ *in* S_j*;*
- $C_{j,\gamma}^{\mathrm{side}} = \inf_{t \in I_{j,\gamma}^{\mathrm{side}}} |\eta'_{j,\gamma}(t)|$
- $C_{j,\gamma}^{\mathrm{mode}} = \inf_{t \in I_{j,\gamma}^{\mathrm{mode}}} |\eta'_{j,\gamma}(t)|$
- $C_{j,\gamma}^{\mathrm{left}} = \inf_{t \in I_{j,\gamma}^{\mathrm{left}}} \eta'_{j,\gamma}(t)$
- $D_{j,\gamma}^{\mathrm{mode}} = \inf_{t \in I_{j,\gamma}^{\mathrm{mode}}} \eta''_{j,\gamma}(t)$
- $\sigma_{1,\mathrm{left}} = \sup_{t \in I_{j,\gamma}^{\mathrm{left}}} (sd(X'_{\gamma}(t)))$

- $\sigma_{1,\text{side}} = \sup_{t \in I_{j,\gamma}^{\text{side}}} (sd(X'_\gamma(t)))$
- $\sigma_{1,\text{mode}} = \sup_{t \in I_{j,\gamma}^{\text{mode}}} (sd(X'_\gamma(t)))$
- $\sigma_{2,\text{mode}} = \sup_{t \in I_{j,\gamma}^{\text{mode}}} (sd(X''_\gamma(t)))$

For $\tilde{T}$ and any threshold u,

$$\begin{aligned}
&P(\#\{t \in \tilde{T} \cap I_{j,\gamma}^{\text{side}}\} = 0) \\
&\quad \geq 1 - \exp(-\frac{a_j^2 C_{j,\gamma}^{\text{side},2}}{2\sigma_{1,\text{side}}^2}) \\
&P(\#\{t \in \tilde{T} \cap I_{j,\gamma}^{\text{mode}}\} = 1) \\
&\quad \geq 2\Phi(\frac{a_j C_{j,\gamma}^{\text{mode}}}{\sigma_1}) - 1 - \exp(-\frac{a_j^2 D_{j,\gamma}^{\text{mode},2}}{2\sigma_{2,\text{mode}}^2}) \\
&P(\#\{t \in \tilde{T} \cap I_j^{\text{mode}} : f_\gamma(t) > u\} = 1) \\
&\quad \geq 1 - \Phi(u - a_j M_j) - \exp(-\frac{a_j^2 D_{j,\gamma}^{\text{mode},2}}{2\sigma_{2,\text{mode}}^2})
\end{aligned} \tag{4.4}$$

Proof. (1) For the side region of I_j^{side}, we consider I_j^{left} first. The probability that there are no local maxima of $f_\gamma(t)$ in I_j^{left} is greater than the probability that $f'_\gamma(t) > 0$ for all t in the interval. This probability is:

$$\begin{aligned}
P(\#\{t \in \tilde{T} \cap I_{j,\gamma}^{\text{left}}\} = 0) &\geq P(\inf_{I_{j,\gamma}^{\text{left}}} f'_\gamma(t) > 0) \\
&\geq P(\inf_{I_{j,\gamma}^{\text{left}}} X'_\gamma(t) > -\inf_{I_{j,\gamma}^{\text{left}}} \left[\frac{\mu_\gamma(t)}{\sqrt{\text{var}(\text{z}_\gamma(\text{t}))}}\right]') \\
&= 1 - P(\sup_{I_{j,\gamma}^{\text{left}}}[-X'_\gamma(t)] > \sup_{I_{j,\gamma}^{\text{left}}} a_j \eta'_{j,\gamma}(t)) \\
&\geq 1 - \exp(-\frac{a_j^2 C_{j,\gamma}^{\text{left},2}}{2\sigma_{1,\text{left}}^2})
\end{aligned} \tag{4.5}$$

Which can be achieved by applying Borell-TIS Inequality because the process $-X'_\gamma(t)$ is zero-mean for every t. For $I_{j,\gamma}^{\text{right}}$, we can get similar result, combine them all. We can get the result.

(2) The probability that $f_\gamma(t)$ has no local maxima in $I_{j,\gamma}^{\text{mode}}$ is less than the probability that $f'_\gamma(\tau_j - \delta) \le 0$ or $f'_\gamma(\tau_j + \delta) \ge 0$, then the probability is bounded above by:

$$\begin{aligned}
&P(\#\{t \in \tilde{T} \cap I_{j,\gamma}^{\text{mode}}\} = 0) \\
&\le P(f'_\gamma(\tau_j - \delta) \le 0) + P(f'_\gamma(\tau_j + \delta) \ge 0) \\
&= \Phi(-\frac{f'_\gamma(\tau_j - \delta)}{\sigma_1(\tau_j - \delta)}) + \Phi(\frac{f'_\gamma(\tau_j + \delta)}{\sigma_1(\tau_j + \delta)}) \\
&= 1 - \Phi(\frac{f'_\gamma(\tau_j - \delta)}{\sigma_1(\tau_j - \delta)}) + 1 - \Phi(-\frac{f'_\gamma(\tau_j + \delta)}{\sigma_1(\tau_j + \delta)}) \\
&\le 2 - 2\Phi(\frac{a_j C_{j,\gamma}^{\text{mode}}}{\sigma_{1,\text{mode}}})
\end{aligned} \tag{4.6}$$

The inequality holds because $f'_\gamma(t) \sim N(a_j \eta'_{j,\gamma}(t), \sigma_1(t))$ for all t.

On the other hand, the probability that $f'_\gamma(t)$ has at least two local maxima in $I_{j,\gamma}^{\text{mode}}$ is less than the probability that $f''_\gamma(t) > 0$ for some $t \in I_{j,\gamma}^{\text{mode}}$. That is:

$$\begin{aligned}
&P(\#\{t \in \tilde{T} \cap I_{j,\gamma}^{\text{mode}}\} \ge 2) \\
&\le P(\sup_{I_{j,\gamma}^{\text{mode}}} f''_\gamma(t) > 0) \\
&\le P(\sup_{I_{j,\gamma}^{\text{mode}}} X''_\gamma(t) > \inf_{I_{j,\gamma}^{\text{mode}}} -a_j \eta''_{j,\gamma}(t)) \\
&\le \exp(-\frac{a_j^2 D_{j,\gamma}^{\text{mode},2}}{2\sigma_{2,\text{mode}}^2})
\end{aligned} \tag{4.7}$$

The probability that $f_\gamma(t)$ has exact one local maxima in $I_{j,\gamma}^{\text{mode}}$ can be calculated from the above two inequalities:

$$\begin{aligned}
&P(\#\{t \in \tilde{T} \cap I_{j,\gamma}^{\text{mode}}\} = 1) \\
&= 1 - P(\#\{t \in \tilde{T} \cap I_{j,\gamma}^{\text{mode}}\} \ge 2) - P(\#\{t \in \tilde{T} \cap I_{j,\gamma}^{\text{mode}}\} = 0) \\
&\ge 2\Phi(\frac{a_j C_{j,\gamma}}{\sigma_1}) - 1 - \exp(-\frac{a_j^2 D_{j,\gamma}^{\text{mode},2}}{2\sigma_{2,\text{mode}}^2})
\end{aligned} \tag{4.8}$$

(3) The probability that no local maxima of $f_\gamma(t)$ in $I_{j,\gamma}^{\text{mode}}$ exceed the threshold u is less than the probability that $f_\gamma(t)$ is below u anywhere in $I_{j,\gamma}^{\text{mode}}$, so it is bounded above by

$\Phi(u - a_j M_j)$. On the other hand, the probability that more than one local maxima of $y(t)$ in I_j^{mode} exceed u is less than the probability that there exist more than one local maximum, which is bounded by 4.8. Combine them all, we can get the result. □

Lemma 4.1.3. *Assume the model of section 2.1, For $\tilde{T}$ is the set of candidate peaks, let $\tilde{m}_{1,\gamma} = \#\{\tilde{T} \cap \mathbb{S}_{1,\gamma}\}$ be the number of local maxima in the set $\mathbb{S}_{1,\gamma}$, and $W_\gamma(u) = \#\{t \in \tilde{T} \cap \mathbb{S}_{1,\gamma} : f_\gamma(t) > u\}$ be the number of local maxima in $\mathbb{S}_{1,\gamma}$ above threshold u. Under conditions (C1) and (C2):*

(1) The probability that $f_\gamma(t)$ has any local maxima in the transition region $\mathbb{T}_\gamma$ tends to 0.

$$P(\#\{t \in \tilde{T} \cap \mathbb{T}_\gamma\} \geq 1) \to 0. \tag{4.9}$$

(2) The probability to get exact J local maxima in the set $\mathbb{S}_{1,\gamma}$,

$$P(\tilde{m}_{1,\gamma} = J) = P(\#\{t \in \tilde{T} \cap \mathbb{S}_{1,\gamma}\} = J) \to 1. \tag{4.10}$$

(3) The probability to get exact J local maxima in the set $\mathbb{S}_{1,\gamma}$ that exceed any fixed threshold u,

$$P[W_\gamma(u) = J] = P[\#\{t \in \tilde{T} \cap \mathbb{S}_{1,\gamma} : f_\gamma(t) > u\} = J] \to 1. \tag{4.11}$$

(4) $W_\gamma(u)/\tilde{m}_{1,\gamma} \to 1$ in probability.

Proof. (1) First, we can get $\mathbb{T}_\gamma = \bigcup_{j=1}^{J} T_{j,\gamma}$, where $T_{j,\gamma}$=$S_{j,\gamma} \backslash S_j$ is a subset of $I_{j,\gamma}^{\text{side}}$. So we have $\mathbb{T}_\gamma$ is a subset of $\bigcup_{j=1}^{J} I_{j,\gamma}^{\text{side}}$. Then we have:

$$\begin{aligned} P(\#\{t \in \tilde{T} \cap \mathbb{T}_\gamma\} \geq 1) &\leq P(\#\{t \in \tilde{T} \cap \bigcup_{j=1}^{J} I_{j,\gamma}^{\text{side}}\} \geq 1) \\ &= P(\bigcup_{j=1}^{J} \#\{t \in \tilde{T} \cap I_{j,\gamma}^{\text{side}}\} \geq 1) \\ &\leq \sum_{j=1}^{J} [1 - P(\#\{t \in \tilde{T} \cap I_{j,\gamma}^{\text{side}}\} = 0)] \end{aligned} \tag{4.12}$$

Under condition (C2), $a_j \to \infty$, plug in the first result of lemma 4.1.2, the result can be obtained directly.

(2) The probability is larger than get one local maximum in $I_{j,\gamma}^{\text{mode}}$ and 0 in $I_{j,\gamma}^{\text{side}}$ for all j. That is:

$$\begin{aligned} &P(\#\{t \in \tilde{T} \cap \mathbb{S}_{1,\gamma}\} = J) \geq P(\cap_{j=1}^{J} \#\{t \in \tilde{T} \cap I_{j,\gamma}^{\text{mode}}\} = 1 \bigcap \#\{t \in \tilde{T} \cap I_{j,\gamma}^{\text{side}}\} = 0) \\ &\geq 1 - \sum_{j=1}^{J} [1 - P(\#\{t \in \tilde{T} \cap I_{j,\gamma}^{\text{mode}}\} = 1 \bigcap \#\{t \in \tilde{T} \cap I_{j,\gamma}^{\text{side}}\} = 0)] \\ &\geq 1 - \sum_{j=1}^{J} [2 - P(\#\{t \in \tilde{T} \cap I_{j,\gamma}^{\text{mode}}\} = 1) - P(\#\{t \in \tilde{T} \cap I_{j,\gamma}^{\text{side}}\} = 0)] \end{aligned} \tag{4.13}$$

Plug in the results in lemma 4.1.2, under condition (C2), we can get the result.

(3) The proof is very similar to the second part.

(4) With the proof of (2) and (3), the result can be obtained directly. □

Theorem 4.1.4. *Suppose that Algorithm is applied with the BH threshold $\tilde{u}_{BH}$. Then, under conditions(C1) and (C2),*

$$\limsup \mathit{FDR}(\tilde{u}_{BH}) \leq \alpha \tag{4.14}$$

Proof. : Let $\tilde{G}_k(u) = \left(\sum_{n=1}^{N} \#\{t \in \tilde{T}_n \cap L_k : f_{n,\gamma}(t) > u\}\right) / \left(\sum_{n=1}^{N} \#\{t \in \tilde{T}_n \cap L_k\}\right)$ be the empirical marginal right cdf of $f_\gamma(t)$ given $t \in \tilde{T}_n$ and t is located in L_k of trial n , where $f_{n,\gamma}(t)$ is the standardized process for trial n and $\tilde{T}_n$ is the candidate peaks for trial n. Now we assume $K = 1$, which means the whole support are seen as one region. Then we have $\tilde{G}(u) = \left(\sum_{n=1}^{N} \#\{t \in \tilde{T}_n : f_{n,\gamma}(t) > u\}\right) / \left(\sum_{n=1}^{N} \#\{t \in \tilde{T}_n\}\right)$ be the empirical marginal right cdf of $f_\gamma(t)$ given $t \in \tilde{T}$. Then the BH threshold for trial n, $\tilde{u}_{\text{BH},n}$ satisfies $\alpha\tilde{G}(\tilde{u}_{BH,n}) = p\alpha/\widetilde{m}_n = F_\gamma(\tilde{u}_{BH,n})$, where p is the largest index for which ith smallest p-value is less than $\frac{i\alpha}{\widetilde{m}_n}$, where $\widetilde{m}_n$ is the number of p-values for trial n. Therefore, $\tilde{u}_{BH,n}$ is the largest u that solves the equation:

$$\alpha\tilde{G}(u) = F_\gamma(u) \tag{4.15}$$

The strategy is to solve equation (4.15) in the limit when $a, N \to \infty$, where $a = \inf a_j$. We first find the limit of $\tilde{G}(u)$. Define:

$$\begin{aligned} V_{n,\gamma}(u) &= \#\{t \in \tilde{T}_n \cap \mathbb{S}_{0,\gamma} : f_{n,\gamma}(t) > u\} \\ W_{n,\gamma}(u) &= \#\{t \in \tilde{T}_n \cap \mathbb{S}_{1,\gamma} : f_{n,\gamma}(t) > u\} \\ R_{n,\gamma}(u) &= V_{n,\gamma}(u) + W_{n,\gamma}(u) \end{aligned} \tag{4.16}$$

$$\begin{aligned} \tilde{G}(u) &= \frac{\sum_{n=1}^{N} R_{n,\gamma}(u)}{\sum_{n=1}^{N} \widetilde{m}_n} = \frac{\sum_{n=1}^{N} V_{n,\gamma}(u)}{\sum_{n=1}^{N} \widetilde{m}_n} + \frac{\sum_{n=1}^{N} W_{n,\gamma}(u)}{\sum_{n=1}^{N} \widetilde{m}_n} \\ &= \frac{\sum_{n=1}^{N} V_{n,\gamma}(u)}{\sum_{n=1}^{N} \widetilde{m}_{0,n,\gamma}} \frac{\sum_{n=1}^{N} \widetilde{m}_{0,n,\gamma}}{\sum_{n=1}^{N} \widetilde{m}_{0,n,\gamma} + \sum_{n=1}^{N} \tilde{m}_{1,n,\gamma}} \\ &+ \frac{\sum_{n=1}^{N} W_{n,\gamma}(u)}{\sum_{n=1}^{N} \widetilde{m}_{1,n,\gamma}} \frac{\sum_{n=1}^{N} \widetilde{m}_{1,n,\gamma}}{\sum_{n=1}^{N} \tilde{m}_{0,n,\gamma} + \sum_{n=1}^{N} \tilde{m}_{1,n,\gamma}} \end{aligned} \tag{4.17}$$

where $\widetilde{m}_n = \#\{t \in \tilde{T}_n\}$, the total number of local maxima of smoothed and standardized trial n, $\tilde{m}_{0,n,\gamma} = \#\{t \in \tilde{T}_n \cap \mathbb{S}_{0,\gamma}\}$ and $\tilde{m}_{1,n,\gamma} = \#\{t \in \tilde{T}_n \cap \mathbb{S}_{1,\gamma}\}$.

By the weak law of large numbers:

$$\frac{\sum_{n=1}^{N} \tilde{m}_{0,n,\gamma}}{\sum_{n=1}^{N} \tilde{m}_{0,n,\gamma} + \sum_{n=1}^{N} \tilde{m}_{1,n,\gamma}} = \frac{\sum_{n=1}^{N} \tilde{m}_{0,n,\gamma}/N}{\sum_{n=1}^{N} \tilde{m}_{0,n,\gamma}/N + \sum_{n=1}^{N} \tilde{m}_{1,n,\gamma}/N} \to \frac{E[\tilde{m}_{0,n,\gamma}]}{E[\tilde{m}_{0,n,\gamma}] + E[\tilde{m}_{1,n,\gamma}]} \tag{4.18}$$

As $N \to \infty$. Replacing the limits in 4.17, we obtain:

$$\tilde{G}(u) \to F_\gamma(u) \frac{E[\tilde{m}_{0,n,\gamma}]}{E[\tilde{m}_{0,n,\gamma}] + E[\tilde{m}_{1,n,\gamma}]} + \frac{E[\tilde{m}_{1,n,\gamma}]}{E[\tilde{m}_{0,n,\gamma}] + E[\tilde{m}_{1,n,\gamma}]} \tag{4.19}$$

By 4.15, we can get the deterministic solution:

$$F_\gamma(u^*_{BH,n}) = \frac{\alpha E[\tilde{m}_{1,n,\gamma}]}{E[\tilde{m}_{1,n,\gamma}] + E[\tilde{m}_{0,n,\gamma}](1-\alpha)} \tag{4.20}$$

The FDR at the threshold $u^*_{BH,n}$ is bounded by:

$$\begin{aligned} \text{FDR}(u^*_{BH,n}) &\le P(W_n(u^*_{BH,k}) \le (J-1)) + \frac{\mathbb{E}[V_n(u^*_{BH,n})]}{\mathbb{E}[V_n(u^*_{BH,n})] + J} \\ &= P(W_n(u^*_{BH,k}) \le (J-1)) \\ &+ \frac{\mathbb{E}[V_{n,\gamma}(u^*_{BH,n})] + \mathbb{E}[\#\{t \in \tilde{T}_n \cap T_{n,\gamma} : y_\gamma(t) > u^*_{BH,n}\}]}{\mathbb{E}[V_{n,\gamma}(u^*_{BH,n})] + \mathbb{E}[\#\{t \in \tilde{T}_n \cap T_{n,\gamma} : y_\gamma(t) > u^*_{BH,n}\}] + J} \end{aligned} \tag{4.21}$$

Where we have split $V_n(u^*_{BH,n})$ into the reduced null region $S_{0,\gamma}$ and the transition region $\mathbb{T}_\gamma = S_0 \backslash S_{0,\gamma}$ From the lemma and outcomes before:

$$0 \le \mathbb{E}[\#\{t \in \tilde{T}_n \cap \mathbb{T}_{n,\gamma} : y_\gamma(t) > u^*_{BH,n}\}] \le \mathbb{E}[\#\{t \in \tilde{T}_n \cap \mathbb{T}_{n,\gamma}\}] \to 0 \tag{4.22}$$

The remaining term can be written as:

$$\begin{aligned} &\frac{\mathbb{E}[V_{n,\gamma}(u^*_{BH,n})]}{\mathbb{E}[V_{n,\gamma}(u^*_{BH,n})] + J} \\ &= \frac{F_\gamma(u^*_{BH,n})\mathbb{E}[\tilde{m}_{0,n,\gamma}]}{F_\gamma(u^*_{BH,n})\mathbb{E}[\tilde{m}_{0,n,\gamma}] + J} \\ &= \alpha \frac{\mathbb{E}[\tilde{m}_{0,n,\gamma}]\mathbb{E}[\tilde{m}_{1,n,\gamma}]}{\alpha\mathbb{E}[\tilde{m}_{0,n,\gamma}]\mathbb{E}[\tilde{m}_{1,n,\gamma}] + J(\mathbb{E}[\tilde{m}_{1,n,\gamma}] + \mathbb{E}[\tilde{m}_{0,n,\gamma}]) - \alpha J\mathbb{E}[\tilde{m}_{0,n,\gamma}]} \end{aligned} \tag{4.23}$$

From the lemma before, we know that $P(\widetilde{m}_{1,n,\gamma} = J) \to 1$, and because L is limited, so $\widetilde{m}_{1,n,\gamma} < \infty$, then we can get $\mathbb{E}[\tilde{m}_{1,n,\gamma}] = J$. Plug in, we can get:

$$\frac{E[V_{n,\gamma}(u^*_{BH,n})]}{E[V_{n,\gamma}(u^*_{BH,n})] + J} \le \alpha \tag{4.24}$$

Combine all, we can get $\text{FDR}(u^*_{BH,n}) \le \alpha$ for all n. Because $F_\gamma(u)$ is continuous, we can say $\limsup \text{FDR}(\tilde{u}_{\text{BH}}) \le \alpha$. □

4.1.2 Power Consistency

First, explain the lemma 2.3.4. If the standardized and smoothed process $f_\gamma(t)$ satisfies $\sup_{t \in S_0 \cap S_{1,\gamma}} [\frac{\mu_\gamma(t)}{\sqrt{\text{var}(z_\gamma(t))}}] < \sup_{t \in S_1} [\frac{\mu_\gamma(t)}{\sqrt{\text{var}(z_\gamma(t))}}]$, then the maximum value of standardized and smoothed signal in the support of signal is larger than the maximum value of standardized and smoothed signal in the transition region. From the proof before, the local maxima of $f_\gamma(t)$ will asymptotically locates in the support of signal with probability 1.

Now the proof of theorem 2.44:

Proof. For the random threshold $\tilde{u}_{\text{BH}}$ and arbitrary $\delta > 0$, we have

$$\begin{aligned} & P(\#\left\{t \in \tilde{T}(\tilde{u}_{\text{BH}}) \cap S_j\right\} \geq 1) \\ =& P(\#\left\{t \in \tilde{T}(\tilde{u}_{\text{BH}}) \cap S_j\right\} \geq 1, |\tilde{u}_{\text{BH}} - u^*_{\text{BH}}| \leq \delta) \\ +& P(\#\left\{t \in \tilde{T}(\tilde{u}_{\text{BH}}) \cap S_j\right\} \geq 1, |\tilde{u}_{\text{BH}} - u^*_{\text{BH}}| > \delta) \end{aligned} \tag{4.25}$$

From the proof of FDR, we have:

$$P(\#\left\{t \in \tilde{T}(\tilde{u}_{\text{BH}}) \cap S_j\right\} \geq 1, |\tilde{u}_{\text{BH}} - u^*_{\text{BH}}| > \delta) \leq P(|\tilde{u}_{\text{BH}} - u^*_{\text{BH}}| > \delta) = 0 \tag{4.26}$$

Then:

$$\begin{aligned} & P(\#\left\{t \in \tilde{T}(\tilde{u}_{\text{BH}}) \cap S_j\right\} \geq 1) \\ =& P(\#\left\{t \in \tilde{T}(\tilde{u}_{\text{BH}}) \cap S_j\right\} \geq 1, |\tilde{u}_{\text{BH}} - u^*_{\text{BH}}| \leq \delta) \\ \geq& P(\#\left\{t \in \tilde{T}(u^*_{\text{BH}} + \delta) \cap S_j\right\} \geq 1, |\tilde{u}_{\text{BH}} - u^*_{\text{BH}}| \leq \delta) \\ =& P(\#\left\{t \in \tilde{T}(u^*_{\text{BH}} + \delta) \cap S_j\right\} \geq 1) \end{aligned} \tag{4.27}$$

Similarly, we can also get:

$$\begin{aligned} & P(\#\left\{t \in \tilde{T}(\tilde{u}_{\text{BH}}) \cap S_j\right\} \geq 1) \\ \leq& P(\#\left\{t \in \tilde{T}(u^*_{\text{BH}} - \delta) \cap S_j\right\} \geq 1, |\tilde{u}_{\text{BH}} - u^*_{\text{BH}}| \leq \delta) \\ =& P(\#\left\{t \in \tilde{T}(u^*_{\text{BH}} - \delta) \cap S_j\right\} \geq 1) \end{aligned} \tag{4.28}$$

Because δ is arbitrary, we let $\delta \to 0$. Then by the lemma before:

$$\begin{aligned} P(\#\left\{t \in \tilde{T}(u^*_{\text{BH}} + \delta) \cap S_j\right\} \geq 1) \to 1 \\ P(\#\left\{t \in \tilde{T}(u^*_{\text{BH}} - \delta) \cap S_j\right\} \geq 1) \to 1 \end{aligned} \tag{4.29}$$

So $\text{Power}_j(\tilde{u}_{\text{BH}}) \to 1$. So that $\text{Power}(\tilde{u}_{\text{BH}}) \to 1$ □

Chapter 5

APPLICATION OF THE ALGORITHM CHANGE POINTS

5.1 Introduction

This part is an application of the theory discussed before. A new algorithm named 'differential Smoothing and TEsting of Maxima/Minima'(dSTEM) in previous work to detect the change points is introduced in the work of Cheng, He and Schwartzman [11]. In that work, the noise is assumed to be stationary, in this project. We assume the noise is non-stationary and try to detect the change points using the non-stationary theory.

5.2 The Model

We also use the signal-plus-noise model in this section:

$$y(t) = \mu(t) + z(t), \quad t \in R, \tag{5.1}$$

where the signal $\mu(t)$ is a step function can be written as:

$$\mu(t) = \sum_{j=0}^{\infty} a_j h_j(t), \qquad a_j \in R\backslash\{0\},$$

where $h_j = \mathbb{1}(t \geq v_j)$ for $v_j \in R$. Finding the change points v_j is our target. We assume

$$a = \inf_j |a_j| > 0 \quad \text{and} \quad d = \inf_j |v_j - v_{j-1}| > 0 \tag{5.2}$$

With the assumptions, the jump of change points is large enough to be detected in and they will not be close to each other.

Convolving the process 5.1 with the kernel $w_\gamma(t)$ can generate the smoothed process:

$$y_\gamma(t) = \omega_\gamma(t) * y(t) = \int_{-\infty}^{\infty} \omega_\gamma(t-s) y(s) ds = \mu_\gamma(t) + z_\gamma(t), \tag{5.3}$$

the smoothed signal and smoothed noise are defined as

$$\mu_\gamma(t) = \omega_\gamma(t) * \mu(t) = \sum_{j=0}^{\infty} a_j h_{j,\gamma}(t), \qquad z_\gamma(t) = \omega_\gamma(t) * z(t) \tag{5.4}$$

and the smoothed indicator function can be written as:

$$h_{j,\gamma}(t) = \omega_\gamma(t) * h_j(t) \tag{5.5}$$

The smoothed noise $z_\gamma(t)$ by 5.4 is a non-stationary Gaussian process whose mean is 0 and can be differentiated four times.

Consider the derivative of the smoothed observed process, the work of Cheng, He and Schwartzman[11]:

$$y'_\gamma(t) = \omega'_\gamma(t) * y(t) = \int_R \omega'_\gamma(t-s)y(s)ds = \mu'_\gamma(t) + z'_\gamma(t) \tag{5.6}$$

the derivatives of the smoothed signal and smoothed noise can be written as:

$$\mu'_\gamma(t) = \omega'_\gamma(t) * \mu(t) = \sum_{j=1}^{\infty} a_j h'_{j,\gamma}(t) \text{ and } z'_\gamma(t) = \omega'_\gamma(t) * z(t) \tag{5.7}$$

The core idea for the algorithm is the finding:

$$\begin{aligned} h'_{j,\gamma}(t) &= \int_R \omega'_\gamma(t-s)h_j(s)ds = \int_R \omega'_\gamma(s)h_j(t-s)ds \\ &= \int_R \omega'_\gamma(s)\mathbb{1}(t-s \geq v_j)ds = \int_{-\infty}^{t-v_j} \omega'_\gamma(s)ds = \omega_\gamma(t-v_j) \end{aligned} \tag{5.8}$$

The derivative of smoothed process:

$$\mu'_\gamma(t) = \sum_{j=0}^{\infty} a_j h'_{j,\gamma}(t) = \sum_{j=0}^{\infty} a_j \omega_\gamma(t-v_j) \tag{5.9}$$

is a sequence of unimodal peaks. Then we can transform the problem of detecting change points in $y_\gamma(t)$ to finding the local extrema in $y'_\gamma(t)$. The figure 5.2 displays the main idea of this method, that is, transform the problem of detecting the change points to the problem of detecting the local extrema in the first derivatives. However, a local extrema can also be generated from the noise. Then, multiple testing is needed based on the peak height density of $z'_\gamma(t)$ to detect the true change points.

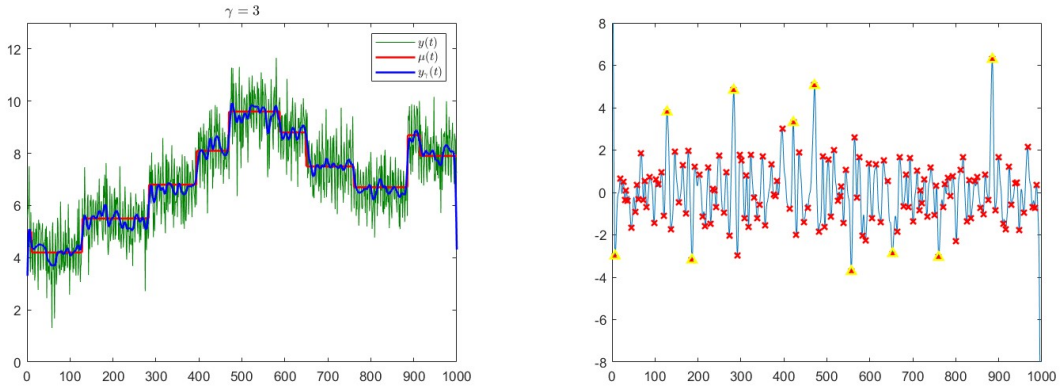

Figure 5.1: For the left plot, the green line is observed sequence $y(t)$, the red line is the original signal $\mu(t)$, the blue line is smoothed sequence $y_\gamma(t)$. For the right plot, the red crosses are local maxima detected, which are the candidate peaks. The yellow triangles are the detected change points after multiple testing

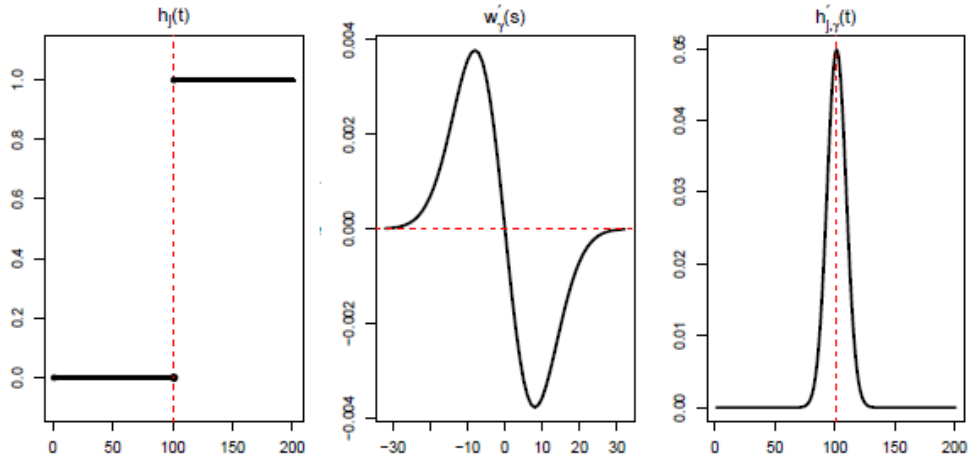

Figure 5.2: Following the notation, the left plot is the step function $h_j(t)$. The middle plot is $w'_\gamma(s)$. The right plot is $h'_{j,\gamma}(t)$. By doing this transformation, the change point detection problems is transformed to the peak detection problems.

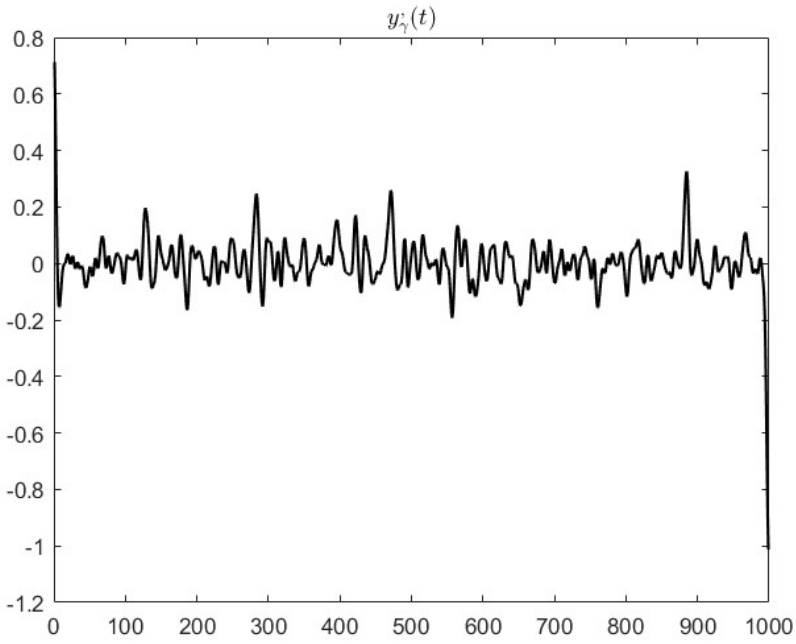

Figure 5.3: This black line is the differential kernel smoothed process. We can see there are many local extrema in this line, which is caused by both change points or noise. We will do the standardization in the next step

5.2.1 Algorithm

To detect the change points of step function, we can transform the problem to finding the peaks of a process. The algorithm has following steps:

1.**Differential kernel smoothing**: In this step, we achieve the process $y'_\gamma(t)$. The main idea of this step is illustrated in figure 5.2.

2.**Standardization**: Divide the kernel smoothed process $y'_\gamma(t)$ with the standard deviation of the differential kernel smoothed noise $z'_\gamma(t)$ and get the new process $f_\gamma(t)$.

$$f_\gamma(t) = \frac{\mu'_\gamma(t)}{\sqrt{\text{var}(z'_\gamma(t))}} + \frac{z'_\gamma(t)}{\sqrt{\text{var}(z'_\gamma(t))}} \tag{5.10}$$

And we define $X_\gamma(t) = \frac{z'_\gamma(t)}{\sqrt{\text{var}(z'_\gamma(t))}}$ as the smoothed and standardized noise.

3.**Candidate peaks**: Find the set of local extrema of $y'_\gamma(t)$ in $[0, L]$, denoted by $\tilde{T}_\gamma$ =

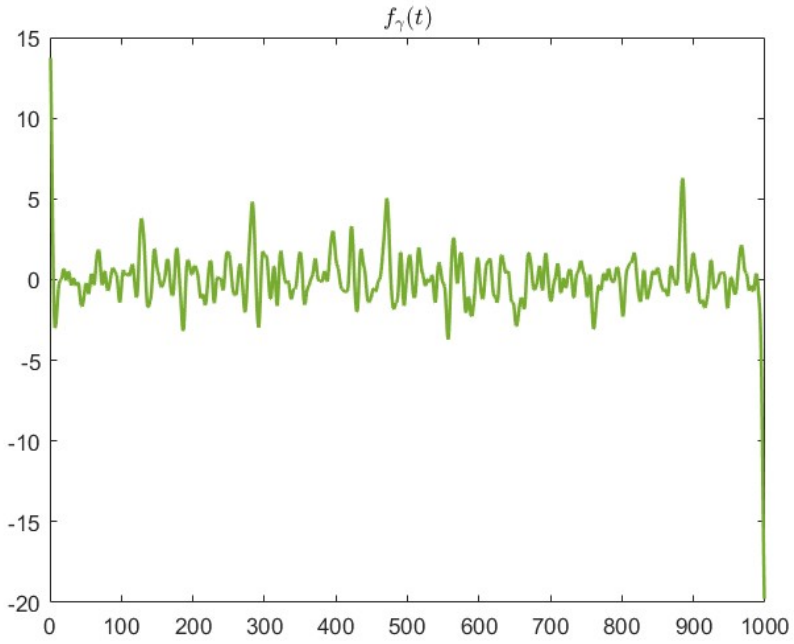

Figure 5.4: This green line is the standardized process. We will calculate the p-values for the local extrema in this process

$\tilde{T}_\gamma^+ \cup \tilde{T}_\gamma^-$, where

$$\tilde{T}_\gamma^+ = \left\{ t \in [0, L] : f'_\gamma(t) = \frac{df_\gamma(t)}{dt} = 0,\ f''_\gamma(t) = \frac{d^2 f_\gamma(t)}{dt^2} < 0 \right\}$$
$$\tilde{T}_\gamma^- = \left\{ t \in [0, L] : f'_\gamma(t) = \frac{df_\gamma(t)}{dt} = 0,\ f''_\gamma(t) = \frac{d^2 f_\gamma(t)}{dt^2} > 0 \right\}$$

4.**P-values**: For each $t \in \tilde{T}_\gamma^+$ compute the p-values $p_\gamma(t)$ for testing the (conditional) hypothesis:

$$H_0(t) : \{\mu'(s) = 0 \text{ for all } s \in (t-b, t+b)\} \text{ vs}$$
$$H_A(t) : \{\mu(s+) > \mu(s-) \text{ for some } s \in (t-b, t+b)\}$$

where $\mu(s+) = \lim_{x \to s+} \mu(x)$ and $\mu(s-) = \lim_{x \to s-} \mu(x)$ are the right and left limit of μ at s and for each $t \in \tilde{T}_\gamma^-$, compute the p-values $p_\gamma(t)$ for testing the (conditional) hypothesis:

$$H_0(t) : \{\mu'(s) = 0 \text{ for all } s \in (t-b, t+b)\} \text{ vs}$$
$$H_A(t) : \{\mu(s+) < \mu(s-) \text{ for some } s \in (t-b, t+b)\}$$

where $b > 0$ is a tolerance parameter because detecting the exact position of v_j is hard after two steps of transformations.

5.**Multiple testing**: Let $\tilde{m}$ be the number of local extrema in $\tilde{T}_\gamma$. Apply BH procedure on $\tilde{m}$ p-values and define the local extrema as significant if their p-values are smaller than the threshold. The figure 5.1 shows the output of example.

5.2.2 P-values

Suppose that we observed the heights $f_\gamma(t)$ at the local extrema, the p-values can be computed as:

$$p_\gamma(t) = \begin{cases} F_\gamma(f'_\gamma(t)), & t \in \tilde{T}^+_\gamma \\ F_\gamma(-f'_\gamma(t)), & t \in \tilde{T}^-_\gamma \end{cases} \tag{5.11}$$

Where $F_\gamma(u)$ is the right cdf of $X_\gamma(t)$. As $X_\gamma(t)$ is a Gaussian process, the calculation of the distribution of $X_\gamma(t)$ is provided in chapter 2. One thing to notice is that, the change point problem uses the first derivative of $z_\gamma(t)$ instead of $z_\gamma(t)$ itself, one example is provided in the following section.

5.2.3 Error Definitions

Assuming the model is defined as 5.1, then the signal region is defined as $\mathbb{S}_1^b = \cup_{j=1}^J (v_j - b, v_j + b)$ and the null region is defined as $\mathbb{S}_0^b = [0, L] \backslash \mathbb{S}_1^b$. For $u > 0$, let $\tilde{T}_\gamma = \tilde{T}^+_\gamma \cup \tilde{T}^-_\gamma$, where

$$\tilde{T}^+_\gamma(u) = \left\{ t \in [0, L] : f_\gamma(t) > u, f'_\gamma(t) = \frac{df_\gamma(t)}{dt} = 0,\ f''_\gamma(t) = \frac{d^2 f_\gamma(t)}{dt^2} < 0 \right\}$$
$$\tilde{T}^-_\gamma(u) = \left\{ t \in [0, L] : f_\gamma(t) < -u, f'_\gamma(t) = \frac{df_\gamma(t)}{dt} = 0,\ f''_\gamma(t) = \frac{d^2 f_\gamma(t)}{dt^2} > 0 \right\}$$

$\tilde{T}^+_\gamma(u)$ is the set of local maxima of $f_\gamma(t)$ above u and $\tilde{T}^-_\gamma(u)$ is the set of local minima of $f_\gamma(t)$ below $-u$. Then we can define the following notations:

$$\begin{aligned} R_\gamma(u) &= \#\left\{ t \in \tilde{T}^+_\gamma(u) \right\} + \#\left\{ t \in \tilde{T}^-_\gamma(u) \right\} \\ V_\gamma(u; b) &= \#\left\{ t \in \tilde{T}^+_\gamma(u) \cap \mathbb{S}_0^b \right\} + \#\left\{ t \in \tilde{T}^-_\gamma(u) \cap \mathbb{S}_0^b \right\} \end{aligned} \tag{5.12}$$

as the number of all detected and falsely detected change points with the threshold u. The two are defined as zero if $\tilde{T}_\gamma(u)$ contains no elements. We can also define the FDR as the expected proportion of falsely detected change points as follows:

$$\mathrm{FDR}_\gamma(u;b) = \mathrm{E}\left\{\frac{V_\gamma(u;b)}{R_\gamma(u)\vee 1}\right\} \tag{5.13}$$

at threshold u and tolerance parameter b.

5.2.4 Control of FDR

BH procedure is applied in the algorithm. For a fixed $\alpha \in (0,1)$, let k be the largest index for which the ith smallest p-value is less than $i\alpha/\tilde{m}_\gamma$. Then the null hypothesis $\mathcal{H}_0(t)$ at $t \in \tilde{T}_\gamma$ is rejected if

$$P_\gamma(t) < \frac{k\alpha}{\tilde{m}_\gamma} \qquad \Longleftrightarrow \qquad \begin{cases} f_\gamma(t) > \tilde{u}_{\mathrm{BH}} = F_\gamma^{-1}(\frac{k\alpha}{\tilde{m}_\gamma}) & t \in \tilde{T}_\gamma^+ \\ f_\gamma(t) < -\tilde{u}_{\mathrm{BH}} = -F_\gamma^{-1}(\frac{k\alpha}{\tilde{m}_\gamma}) & t \in \tilde{T}_\gamma^- \end{cases} \tag{5.14}$$

where $k\alpha/\tilde{m}_\gamma$ is defined as 1 if $\tilde{m}_\gamma = 0$. $\tilde{u}_{\mathrm{BH}}$ is random, we define FDR in the BH procedure as

$$\mathrm{FDR}_{\mathrm{BH},\gamma}(b) = \mathbb{E}\left\{\frac{V_\gamma(\tilde{u}_{\mathrm{BH}};b)}{R_\gamma(\tilde{u}_{\mathrm{BH}})\vee 1}\right\} \tag{5.15}$$

Define the following conditions:

(C_1) The assumptions of the 5.1 hold.

(C_2) The number of trials $N \to \infty$ and $a \to \infty$.

Theorem 5.2.1. *Suppose that algorithm is applied with the random threshold $\tilde{u}_{BH}$. Then under conditions* $(\mathrm{C1})$ *and* $(\mathrm{C2})$.

$$\limsup \mathrm{FDR}_{\mathrm{BH},\gamma}(b) \le \alpha \tag{5.16}$$

The proof of theorem is similar to the proof in chapter 4.

5.2.5 Power Consistency

The power of Algorithm is defined as the expected fraction of truly detected change points

$$\begin{aligned}&\text{Power}_{\gamma}(u;b) = \frac{1}{J}\sum_{j=1}^{J}\text{Power}_{j,\gamma}(u;b)\\&= \mathbb{E}\left[\frac{1}{J}\left(\sum_{j\in I^{+}}\mathbb{1}(\tilde{T}_{\gamma}^{+}\cap(v_j-b,v_j+b)\neq\varnothing)+\sum_{j\in I^{-}}\mathbb{1}(\tilde{T}_{\gamma}^{-}\cap(v_j-b,v_j+b)\neq\varnothing)\right)\right]\end{aligned} \tag{5.17}$$

$\text{Power}_{j,\gamma}(u;b)$ is the probability of detecting peak j within a tolerance distance b.

$$\text{Power}_{j,\gamma}(u;b) = \begin{cases} \text{P}(\tilde{T}_{\gamma}^{+}\cap(v_j-b,v_j+b)\neq\varnothing), & j\in I^{+}\\ \text{P}(\tilde{T}_{\gamma}^{-}\cap(v_j-b,v_j+b)\neq\varnothing), & j\in I^{-}\end{cases} \tag{5.18}$$

where I^{+} is the set of increasing change points and I^{-} is the set of decreasing change points. The indicator function guarantees there will only be one significant local extrema is counted in a change points support, which is $(v_j - b, v_j + b)$, so the power will not be inflated. If we fix the γ and u, the power will increase by b because the support will be larger. The definition of $\text{Power}_{\text{BH},\gamma}(b)$ is defined:

$$\begin{aligned}&\text{Power}_{\text{BH},\gamma}(b)\\&= \mathbb{E}\left[\frac{1}{J}\left(\sum_{j\in I^{+}}\mathbb{1}(\tilde{T}_{\gamma}^{+}(\tilde{u}_{\text{BH}})\cap(v_j-b,v_j+b)\neq\varnothing)+\sum_{j\in I^{-}}\mathbb{1}(\tilde{T}_{\gamma}^{-}(\tilde{u}_{\text{BH}})\cap(v_j-b,v_j+b)\neq\varnothing)\right)\right]\end{aligned} \tag{5.19}$$

Theorem 5.2.2. *Let conditions (C_1) and (C_1) hold, suppose Algorithm is applied with the random threshold $\tilde{u}_{BH}$, then*

$$\text{Power}_{\text{BH},\gamma}(\text{b}) \to 1 \tag{5.20}$$

The proof of this theorem is similar to that of chapter 4.

5.3 Example

We also use the noise function created before and the different thing is that we need to use the derivative of $z(t)$ to construct our new process instead of $z(t)$ itself:

Example 5.3.1. Consider the following non-stationary Gaussian process as our noise $z(t)$:

$$z(t) = cos(t) \cdot \xi + sin(t) \cdot dB(t) \tag{5.21}$$

where ξ is a standard Gaussian random variable, $dB(t)$ is white noise which is independent of ξ. From the assumption and transformation of the algorithm, we can get:

$$X_\gamma(t) = \frac{z'_\gamma(t)}{\sqrt{var(z'_\gamma(t))}} \tag{5.22}$$

Then we can calculate the parameters needed to calculate the height density:

$$\begin{aligned} X'_\gamma(t) &= \frac{z''_\gamma(t)\sqrt{var(z'_\gamma(t))} - (\sqrt{var(z'_\gamma(t))})' z'_\gamma(t)}{var(z'_\gamma(t))} \\ &= \frac{z''_\gamma(t)}{\sqrt{var(z'_\gamma(t))}} - \frac{z'_\gamma(t)[var(z'_\gamma(t))]'}{2[var(z'_\gamma(t))]^{\frac{3}{2}}} \end{aligned} \tag{5.23}$$

And:

$$\begin{aligned} X''_\gamma(t) = &\frac{z'''_\gamma(t)}{\sqrt{var(z'_\gamma(t))}} - \frac{z''_\gamma(t)[var(z'_\gamma(t))]'}{2(var(z'_\gamma(t)))^{\frac{3}{2}}} \\ &- \frac{2\{z''_\gamma(t)[var(z'_\gamma(t))]' + z'_\gamma(t)[var(z'_\gamma(t))]''\}[var(z'_\gamma(t))]^{\frac{3}{2}}}{4[var(z'_\gamma(t))]^3} \\ &+ \frac{3z'_\gamma(t)var(z'_\gamma(t))^{\frac{1}{2}}\{[var(z'_\gamma(t))]'\}^2}{4[var(z'_\gamma(t))]^3} \end{aligned} \tag{5.24}$$

$$var(z'_\gamma(t)) = \left(\int_{-\infty}^{\infty} \frac{cos(s)(s-t)}{\gamma^3}\phi(\frac{t-s}{\gamma})ds\right)^2 + \int_{-\infty}^{\infty} \frac{sin^2(s)(s-t)^2}{\gamma^6}\phi^2(\frac{s-t}{\gamma})ds \tag{5.25}$$

$$\begin{aligned} [var(z'_\gamma(t))]' =& 2\int_{-\infty}^{\infty} \frac{cos(s)(s-t)}{\gamma^3}\phi(\frac{t-s}{\gamma})ds \int_{-\infty}^{\infty} \frac{cos(s)[(s-t)^2-\gamma^2]}{\gamma^5}\phi(\frac{t-s}{\gamma})ds \\ &+ \int_{-\infty}^{\infty} \frac{2sin^2(s)(s-t)[(s-t)^2-\gamma^2]}{\gamma^8}\phi^2(\frac{t-s}{\gamma})ds \end{aligned} \tag{5.26}$$

$$
\begin{aligned}
[var(z'_\gamma(t))]'' =& 2\Big(\int_{-\infty}^{\infty} \frac{cos(s)[(s-t)^2-\gamma^2]}{\gamma^5}\phi(\frac{t-s}{\gamma})ds\Big)^2 \\
&+2\int_{-\infty}^{\infty} \frac{cos(s)(s-t)}{\gamma^3}\phi(\frac{t-s}{\gamma})ds \\
&\times \int_{-\infty}^{\infty} \frac{cos(s)(s-t)[(s-t)^2-3\gamma^2]}{\gamma^7}\phi(\frac{t-s}{\gamma})ds \\
&+\int_{-\infty}^{\infty} \frac{2sin^2(s)[\gamma^2-3(s-t)^2]}{\gamma^8}\phi^2(\frac{t-s}{\gamma})ds \\
&+\int_{-\infty}^{\infty} \frac{4sin^2(s)(s-t)^2[(s-t)^2-\gamma^2]}{\gamma^{10}}\phi^2(\frac{t-s}{\gamma})ds
\end{aligned}
\tag{5.27}
$$

Then calculate the λ_1, λ_2 and λ_1':

$$
\begin{aligned}
X'_\gamma(t) &= \frac{z''_\gamma(t)}{\sqrt{var(z'_\gamma(t))}} - \frac{z'_\gamma(t)[var(z'_\gamma(t))]'}{2[var(z'_\gamma(t))]^{\frac{3}{2}}} \\
&= a(t)z'_\gamma(t) + b(t)z''_\gamma(t)
\end{aligned}
\tag{5.28}
$$

Where $a(t) = -\frac{[var(z'_\gamma(t))]'}{2[var(z'_\gamma(t))]^{\frac{3}{2}}}$ and $b(t) = \frac{1}{\sqrt{var(z'_\gamma(t))}}$, which are constants when t is fixed, then $var(X'_\gamma(t))$ can be calculated as:

$$
\begin{aligned}
var(X'_\gamma(t)) &= E[(a(t)z'_\gamma(t) + b(t)z''_\gamma(t))(a(t)z'_\gamma(t) + b(t)z''_\gamma(t))] \\
&= a^2(t)var(z'_\gamma(t)) + b^2(t)var(z''_\gamma(t)) + 2a(t)b(t)E(z'_\gamma(t)z''_\gamma(t))
\end{aligned}
\tag{5.29}
$$

where we can calculate:

$$
\begin{aligned}
var(z'_\gamma(t)) &= \Big(\int_{-\infty}^{\infty} \frac{cos(s)(s-t)}{\gamma^3}\phi(\frac{t-s}{\gamma})ds\Big)^2 + \int_{-\infty}^{\infty} \frac{sin^2(s)(s-t)^2}{\gamma^6}\phi^2(\frac{s-t}{\gamma})ds \\
var(z''_\gamma(t)) &= \Big(\int_{-\infty}^{\infty} \frac{cos(s)(s-t)}{\gamma^3}\phi(\frac{t-s}{\gamma})ds\Big)^2 + \int_{-\infty}^{\infty} \frac{sin^2(s)(s-t)^2}{\gamma^6}\phi^2(\frac{s-t}{\gamma})ds \\
E(z'_\gamma(t)z''_\gamma(t)) &= \Big(\int_{-\infty}^{\infty} \frac{cos(s)(s-t)}{\gamma^3}\phi(\frac{t-s}{\gamma})ds\Big)\Big(\int_{-\infty}^{\infty} \frac{cos(s)[(s-t)^2-\gamma^2]}{\gamma^5}\phi(\frac{t-s}{\gamma})ds\Big) \\
&\quad + \int_{-\infty}^{\infty} \frac{sin^2(s)(s-t)[(s-t)^2-\gamma^2]}{\gamma^8}\phi^2(\frac{s-t}{\gamma})ds
\end{aligned}
$$

They are all constants when t is fixed. So we can calculate $var(X'_\gamma(t))$ when t is fixed.

Now we calculate $var(X''_\gamma(t))$:

$$
X''_\gamma(t) = c(t)z'_\gamma(t) + d(t)z''_\gamma(t) + g(t)z'''_\gamma(t) \tag{5.30}
$$

where $c(t) = \frac{-2[var(z'_\gamma(t))''][var(z'_\gamma(t))]^{\frac{3}{2}} + 3var(z'_\gamma(t))^{\frac{1}{2}}[var(z'_\gamma(t))]'^2}{4[var(z'_\gamma(t))]^3}$,
$d(t) = -\frac{[var(z'_\gamma(t))]'}{2[var(z'_\gamma(t))]^{\frac{3}{2}}} - \frac{[var(z'_\gamma(t))]'}{2[var(z'_\gamma(t))]^3}$ and $g(t) = \frac{1}{\sqrt{var(z'_\gamma(t))}}$, which are constants when t is fixed, then $var(X''_\gamma(t))$ can be calculated as:

$$\begin{aligned} var(X''_\gamma(t)) &= E[(c(t)z'_\gamma(t) + d(t)z''_\gamma(t) + g(t)z'''_\gamma(t))(c(t)z'_\gamma(t) \\ &\quad + d(t)z''_\gamma(t) + g(t)z'''_\gamma(t))] \\ &= c^2(t)var(z'_\gamma(t)) + d^2(t)var(z''_\gamma(t)) + g^2(t)var(z'''_\gamma(t)) \\ &\quad + 2c(t)d(t)E(z'_\gamma(t)z''_\gamma(t)) + 2c(t)g(t)E(z'_\gamma(t)z'''_\gamma(t)) \\ &\quad + 2d(t)g(t)E(z''_\gamma(t)z'''_\gamma(t)) \end{aligned} \tag{5.31}$$

where we can calculate:

$$\begin{aligned} var(z'''_\gamma(t)) =& \Big(\int_{-\infty}^{\infty} \frac{cos(s)(s-t)[(s-t)^2 - 3\gamma^2]}{\gamma^7}\phi(\frac{t-s}{\gamma})ds\Big)^2 \\ &+ \int_{-\infty}^{\infty} \frac{sin^2(s)(s-t)^2[(s-t)^2 - 3\gamma^2]^2}{\gamma^{14}}\phi^2(\frac{t-s}{\gamma})ds \\ E(z'_\gamma(t)z'''_\gamma(t)) =& \Big(\int_{-\infty}^{\infty} \frac{cos(s)(s-t)}{\gamma^3}\phi(\frac{t-s}{\gamma})ds\Big) \\ &\times \Big(\int_{-\infty}^{\infty} \frac{cos(s)(s-t)[(s-t)^2 - 3\gamma^2]}{\gamma^7}\phi(\frac{t-s}{\gamma})ds\Big) \\ &+ \int_{-\infty}^{\infty} \frac{sin^2(s)(s-t)^2[(s-t)^2 - 3\gamma^2]}{\gamma^{10}}\phi^2(\frac{s-t}{\gamma})ds \\ E(z''_\gamma(t)z'''_\gamma(t)) =& \Big(\int_{-\infty}^{\infty} \frac{cos(s)[(s-t)^2 - \gamma^2]}{\gamma^5}\phi(\frac{t-s}{\gamma})ds\Big) \\ &\times \Big(\int_{-\infty}^{\infty} \frac{cos(s)(s-t)[(s-t)^2 - 3\gamma^2]}{\gamma^7}\phi(\frac{t-s}{\gamma})ds\Big) \\ &+ \int_{-\infty}^{\infty} \frac{sin^2(s)(s-t)[(s-t)^2 - \gamma^2][(s-t)^2 - 3\gamma^2]}{\gamma^{12}}\phi^2(\frac{s-t}{\gamma})ds \end{aligned}$$

They are all constants when t is fixed. So we can calculate $var(X''_\gamma(t))$ when t is fixed.

Now we calculate $E(X'_\gamma(t)X''_\gamma(t))$, from the definitions given before, we can get:

$$\begin{aligned} E(X'_\gamma(t)X''_\gamma(t)) &= E[(a(t)z'_\gamma(t) + b(t)z''_\gamma(t))(c(t)z'_\gamma(t) + d(t)z''_\gamma(t) + g(t)z'''_\gamma(t))] \\ &= a(t)c(t)var(z'_\gamma(t)) + b(t)d(t)var(z''_\gamma(t)) \\ &+ [a(t)d(t) + b(t)c(t)]E(z'_\gamma(t)z''_\gamma(t)) + a(t)g(t)E(z'_\gamma(t)z'''_\gamma(t)) \\ &+ b(t)g(t)E(z''_\gamma(t)z'''_\gamma(t)) \end{aligned} \tag{5.32}$$

With all the parameters calculated, the density can be calculated with the formula 2.16.

5.4 Simulation Studies

Simulations were performed to assess the performance of the algorithm with moderate signal strength a and finite repetitions N, where $L = 3000$, $J = 30$, the signal $\mu(t)$ is constructed as the model 5.1, where the signal strength $a = 1.5$, and the locations of change points were given as $\tau_j = (j - 1/2)L/J$, $j = 1, \ldots, J$, and sampled at integer values of t, the noise $z(t)$ was constructed as equation 5.21. The process repeats $N = 1000$ times to get the average FDR and corresponding power.

The smoothing kernel in the simulation is a truncated Gaussian density with $c = 3$:

$$w_\gamma(t) = (1/\gamma)\phi(t/\gamma)\mathbf{1}[-c\gamma, c\gamma]$$

We can estimate the noise parameter of $z(t)$ by calculating its first, second and third-order differences to approximate the corresponding first second and third derivatives. With the same smoothing kernel, the level α of BH procedures is 0.05 in this simulation.

Figure 5.5 displays the FDR levels. Error rates are kept below the nominal level of $\alpha = 0.05$ for bandwidths larger than 2 and large enough signal strength $a = 1.5$. The points above the nominal level occur because when the bandwidth is small, the smoothed process is not smooth enough to apply the algorithm effectively, similar to the simulation conducted

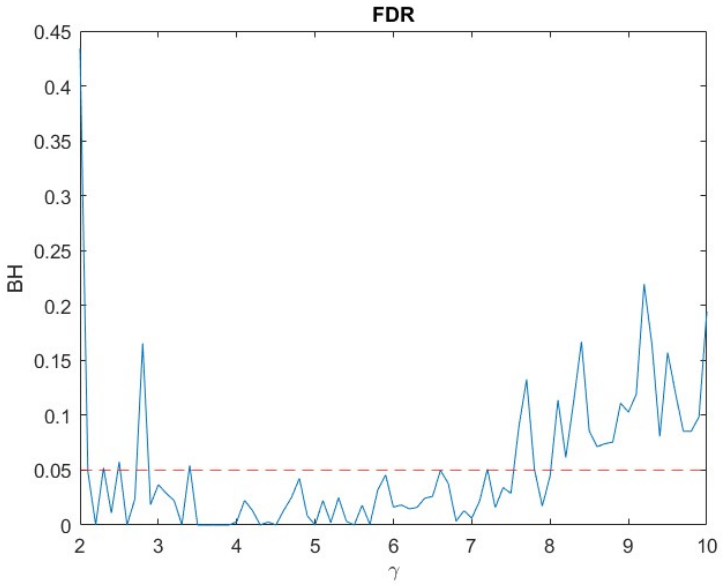

Figure 5.5: FDR of the BH procedure for different bandwidth

previously. When γ is large, that is, when $\gamma > 7$, the FDR is beyond the nominal level, that is because when γ is too large, the $\rho(t)$ used for calculating the p-values varies significantly. In certain regions, the $\rho(t)$ can be extremely small, approaching 0. As a result, when calculating the regional peak height density, the threshold for observation becomes too small, leading to an excessive number of falsely detected change points. Additionally, when the bandwidth is large, neighboring change points may interact with each other, leading to an increase in the FDR.

Figure 5.6 shows the realized power of BH procedures, we can see as the bandwidth γ increase, the power is approaching 1. When the bandwidth increases, just as described in FDR part, the threshold decreases because the region in which $\rho(t)$ approaches 0 becomes large. Consequently, the power of the algorithm increases correspondingly.

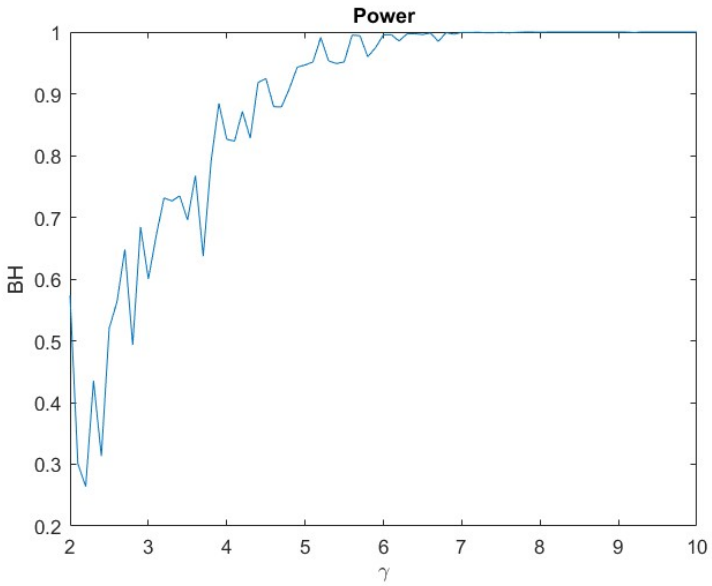

Figure 5.6: Power of the BH procedure for different bandwidth

Chapter 6

HEIGHT DISTRIBUTIONS OF CRITICAL POINTS OF SMOOTH ISOTROPIC GAUSSIAN FIELDS: COMPUTATIONS, SIMULATIONS AND ASYMPTOTICS

This chapter is another project that focuses on the height distributions of critical points in smooth isotropic Gaussian fields. The project is divided into three main components: computations, simulations, and asymptotics.

In the computations part, building upon the work of Cheng and Schwartzman [14], the explicit form of the peak height density of critical points in smooth isotropic Gaussian random fields can be calculated when the dimension N is small (3 and 4).

However, as the dimension N increases, obtaining the explicit form of the peak height density becomes increasingly challenging. In such cases, it becomes necessary to explore simulation methods to research the height distribution. Simulation approaches for both the Gaussian Orthogonal Ensemble (GOE) and the Gaussian Isotropic Ensemble (GOI) matrices are provided, based on the implicit form of the height density.

When the dimension N becomes sufficiently large (specifically, $N > 50$), the asymptotic distributions of the height density can be determined. As $N \to \infty$, $\kappa^2 = (N+2)/N \to 1$, implying that nearly all κ^2 values are less than 1. In this scenario, the implicit form of the height density with respect to the GOE matrix can be utilized. Drawing from the work of O'Rourke, S.[29], the distribution of all eigenvalues of the GOE matrix, except for the largest one, can be explicitly calculated, enabling the derivation of the explicit form of the asymptotic distribution of the height density. The Tracy-Widom distribution can be employed for the distribution of the largest eigenvalue, allowing for the simulation of the largest eigenvalue of the GOE matrix. Consequently, an algorithm for simulating the height density can be provided.

Overall, this project combines computations, simulations, and asymptotic analysis to explore the height distributions of critical points in smooth isotropic Gaussian fields.

6.1 Height Distributions of Critical Points of Gaussian Fields with $\kappa \leq 1$

When $\kappa \leq 1$, or equivalently, $\kappa^2 \leq 1$, the height density of critical points given by formula 1.3 can also be expressed in the following form with respect to the GOE matrix.

Theorem 6.1.1. *We have that, for* $\kappa < 1$

$$h_i(x) = \frac{\phi(x)\mathbb{E}^{N+1}_{\mathrm{GOE}}\left[e^{\frac{\lambda_{i+1}^2}{2} - \frac{(\lambda_{i+1} - \kappa x/\sqrt{2})^2}{1-\kappa^2}}\right]}{\sqrt{1-\kappa^2}\,\mathbb{E}^{N+1}_{\mathrm{GOE}}\left[e^{-\frac{\lambda_{i+1}^2}{2}}\right]}. \tag{6.1}$$

For $\kappa = 1$,

$$h_i(x) = \frac{e^{-\frac{x^2}{4}} f_{i+1}(x/\sqrt{2})}{\sqrt{2}\,\mathbb{E}^{N+1}_{\mathrm{GOE}}\left[e^{-\frac{\lambda_{i+1}^2}{2}}\right]} \tag{6.2}$$

Where f_{i+1} *is the density of* λ_{i+1} *of* GOE *matrix with dimension* $N+1$.

Theorem 6.1.1 introduces two special cases of the height distribution of the critical points of a Gaussian field with $\kappa < 1$ and $\kappa = 1$. In comparison to the density 1.3, the new densities have a more concise form, which facilitates the calculation of the explicit expression and simplifies the application of the simulation algorithm.

6.2 Evaluating Peak Height Distributions by Gaussian Densities

The following result is Lemma 2.2 in the Cheng and Schwartzman[14].

Lemma 6.2.1. *Let* M *be an* $N \times N$ *non-degenerate* $\mathrm{GOI}(c)$ *random matrix (*$c > -1/N$*). Then the density of the ordered eigenvalues* $\lambda_1 \leq \ldots \leq \lambda_N$ *of* M *is given by*

$$\begin{aligned} f_c(\lambda_1, \ldots, \lambda_N) = {} & \frac{1}{K_N\sqrt{1+Nc}} \exp\left\{-\frac{1}{2}\sum_{i=1}^{N}\lambda_i^2 + \frac{c}{2(1+Nc)}\left(\sum_{i=1}^{N}\lambda_i\right)^2\right\} \\ & \times \prod_{1\leq i<j\leq N} |\lambda_i - \lambda_j| \mathbb{1}_{\{\lambda_1 \leq \ldots \leq \lambda_N\}}, \end{aligned} \tag{6.3}$$

where

$$K_N = 2^{N/2} \prod_{i=1}^{N} \Gamma\left(\frac{i}{2}\right). \tag{6.4}$$

Use the notation $\mathbb{E}^N_{\mathrm{GOI}(c)}$ to represent the expectation under the GOI density (6.3), i.e., for a measurable function g,

$$\mathbb{E}^N_{\mathrm{GOI}(c)}[g(\lambda_1, \ldots, \lambda_N)] = \int_{\mathbb{R}^N} g(\lambda_1, \ldots, \lambda_N) f_c(\lambda_1, \ldots, \lambda_N) d\lambda_1 \cdots d\lambda_N. \tag{6.5}$$

We are interested in computing the following height density of local maxima of Gaussian random fields [See Corollary 3.6 in the [14] with $i = N$, implying $\lambda_{N+1} = \infty$. The density below is the derivative $-F'_N(x)$.]

Lemma 6.2.2. *The peak height density of local max of Gaussian random fields can be written as:*

$$h(x) = \frac{\phi(x)\mathbb{E}^N_{\mathrm{GOI}((1-\kappa^2)/2)}\left[\prod_{j=1}^{N} \left|\lambda_j - \kappa x/\sqrt{2}\right| \mathbb{1}_{\{\lambda_N < \kappa x/\sqrt{2}\}}\right]}{\mathbb{E}^N_{\mathrm{GOI}(1/2)}\left[\prod_{j=1}^{N} |\lambda_j| \mathbb{1}_{\{\lambda_N < 0\}}\right]}, \tag{6.6}$$

where $0 < \kappa^2 < (N+2)/N$ *and* $\phi(x) = \frac{1}{\sqrt{2\pi}} e^{-x^2/2}$ *is the density of standard Normal distribution.*

The computation of the GOI expectation (6.5) remains difficult because the exponential term of the GOI density in (6.3) has the form of a multivariate Gaussian density with correlation. Our next result shows that the expectation (6.5) can be expressed in terms of an expectation with respect to a GOE instead, where the correlation in the exponential term is no longer present.

Corollary 6.2.2.1. From lemma 6.2.2, when $\kappa^2 = 1$, the peak height density of local max of Gaussian random field is:

$$h(u) = \frac{e^{-\frac{u^2}{4}} f(u/\sqrt{2})}{\sqrt{2}\mathbb{E}^{N+1}_{\mathrm{GOE}}\left[e^{-\frac{\lambda^2_{N+1}}{2}}\right]} \tag{6.7}$$

Where f is the density of the largest eigenvalue of GOE matrix with dimension $N+1$.

Proof. From the equations before, we know that when $\kappa^2 = 1$, the numerator of the CDF of local max of Gaussian random fields can be written as:

$$\begin{aligned}
&\int_{-\infty}^{u} \phi(x)\mathbb{E}^N_{\mathrm{GOE}}[\prod_{j=1}^{N}|\lambda_j - x/\sqrt{2}|\mathbb{1}_{\{\lambda_N<x/\sqrt{2}\}}dx \\
=&\int_{-\infty}^{u} \frac{1}{\sqrt{2\pi}}e^{-\frac{x^2}{2}}\mathbb{E}^N_{\mathrm{GOE}}[\prod_{j=1}^{N}|\lambda_j - x/\sqrt{2}|\mathbb{1}_{\{\lambda_N<x/\sqrt{2}\}}dx \\
=&\frac{1}{\sqrt{2\pi}}\int_{-\infty}^{u}\int_{\mathbb{R}^N} e^{-\frac{x^2}{2}}\frac{1}{K_N}e^{-\frac{\Sigma_{i=1}^N\lambda_i^2}{2}}\prod_{1\le i<j\le N}|\lambda_i-\lambda_j| \\
&\times\prod_{k=1}^{N}|\lambda_k - x/\sqrt{2}|\mathbb{1}_{\{\lambda_1\le\ldots\le\lambda_N\le x/\sqrt{2}\}}d\lambda_1\ldots d\lambda_N dx
\end{aligned}$$

Then we take $\lambda_{N+1} = x/\sqrt{2}$, that is, $x = \sqrt{2}\lambda_{N+1}$, then we can get:

$$\begin{aligned}
&\frac{1}{\sqrt{\pi}}\int_{-\infty}^{u/\sqrt{2}}\int_{\mathbb{R}^N} e^{-\lambda_{N+1}^2}\frac{1}{K_N}e^{-\frac{\Sigma_{i=1}^N\lambda_i^2}{2}}\prod_{1\le i<j\le N+1}|\lambda_i-\lambda_j|\mathbb{1}_{\{\lambda_1\le\ldots\le\lambda_N\le\lambda_{N+1}\}}d\lambda_1\ldots d\lambda_N d\lambda_{N+1} \\
=&\frac{1}{\sqrt{\pi}}\int_{-\infty}^{u/\sqrt{2}}\int_{\mathbb{R}^N} e^{-\frac{\lambda_{N+1}^2}{2}}\frac{\sqrt{2}\Gamma(\frac{N+1}{2})}{K_{N+1}}e^{-\frac{\Sigma_{i=1}^{N+1}\lambda_i^2}{2}} \\
&\times\prod_{1\le i<j\le N+1}|\lambda_i-\lambda_j|\mathbb{1}_{\{\lambda_1\le\ldots\le\lambda_N\le\lambda_{N+1}\}}d\lambda_1\ldots d\lambda_N d\lambda_{N+1} \\
=&\frac{\sqrt{2}\Gamma(\frac{N+1}{2})}{\sqrt{\pi}}\mathbb{E}^{N+1}_{\mathrm{GOE}}\left[e^{-\frac{\lambda_{N+1}^2}{2}}\mathbb{1}_{\{\lambda_{N+1}\le u/\sqrt{2}\}}\right] \\
=&\frac{\sqrt{2}\Gamma(\frac{N+1}{2})}{\sqrt{\pi}}\int_{-\infty}^{u/\sqrt{2}} e^{-\frac{\lambda_{N+1}^2}{2}}f(\lambda_{N+1})d\lambda_{N+1}
\end{aligned}$$

Where f is the density of the largest eigenvalue of GOE matrix with dimension $N+1$.

The denominator can be written as:

$$\mathbb{E}^N_{\mathrm{GOI}(1/2)}\left[\prod_{j=1}^{N}|\lambda_j|\mathbb{1}_{\{\lambda_N\le 0\}}\right] = \frac{\Gamma(\frac{N+1}{2})}{\sqrt{\pi/2}}\mathbb{E}^{N+1}_{\mathrm{GOE}}\left[e^{-\frac{\lambda_{N+1}^2}{2}}\right]$$

Then the CDF can be written as:

$$P(Y\le u) = \frac{\int_{-\infty}^{u/\sqrt{2}} e^{-\frac{\lambda_{N+1}^2}{2}}f(\lambda_{N+1})d\lambda_{N+1}}{\mathbb{E}^{N+1}_{\mathrm{GOE}}\left[e^{-\frac{\lambda_{N+1}^2}{2}}\right]}$$

Then the PDF is:

$$h(u) = \frac{e^{-\frac{u^2}{4}} f(u/\sqrt{2})}{\sqrt{2}\mathbb{E}_{\mathrm{GOE}}^{N+1}\left[e^{-\frac{\lambda_{N+1}^2}{2}}\right]}$$

Where f is the density of the largest eigenvalue of GOE matrix with dimension $N+1$. □

Recall that the density of the ordered eigenvalues $\lambda_1 \le \ldots \le \lambda_N$ of a GOE matrix H is given by

$$f_0(\lambda_1, \ldots, \lambda_N) = \frac{1}{K_N} \exp\left\{-\frac{1}{2}\sum_{i=1}^{N} \lambda_i^2\right\} \prod_{1\le i<j\le N} |\lambda_i - \lambda_j| \mathbb{1}_{\{\lambda_1 \le \ldots \le \lambda_N\}}, \tag{6.8}$$

which is of the special case of GOI densities $f_c(\lambda_1, \ldots, \lambda_N)$ when $c = 0$. A nice property is that the exponential function is the kernel of multiple independent Gaussian densities, which can simplify the calculations a lot.

To achieve this, we rewrite the GOI density as follows. For $\sigma > 0$, let

$$\phi_\sigma(x) = \frac{1}{\sqrt{2\pi}\sigma} e^{-\frac{x^2}{2\sigma^2}}.$$

For simplicity, denote $\phi(x) = \phi_1(x)$ and let $\Phi(x) = \int_{-\infty}^{x} \phi(y)dy$. Let $\bar{\lambda} = \sum_{i=1}^{N} \lambda_i/N$. By careful calculations, we may check that (6.3) can be written as the following decomposition

$$\begin{aligned} &f_c(\lambda_1, \ldots, \lambda_N) \\ &= \frac{\sqrt{2\pi}}{K_N\sqrt{N}} \phi_{\sigma_c}(\bar{\lambda}) \exp\left\{-\frac{1}{2}\sum_{i=1}^{N}(\lambda_i - \bar{\lambda})^2\right\} \prod_{1\le i<j\le N} |\lambda_i - \lambda_j| \mathbb{1}_{\{\lambda_1 \le \ldots \le \lambda_N\}}, \end{aligned} \tag{6.9}$$

where $\sigma_c = \sqrt{(1+Nc)/N}$. Notice that the form of (6.9) is similar to the product of a Gaussian density and a GOE density. In particular, the covariance parameter c is only included in the Gaussian density ϕ_{σ_c}.

Lemma 6.2.3. *Let $c > -1/N$. Then for a measurable function g and a constant b,*

$$\begin{aligned} &\mathbb{E}_{\mathrm{GOI}(c)}^{N}[g(\lambda_1 - b, \ldots, \lambda_N - b)] \\ &= \sqrt{\frac{2\pi}{N}} \int_{\mathbb{R}} \phi_{\sigma_c}(z+b) \mathbb{E}_{\mathrm{GOE}}^{N}\left[g(r_1 + z, \ldots, r_N + z)\delta\left(\sum_{i=1}^{N} r_i = 0\right)\right] dz, \end{aligned} \tag{6.10}$$

where $\sigma_c = \sqrt{(1+Nc)/N}$, $\delta(\cdot)$ *is the Dirac delta function and the expectation* $\mathbb{E}^N_{\mathrm{GOE}}$ *is taken with respect to* $r_1, \cdots, r_N$.

Proof. Plugging (6.9) into (6.5) and making change of variables $\xi_i = \lambda_i - b$, $1 \le i \le N$, we have that

$$\begin{aligned}
&\mathbb{E}^N_{\mathrm{GOI}(c)}[g(\lambda_1 - b, \ldots, \lambda_N - b)] \\
&\quad = \frac{\sqrt{2\pi}}{K_N\sqrt{N}} \int_{\mathbb{R}^N} \phi_{\sigma_c}(\bar{\lambda}) \exp\left\{-\frac{1}{2}\sum_{i=1}^N (\lambda_i - \bar{\lambda})^2\right\} \prod_{1\le i<j\le N} |\lambda_i - \lambda_j| \mathbb{1}_{\{\lambda_1 \le \ldots \le \lambda_N\}} \\
&\qquad \times g(\lambda_1 - b, \ldots, \lambda_N - b) d\lambda_1 \cdots d\lambda_N \\
&\quad = \frac{\sqrt{2\pi}}{K_N\sqrt{N}} \int_{\mathbb{R}^N} \phi_{\sigma_c}(\bar{\xi} + b) \exp\left\{-\frac{1}{2}\sum_{i=1}^N (\xi_i - \bar{\xi})^2\right\} \prod_{1\le i<j\le N} |\xi_i - \xi_j| \mathbb{1}_{\{\xi_1 \le \ldots \le \xi_N\}} \\
&\qquad \times g(\xi_1, \ldots, \xi_N) d\xi_1 \cdots d\xi_N,
\end{aligned}$$

where $\bar{\xi} = \sum_{i=1}^N \xi_i / N$. Adding an additional integral variable $\bar{\xi}$ and introducing the Dirac delta function, and making again change of variables

$$z = \bar{\xi} \quad \text{and} \quad r_i = \xi_i - \bar{\xi}, \quad i = 1, \ldots, N,$$

we obtain

$$\begin{aligned}
&\mathbb{E}^N_{\mathrm{GOI}(c)}[g(\lambda_1 - b, \ldots, \lambda_N - b)] \\
&\quad = \frac{\sqrt{2\pi}}{K_N\sqrt{N}} \int_{\mathbb{R}} d\bar{\xi} \int_{\mathbb{R}^N} \phi_{\sigma_c}(\bar{\xi} + b) \exp\left\{-\frac{1}{2}\sum_{i=1}^N (\xi_i - \bar{\xi})^2\right\} \prod_{1\le i<j\le N} |\xi_i - \xi_j| \mathbb{1}_{\{\xi_1 \le \ldots \le \xi_N\}} \\
&\qquad \times \delta\left(\sum_{i=1}^N \xi_i = N\bar{\xi}\right) g(\xi_1, \ldots, \xi_N) d\xi_1 \cdots d\xi_N \\
&\quad = \frac{\sqrt{2\pi}}{K_N\sqrt{N}} \int_{\mathbb{R}} dz \int_{\mathbb{R}^N} \phi_{\sigma_c}(z + b) \exp\left\{-\frac{1}{2}\sum_{i=1}^N r_i^2\right\} \prod_{1\le i<j\le N} |r_i - r_j| \mathbb{1}_{\{r_1 \le \ldots \le r_N\}} \\
&\qquad \times \delta\left(\sum_{i=1}^N r_i = 0\right) g(r_1 + z, \ldots, r_N + z) dr_1 \cdots dr_N \\
&\quad = \sqrt{\frac{2\pi}{N}} \int_{\mathbb{R}} \phi_{\sigma_c}(z + b) \mathbb{E}^N_{\mathrm{GOE}}\left[g(r_1 + z, \ldots, r_N + z)\delta\left(\sum_{i=1}^N r_i = 0\right)\right] dz.
\end{aligned}$$

□

A nice feature of expression (6.10) is that the inner GOE integral does not depend on the GOI parameter c. The effect of the GOI parameter c is only in the univariate outer integral. Expression (6.10) will be used to simplify the computation of the expected number of critical points of isotropic Gaussian fields.

Lemma 6.2.4. *Let $c > -1/N$ and $\sigma_c = \sqrt{(1+Nc)/N}$. Then for $b \in \mathbb{R}$,*

$$\begin{aligned}
&\mathbb{E}^N_{\mathrm{GOI}(c)}\left[\prod_{j=1}^{N}|\lambda_j - b|\mathbb{1}_{\{\lambda_N<b\}}\right] \\
&= \frac{\sqrt{2\pi}}{K_N\sqrt{N}}\int_{-\infty}^{0}\phi_{\sigma_c}(z+b)dz\int_0^{-\sqrt{\frac{N}{N-1}}z} ds_{N-1}\int_0^{\sqrt{\frac{N}{N-2}}s_{N-1}} ds_{N-2}\cdots\int_0^{\sqrt{3}s_2} ds_1 \\
&\quad\times\exp\left\{-\frac{1}{2}\sum_{i=1}^{N-1}s_i^2\right\}\prod_{2\le j\le N}\left(\sqrt{\frac{j-1}{j}}s_{j-1}+\frac{1}{\sqrt{2}}s_1+\sum_{\ell=2}^{j-1}\frac{1}{\sqrt{\ell(\ell+1)}}s_\ell\right) \\
&\quad\times\prod_{2\le i<j\le N}\left(\sqrt{\frac{j-1}{j}}s_{j-1}-\sqrt{\frac{i-1}{i}}s_{i-1}+\sum_{\ell=i}^{j-1}\frac{1}{\sqrt{\ell(\ell+1)}}s_\ell\right) \\
&\quad\times\left(-z+\frac{1}{\sqrt{2}}s_1+\sum_{\ell=2}^{N-1}\frac{1}{\sqrt{\ell(\ell+1)}}s_\ell\right)\prod_{j=2}^{N}\left(-z-\sqrt{\frac{j-1}{j}}s_{j-1}+\sum_{\ell=j}^{N-1}\frac{1}{\sqrt{\ell(\ell+1)}}s_\ell\right)
\end{aligned}$$

Proof. Applying Lemma 6.2.3 with

$$g(\lambda_1-b,\dots,\lambda_N-b)=\prod_{j=1}^{N}|\lambda_j-b|\mathbb{1}_{\{\lambda_N-b<0\}},$$

or equivalently

$$g(x_1,\dots,x_N)=\prod_{j=1}^{N}|x_j|\mathbb{1}_{\{x_N<0\}},$$

we have

$$\begin{aligned}
&\mathbb{E}^N_{\mathrm{GOI}(c)}\left[\prod_{j=1}^{N}|\lambda_j-b|\mathbb{1}_{\{\lambda_N<b\}}\right]=\mathbb{E}^N_{\mathrm{GOI}(c)}\left[g(\lambda_1-b,\dots,\lambda_N-b)\right] \\
&=\sqrt{\frac{2\pi}{N}}\int_{\mathbb{R}}\phi_{\sigma_c}(z+b)\mathbb{E}^N_{\mathrm{GOE}}\left[g(r_1+z,\dots,r_N+z)\delta\left(\sum_{i=1}^{N}r_i=0\right)\right]dz \qquad (6.11)\\
&=\sqrt{\frac{2\pi}{N}}\int_{\mathbb{R}}\phi_{\sigma_c}(z+b)\mathbb{E}^N_{\mathrm{GOE}}\left[\prod_{j=1}^{N}|r_j+z|\mathbb{1}_{\{r_N+z<0\}}\delta\left(\sum_{i=1}^{N}r_i=0\right)\right]dz.
\end{aligned}$$

Let

$$V_j = \frac{j}{\sqrt{j(j+1)}} e_{j+1} - \frac{1}{\sqrt{j(j+1)}} \sum_{\ell=1}^{j} e_\ell, \quad j = 1, \ldots, N-1,$$
$$V_N = \frac{1}{\sqrt{N}} \mathbf{1}_N,$$

where $\{e_j : 1 \le j \le N\}$ is the standard basis in $\mathbb{R}^N$ and $\mathbf{1}_N$ is the $N \times 1$ column vector of ones. Then

$$\begin{aligned} \mathbb{V}_N &= (V_1, \ldots, V_{N-1}, V_N) \\ &= \begin{pmatrix} -\frac{1}{\sqrt{2}} & -\frac{1}{\sqrt{6}} & \cdots & -\frac{1}{\sqrt{(N-1)N}} & \frac{1}{\sqrt{N}} \\ \frac{1}{\sqrt{2}} & -\frac{1}{\sqrt{6}} & \cdots & -\frac{1}{\sqrt{(N-1)N}} & \frac{1}{\sqrt{N}} \\ 0 & \frac{2}{\sqrt{6}} & \cdots & -\frac{1}{\sqrt{(N-1)N}} & \frac{1}{\sqrt{N}} \\ \vdots & \vdots & \vdots & \vdots & \vdots \\ 0 & 0 & \cdots & \frac{N-1}{\sqrt{(N-1)N}} & \frac{1}{\sqrt{N}} \end{pmatrix} \end{aligned} \tag{6.12}$$

is an orthonormal basis in $\mathbb{R}^N$ such that $\mathbf{1}_N^T V_j = 0$ for every $j = 1, \ldots, N-1$.

Now, we make the following change of variables,

$$(r_1, \ldots, r_N)^T = \mathbb{V}_N (s_1, \ldots, s_N)^T,$$

which gives

$$\begin{aligned} r_1 &= -\frac{1}{\sqrt{2}} s_1 - \sum_{\ell=2}^{N-1} \frac{1}{\sqrt{\ell(\ell+1)}} s_\ell + \frac{1}{\sqrt{N}} s_N, \\ r_j &= \frac{j-1}{\sqrt{(j-1)j}} s_{j-1} - \sum_{\ell=j}^{N-1} \frac{1}{\sqrt{\ell(\ell+1)}} s_\ell + \frac{1}{\sqrt{N}} s_N, \quad 2 \le j \le N. \end{aligned}$$

Notice that

$$\sum_{j=1}^{N} r_j = 0 \Leftrightarrow s_N = 0. \tag{6.13}$$

Since λ_j, ξ_j and hence r_j are already ordered from low to high, we have

$$\begin{aligned} r_2 - r_1 &= \sqrt{2} s_1 > 0, \\ r_j - r_{j-1} &= \sqrt{\frac{j}{j-1}} s_{j-1} - \sqrt{\frac{j-2}{j-1}} s_{j-2} > 0, \quad 3 \le j \le N, \end{aligned} \tag{6.14}$$

implying that

$$s_j < \sqrt{\frac{j+2}{j}} s_{j+1}, \quad 1 \le j \le N-2. \tag{6.15}$$

For $b \in \mathbb{R}$, under $s_N = 0$,

$$\begin{aligned} \lambda_N < b &\Leftrightarrow \xi_N < 0 \Leftrightarrow r_N + z < 0 \\ &\Leftrightarrow r_N = \sqrt{\frac{N-1}{N}} s_{N-1} < -z \\ &\Leftrightarrow s_{N-1} < -\sqrt{\frac{N}{N-1}} z. \end{aligned} \tag{6.16}$$

Plugging (6.13), (6.14), (6.15) and (6.16) into (6.11) yields the desired results.

□

Lemma 6.2.5. *Let $c > -1/N$ and $\sigma_c = \sqrt{(1+Nc)/N}$. Then for $b \in \mathbb{R}$,*

$$\begin{aligned} &\mathbb{E}^N_{\mathrm{GOI}(c)} \left[\prod_{j=1}^N |\lambda_j| \mathbb{1}_{\{\lambda_N<0\}} \mathbb{1}_{\{\sum_{j=1}^N \lambda_j/N \le -\sqrt{(N+2)/(2N)}u\}} \right] \\ &= \frac{\sqrt{2\pi}}{K_N \sqrt{N}} \int_{-\infty}^{-\sqrt{(N+2)/(2N)}u} \phi_{\sigma_c}(z) dz \int_0^{-\sqrt{\frac{N}{N-1}}z} ds_{N-1} \int_0^{\sqrt{\frac{N}{N-2}}s_{N-1}} ds_{N-2} \cdots \int_0^{\sqrt{3}s_2} ds_1 \\ &\quad \times \exp\left\{ -\frac{1}{2} \sum_{i=1}^{N-1} s_i^2 \right\} \prod_{2 \le j \le N} \left(\sqrt{\frac{j-1}{j}} s_{j-1} + \frac{1}{\sqrt{2}} s_1 + \sum_{\ell=2}^{j-1} \frac{1}{\sqrt{\ell(\ell+1)}} s_\ell \right) \\ &\quad \times \prod_{2 \le i < j \le N} \left(\sqrt{\frac{j-1}{j}} s_{j-1} - \sqrt{\frac{i-1}{i}} s_{i-1} + \sum_{\ell=i}^{j-1} \frac{1}{\sqrt{\ell(\ell+1)}} s_\ell \right) \\ &\quad \times \left(-z + \frac{1}{\sqrt{2}} s_1 + \sum_{\ell=2}^{N-1} \frac{1}{\sqrt{\ell(\ell+1)}} s_\ell \right) \prod_{j=2}^N \left(-z - \sqrt{\frac{j-1}{j}} s_{j-1} + \sum_{\ell=j}^{N-1} \frac{1}{\sqrt{\ell(\ell+1)}} s_\ell \right) \end{aligned}$$

Proof. :The proof is similar as the proof of lemma 6.2.4, the difference is the range of z, which represents $\sum_{j=1}^N \lambda_j/N$ is $(-\infty, -\sqrt{(N+2)(2N)}u)$ □

Example 6.2.1. When $N = 2$, by the lemma 6.2.5, we can calculate the height density by corollary 3.14 of the paper []:

$$F_i(u) = \frac{\mathbb{E}^N_{\mathrm{GOI}(\frac{1}{2})} \left[\prod_{j=1}^N |\lambda_j| \mathbb{1}_{\{\lambda_N<0\}} \mathbb{1}_{\{\sum_{j=1}^N \lambda_j/N \le -\sqrt{\frac{N+2}{2N}}u\}} \right]}{\mathbb{E}^N_{\mathrm{GOI}(\frac{1}{2})} \left[\prod_{j=1}^N |\lambda_j| \mathbb{1}_{\{\lambda_N<0\}} \right]}$$

where u is a constant.

Applying lemma 3.1, we can let:

$$g(\lambda_1,\ldots,\lambda_N)=\prod_{j=1}^{N}|\lambda_j|\mathbb{1}_{\{\lambda_N<0\}}\mathbb{1}_{\{\bar{\lambda_i}\le-\sqrt{\frac{N+2}{/}2N}u\}}$$

Then:

$$\begin{aligned}
&\mathbb{E}^N_{\mathrm{GOI}(\frac{1}{2})}\left[\prod_{j=1}^{N}|\lambda_j|\mathbb{1}_{\{\lambda_N<0\}}\mathbb{1}_{\{\bar{\lambda_i}\le-\sqrt{\frac{N+2}{2N}}u\}}\right]\\
&\quad=\frac{\sqrt{2\pi}}{K_N\sqrt{N}}\int_{-\infty}^{-\sqrt{\frac{N+2}{2N}}u}\phi_{\sigma_c}(z)dz\int_0^{-\sqrt{\frac{N}{N-1}}z}ds_{N-1}\int_0^{\sqrt{\frac{N}{N-2}}s_{N-1}}ds_{N-2}\cdots\int_0^{\sqrt{3}s_2}ds_1\\
&\qquad\times\exp\left\{-\frac{1}{2}\sum_{i=1}^{N-1}s_i^2\right\}\prod_{2\le j\le N}\left(\sqrt{\frac{j-1}{j}}s_{j-1}+\frac{1}{\sqrt{2}}s_1+\sum_{\ell=2}^{j-1}\frac{1}{\sqrt{\ell(\ell+1)}}s_\ell\right)\\
&\qquad\times\prod_{2\le i<j\le N}\left(\sqrt{\frac{j-1}{j}}s_{j-1}-\sqrt{\frac{i-1}{i}}s_{i-1}+\sum_{\ell=i}^{j-1}\frac{1}{\sqrt{\ell(\ell+1)}}s_\ell\right)\\
&\qquad\times\left(-z+\frac{1}{\sqrt{2}}s_1+\sum_{\ell=2}^{N-1}\frac{1}{\sqrt{\ell(\ell+1)}}s_\ell\right)\prod_{j=2}^{N}\left(-z-\sqrt{\frac{j-1}{j}}s_{j-1}+\sum_{\ell=j}^{N-1}\frac{1}{\sqrt{\ell(\ell+1)}}s_\ell\right)
\end{aligned}$$

The output is $1-CDF$, if we plug in $N=2$, we can get the numerator:

$$\begin{aligned}
&\mathbb{E}^2_{\mathrm{GOI}(\frac{1}{2})}\left[\prod_{j=1}^{2}|\lambda_j|\mathbb{1}_{\{\lambda_2<0\}}\mathbb{1}_{\{\bar{\lambda_i}\le-u\}}\right]\\
&\quad=\frac{\sqrt{2\pi}}{K_2\sqrt{2}}\int_{-\infty}^{-u}\phi(z)dz\int_0^{-\sqrt{2}z}e^{-\frac{1}{2}s_1^2}\sqrt{2}s_1(-z-\frac{1}{\sqrt{2}}s_1)(-z+\frac{1}{\sqrt{2}}s_1)ds_1\\
&\quad=\frac{\sqrt{2\pi}}{K_2\sqrt{2}}\{\int_{-\infty}^{-u}z^2\phi(z)dz\int_0^{-\sqrt{2}z}\sqrt{2}s_1e^{-\frac{1}{2}s_1^2}ds_1-\int_{-\infty}^{-u}\phi(z)dz\int_0^{-\sqrt{2}z}\frac{\sqrt{2}}{2}s_1^3e^{-\frac{1}{2}s_1^2}ds_1\}
\end{aligned}$$

The denominator is:

$$\begin{aligned}
&\mathbb{E}^2_{\mathrm{GOI}(\frac{1}{2})}\left[\prod_{j=1}^{2}|\lambda_j|\mathbb{1}_{\{\lambda_2<0\}}\right]\\
&\quad=\frac{\sqrt{2\pi}}{K_2\sqrt{2}}\int_{-\infty}^{0}\phi(z)dz\int_0^{-\sqrt{2}z}e^{-\frac{1}{2}s_1^2}\sqrt{2}s_1(-z-\frac{1}{\sqrt{2}}s_1)(-z+\frac{1}{\sqrt{2}}s_1)ds_1\\
&\quad=\frac{\sqrt{2\pi}}{K_2\sqrt{2}}\{\int_{-\infty}^{0}z^2\phi(z)dz\int_0^{-\sqrt{2}z}\sqrt{2}s_1e^{-\frac{1}{2}s_1^2}ds_1-\int_{-\infty}^{0}\phi(z)dz\int_0^{-\sqrt{2}z}\frac{\sqrt{2}}{2}s_1^3e^{-\frac{1}{2}s_1^2}ds_1\}
\end{aligned}$$

Combine them all, we can get the result:

$$h_2(x) = \frac{2\sqrt{3}}{\sqrt{2\pi}}[(x^2-1)e^{-x^2/2} + e^{-3x^2/2}]\mathbb{1}_{\{x\geq 0\}} \tag{6.17}$$

Lemma 6.2.6. *Let $N = 2$. Let $c > -1/N$ and $\sigma_c = \sqrt{(1+Nc)/N} = \sqrt{(1+2c)/2}$. Then for $b \in \mathbb{R}$,*

$$\begin{aligned}
&\int_{-\infty}^{0} \phi_{\sigma_c}(z+b)dz \int_0^{-\sqrt{2}z} e^{-\frac{s^2}{2}}\sqrt{2}s(-z+\frac{1}{\sqrt{2}}s)(-z-\frac{1}{\sqrt{2}}s)ds \\
&= 2\sqrt{2}[\sigma_c^2 + b^2 - 1]\Phi\left(\frac{b}{\sigma_c}\right) + \frac{2\sigma_c b}{\sqrt{\pi}}e^{-\frac{b^2}{2\sigma_c^2}} + \frac{2\sqrt{2}}{\sqrt{1+2\sigma_c^2}}e^{-\frac{b^2}{1+2\sigma_c^2}}\Phi\left(\frac{b}{\sigma_c\sqrt{1+2\sigma_c^2}}\right).
\end{aligned}$$

Proof.

$$\begin{aligned}
&\int_0^{-\sqrt{2}z} e^{-\frac{s^2}{2}}\sqrt{2}s(-z+\frac{1}{\sqrt{2}}s)(-z-\frac{1}{\sqrt{2}}s)ds \\
&= \sqrt{2}z^2\int_0^{-\sqrt{2}z} se^{-\frac{s^2}{2}}ds - \frac{1}{\sqrt{2}}\int_0^{-\sqrt{2}z} s^3 e^{-\frac{s^2}{2}}ds \\
&= \sqrt{2}z^2(1-e^{-z^2}) - \frac{1}{\sqrt{2}}(-2z^2e^{-z^2} - 2e^{-z^2} + 2) \\
&= \sqrt{2}(e^{-z^2} + z^2 - 1)
\end{aligned}$$

On the other hand,

$$\begin{aligned}
\int_{-\infty}^{0}\phi_{\sigma_c}(z+b)e^{-z^2}dz &= \int_{-\infty}^{b}\phi_{\sigma_c}(y)e^{-(y-b)^2}dy = \frac{1}{\sqrt{2\pi}\sigma_c}\int_{-\infty}^{b} e^{-\frac{y^2}{2\sigma_c^2}-(y-b)^2}dy \\
&= \frac{1}{\sqrt{2\pi}\sigma_c}e^{-\frac{b^2}{1+2\sigma_c^2}}\int_{-\infty}^{b} e^{-\frac{(1+2\sigma_c^2)\left[y-\frac{2b\sigma_c^2}{1+2\sigma_c^2}\right]^2}{2\sigma_c^2}}dy \\
&= \frac{1}{\sqrt{2\pi}\sigma_c}e^{-\frac{b^2}{1+2\sigma_c^2}}\frac{\sigma_c}{\sqrt{1+2\sigma_c^2}}\int_{-\infty}^{\frac{b}{\sigma_c\sqrt{1+2\sigma_c^2}}} e^{-\frac{x^2}{2}}dx \\
&= \frac{1}{\sqrt{1+2\sigma_c^2}}e^{-\frac{b^2}{1+2\sigma_c^2}}\Phi\left(\frac{b}{\sigma_c\sqrt{1+2\sigma_c^2}}\right);
\end{aligned}$$

and

$$\begin{aligned}
\int_{-\infty}^{0}\phi_{\sigma_c}(z+b)z^2dz &= \frac{1}{\sqrt{2\pi}\sigma_c}\int_{-\infty}^{0} e^{-\frac{(z+b)^2}{2\sigma_c^2}}z^2dz \\
&= \frac{b\sigma_c}{\sqrt{2\pi}}e^{-\frac{b^2}{2\sigma_c^2}} + (b^2+\sigma_c^2)\Phi\left(\frac{b}{\sigma_c}\right);
\end{aligned}$$

and

$$\int_{-\infty}^{0} \phi_{\sigma_c}(z+b)dz = \Phi\left(\frac{b}{\sigma_c}\right).$$

Combining all the results above, we obtain

$$\begin{aligned}
&\int_{-\infty}^{0} \phi_{\sigma_c}(z+b)dz \int_{0}^{-\sqrt{2}z} e^{-\frac{s^2}{2}}\sqrt{2}s(-z+\frac{1}{\sqrt{2}}s)(-z-\frac{1}{\sqrt{2}}s)ds \\
&= \sqrt{2}[\sigma_c^2+b^2-1]\Phi\left(\frac{b}{\sigma_c}\right) + \frac{b\sigma_c}{\sqrt{\pi}}e^{-\frac{b^2}{2\sigma_c^2}} + \frac{\sqrt{2}}{\sqrt{1+2\sigma_c^2}}e^{-\frac{b^2}{1+2\sigma_c^2}}\Phi\left(\frac{b}{\sigma_c\sqrt{1+2\sigma_c^2}}\right).
\end{aligned}$$

□

Now, applying Lemma 6.2.4 with $N=2$, $b=\kappa x/\sqrt{2}$, $c=(1-\kappa^2)/2$ and hence $\sigma_c = \sqrt{\frac{2-\kappa^2}{2}}$, together with Lemma 6.2.6, we obtain

$$\begin{aligned}
&\mathbb{E}^N_{\mathrm{GOI}((1-\kappa^2)/2)}\left[\prod_{j=1}^{N}\left|\lambda_j-\kappa x/\sqrt{2}\right|\mathbb{1}_{\{\lambda_N<\kappa x/\sqrt{2}\}}\right] = \mathbb{E}^N_{\mathrm{GOI}(c)}\left[\prod_{j=1}^{N}|\lambda_j-b|\mathbb{1}_{\{\lambda_N<b\}}\right] \\
&= \frac{\sqrt{2\pi}}{K_N\sqrt{N}}\int_{-\infty}^{0}\phi_{\sigma_c}(z+b)dz\int_{0}^{-\sqrt{2}z}e^{-\frac{s^2}{2}}\sqrt{2}s(-z+\frac{1}{\sqrt{2}}s)(-z-\frac{1}{\sqrt{2}}s)ds \\
&= \frac{\sqrt{2\pi}}{K_N\sqrt{N}}\left\{\frac{\kappa^2(x^2-1)}{\sqrt{2}}\Phi\left(\frac{\kappa x}{\sqrt{2-\kappa^2}}\right) + \frac{\kappa\sqrt{2-\kappa^2}}{2\sqrt{\pi}}xe^{-\frac{\kappa^2x^2}{2(2-\kappa^2)}}\right. \\
&\quad \left. + \frac{\sqrt{2}}{\sqrt{3-\kappa^2}}e^{-\frac{\kappa^2x^2}{2(3-\kappa^2)}}\Phi\left(\frac{\kappa x}{\sqrt{(2-\kappa^2)(3-\kappa^2)}}\right)\right\}.
\end{aligned}$$

On the other hand, applying Lemma 6.2.4 with $N=2$, $b=0$, $c=1/2$ and hence $\sigma_c=1$, together with Lemma 6.2.6, we obtain

$$\mathbb{E}^N_{\mathrm{GOI}(1/2)}\left[\prod_{j=1}^{N}\left|\lambda_j\right|\mathbb{1}_{\{\lambda_N<0\}}\right] = \frac{\sqrt{2\pi}}{K_N\sqrt{N}}\frac{1}{\sqrt{6}}.$$

Therefore, the height density of local maxima for $N = 2$ is given by

$$\begin{aligned}
&\frac{\phi(x)\mathbb{E}^N_{\mathrm{GOI}((1-\kappa^2)/2)}\left[\prod_{j=1}^N \left|\lambda_j - \kappa x/\sqrt{2}\right| \mathbb{1}_{\{\lambda_N < \kappa x/\sqrt{2}\}}\right]}{\mathbb{E}^N_{\mathrm{GOI}(1/2)}\left[\prod_{j=1}^N |\lambda_j| \mathbb{1}_{\{\lambda_N<0\}}\right]} \\
&= \sqrt{6}\phi(x)\left\{\frac{\kappa^2(x^2-1)}{\sqrt{2}}\Phi\left(\frac{\kappa x}{\sqrt{2-\kappa^2}}\right) + \frac{\kappa\sqrt{2-\kappa^2}}{2\sqrt{\pi}} x e^{-\frac{\kappa^2 x^2}{2(2-\kappa^2)}}\right. \\
&\quad \left. + \frac{\sqrt{2}}{\sqrt{3-\kappa^2}} e^{-\frac{\kappa^2 x^2}{2(3-\kappa^2)}}\Phi\left(\frac{\kappa x}{\sqrt{(2-\kappa^2)(3-\kappa^2)}}\right)\right\} \\
&= \sqrt{3}\kappa^2(x^2-1)\phi(x)\Phi\left(\frac{\kappa x}{\sqrt{2-\kappa^2}}\right) + \frac{\kappa\sqrt{3(2-\kappa^2)}}{2\pi} x e^{-\frac{x^2}{2-\kappa^2}} \\
&\quad + \frac{\sqrt{6}}{\sqrt{\pi(3-\kappa^2)}} e^{-\frac{3x^2}{2(3-\kappa^2)}}\Phi\left(\frac{\kappa x}{\sqrt{(2-\kappa^2)(3-\kappa^2)}}\right).
\end{aligned} \tag{6.18}$$

6.3 Explicit Distribution on Euclidean Space

This section will display some explicit height densities of local maxima and some index=i_0 of Gaussian random fields when $N = 3, 4$.

6.3.1 Non Degenerate

When $\kappa^2 < \frac{N+2}{N}$, the height density is non-degenerate, we have the following results:

$N = 3$, $i_0 = 1$

$$
\begin{aligned}
h(x) = & \frac{72\phi(x)}{\pi(36+29\sqrt{6})}\{C_{1,x}x^3\Phi(\frac{\kappa x}{\sqrt{3-\kappa^2}}) + C_{2,x}x^3\Phi_{\Sigma_1}(\frac{\sqrt{2}\kappa x}{2},\kappa x) \\
& + C_{3,x}x^2 e^{\frac{\kappa^2 x^2}{2(\kappa^2-3)}}\Phi(\frac{2\kappa x}{\sqrt{(3-\kappa^2)(5-3\kappa^2)}}) + C_{4,x}x^2 e^{\frac{\kappa^2 x^2}{2(\kappa^2-3)}} \\
& + C_{5,x}x^2 e^{\frac{\kappa^2 x^2}{2(\kappa^2-2)}}\Phi(\frac{\sqrt{2}\kappa x}{\sqrt{(4-2\kappa^2)(5-3\kappa^2)}}) + C_{6,x}x e^{\frac{\kappa^2 x^2}{2(\kappa^2-3)}} e^{-\frac{2\kappa^2 x^2}{3\kappa^4-14\kappa^2+15}} \\
& + C_{7,x}x e^{\frac{\kappa^2 x^2}{2(\kappa^2-2)}} e^{-\frac{\kappa^2 x^2}{6\kappa^4-22\kappa^2+20}} + C_{8,x}x e^{\frac{3\kappa^2 x^2}{2(3\kappa^2-5)}} + C_{9,x}x\Phi(\frac{\kappa x}{\sqrt{3-\kappa^2}}) \\
& + C_{10,x}x\Phi_{\Sigma_1}(\frac{\sqrt{2}\kappa x}{2},\kappa x) + C_{11,x}e^{\frac{\kappa^2 x^2}{2(\kappa^2-3)}}\Phi(\frac{2\kappa x}{\sqrt{(3-\kappa^2)(5-3\kappa^2)}}) \\
& + C_{12,x}e^{\frac{\kappa^2 x^2}{2(\kappa^2-3)}} + C_{13,x}e^{\frac{\kappa^2 x^2}{2(\kappa^2-2)}}\Phi(\frac{\sqrt{2}\kappa x}{\sqrt{(4-2\kappa^2)(5-3\kappa^2)}})\}
\end{aligned}
$$

where:

$$C_{1,x} = \frac{\pi\sqrt{\pi}\kappa^3}{2}$$
$$C_{2,x} = -\frac{\pi\sqrt{\pi}\kappa^3}{2}$$
$$C_{3,x} = \frac{2\sqrt{2}\pi\kappa^2(\kappa^6 - 9\kappa^4 + 27\kappa^2 - 43)}{8(3-\kappa^2)^{\frac{5}{2}}}$$
$$C_{4,x} = -\frac{2\sqrt{2}\pi\kappa^2(\kappa^6 - 9\kappa^4 + 27\kappa^2 - 43)}{8(3-\kappa^2)^{\frac{5}{2}}}$$
$$C_{5,x} = \frac{2\pi\kappa^2(\kappa^2-2)^3}{(4-2\kappa^2)^{\frac{5}{2}}}$$
$$C_{6,x} = \frac{2\sqrt{\pi}\kappa(3\kappa^6 - 25\kappa^4 + 101\kappa^2 - 127)}{4(\kappa^2-3)^2(5-3\kappa^2)^{1.5}}$$
$$C_{7,x} = \frac{2\sqrt{\pi}\kappa(3\kappa^2-7)(1-\kappa^2)}{8(5-3\kappa^2)^{\frac{3}{2}}}$$
$$C_{8,x} = \frac{3\sqrt{\pi}\kappa p(1-2\kappa^2)}{(\kappa^2-1)(5-3\kappa^2)^{\frac{3}{2}}}$$
$$C_{9,x} = -\frac{3\pi\sqrt{\pi}\kappa^3}{2}$$
$$C_{10,x} = \frac{3\pi\sqrt{\pi}\kappa^3}{2}$$
$$C_{11,x} = -\frac{\sqrt{2}\pi(2\kappa^8 - 15\kappa^6 + 51\kappa^4 - 101\kappa^2 + 87)}{4(3-\kappa^2)^{\frac{5}{2}}}$$
$$C_{12,x} = \frac{\sqrt{2}\pi(2\kappa^8 - 15\kappa^6 + 51\kappa^4 - 101\kappa^2 + 87)}{4(3-\kappa^2)^{\frac{5}{2}}}$$
$$C_{13,x} = \frac{\sqrt{2}\pi(2\kappa^8 - 15\kappa^6 + 51\kappa^4 - 101\kappa^2 + 87)}{4(3-\kappa^2)^{\frac{5}{2}}}$$
$$\Sigma_1 =: \begin{pmatrix} \frac{3-\kappa^2}{2} & -\frac{\sqrt{2}(\kappa^2-1)}{2} \\ -\frac{\sqrt{2}(\kappa^2-1)}{2} & 2-\kappa^2 \end{pmatrix}$$

$N = 3$, $i_0 = 3$

$$h(x) = \frac{12\sqrt{12}\phi(x)}{29-6\sqrt{6}}\{(\frac{3\kappa^3 x-\kappa^3 x^3}{2\sqrt{2}})\sqrt{\pi}[\Phi(\frac{\sqrt{3}\kappa x}{\sqrt{5-3\kappa^2}})]$$
$$-\Phi_{\Sigma_1}(\sqrt{3}\kappa x,\frac{\sqrt{3}\kappa x}{\sqrt{5-3\kappa^2}})-\Phi_{\Sigma_2}(\frac{\sqrt{3}\kappa x}{2},\frac{\sqrt{3}\kappa x}{\sqrt{5-3\kappa^2}})]$$
$$-\frac{\sqrt{3}(2-\kappa^2)^{\frac{1}{2}}(-\kappa^2x^2+2\kappa^2+2)\sqrt{6\pi}}{12}\phi(\frac{\kappa x}{\sqrt{2-\kappa^2}})\Phi(\frac{\kappa x}{\sqrt{(2-\kappa^2)(5-3\kappa^2)}})$$
$$+\frac{\frac{3\sqrt{\pi}}{\sqrt{2}}(-9\kappa^8x^2+18\kappa^8+81\kappa^6x^2-135\kappa^6-243\kappa^4x^2+459\kappa^4+387\kappa^2x^2-909\kappa^2+783)}{54(3-\kappa^2)^{\frac{5}{2}}}$$
$$\times\phi(\frac{\kappa x}{\sqrt{3-\kappa^2}})\Phi(\frac{2\kappa x}{\sqrt{(3-\kappa^2)(5-3\kappa^2)}})$$
$$+\frac{\sqrt{2\pi(5-3\kappa^2)}\kappa x}{12}\phi(\frac{\kappa x}{\sqrt{2-\kappa^2}})\phi(\frac{\kappa x}{\sqrt{(2-\kappa^2)(5-3\kappa^2)}})$$
$$+\frac{2\kappa x\sqrt{2\pi(5-3\kappa^2)}(\frac{9\kappa^4}{4}-\frac{27\kappa^2}{2}+\frac{189}{4})}{27(\kappa^2-3)^2}\phi(\frac{\kappa x}{\sqrt{3-\kappa^2}})\phi(\frac{2\kappa x}{\sqrt{(3-\kappa^2)(5-3\kappa^2)}})\}$$

$$\Sigma_1 =: \begin{pmatrix} 6-3\kappa^2 & \sqrt{5-3\kappa^2} \\ \sqrt{5-3\kappa^2} & 1 \end{pmatrix}$$

$$\Sigma_2 =: \begin{pmatrix} \frac{9-3\kappa^2}{4} & \frac{\sqrt{5-3\kappa^2}}{2} \\ \frac{\sqrt{5-3\kappa^2}}{2} & 1 \end{pmatrix}$$

$N = 4$, $i_0 = 4$

$$
\begin{aligned}
h(x) = \frac{\phi(x)}{Q}\{ & C_{1,x}\phi(\frac{\kappa x}{\sqrt{2-\kappa^2}})\phi(\frac{\kappa x}{\sqrt{2\kappa^4-7\kappa^2+6}}) + C_{2,x}\phi(\frac{\kappa x}{\sqrt{2-\kappa^2}})\Phi(\frac{\kappa x}{\sqrt{2\kappa^4-7\kappa^2+6}}) \\
& + C_{3,x}\phi(\frac{\sqrt{3}\kappa x}{\sqrt{5-3\kappa^2}})\phi(\frac{\kappa x}{\sqrt{6\kappa^4-19\kappa^2+15}}) + C_{4,x}\phi(\frac{\sqrt{3}\kappa x}{\sqrt{5-3\kappa^2}})\Phi(\frac{\kappa x}{\sqrt{6\kappa^4-19\kappa^2+15}}) \\
& + C_{5,x}\phi(\frac{\kappa x}{\sqrt{3-\kappa^2}})\Phi(\frac{\sqrt{3}\kappa x}{\sqrt{2\kappa^4-9\kappa^2+9}}) \\
& + C_{6,x}\{\phi(\frac{\kappa x}{\sqrt{3-\kappa^2}})\Phi_{\Sigma_2}(-\frac{2\sqrt{3}\kappa x}{\kappa^2-3}, \frac{\sqrt{3}\kappa x}{\sqrt{2\kappa^4-9\kappa^2+9}}) \\
& + \phi(\frac{\kappa x}{\sqrt{3-\kappa^2}})\Phi_{\Sigma_3}(-\frac{\sqrt{3}\kappa x}{\kappa^2-3}, \frac{\sqrt{3}\kappa x}{\sqrt{2\kappa^4-9\kappa^2+9}})\} \\
& + C_{7,x}\Phi(\frac{\sqrt{2}\kappa x}{\sqrt{3-2\kappa^2}}) + C_{8,x}\Phi_{\Sigma_1}(\sqrt{2}\kappa x, \frac{\sqrt{2}\kappa x}{\sqrt{3-2\kappa^2}}) \\
& + C_{9,x}\phi(\frac{\kappa x}{\sqrt{3-\kappa^2}})\phi(\frac{2\kappa x}{\sqrt{3\kappa^4-14\kappa^2+15}})\phi(\frac{\kappa x}{\sqrt{6\kappa^4-19\kappa^2+15}}) \\
& + C_{10,x}\phi(\frac{\kappa x}{\sqrt{3-\kappa^2}})\phi(\frac{2\kappa x}{\sqrt{3\kappa^4-14\kappa^2+15}})\Phi(\frac{\kappa x}{\sqrt{6\kappa^4-19\kappa^2+15}}) \\
& + C_{11,x}\phi(\frac{\kappa x}{\sqrt{3-\kappa^2}})\phi(\frac{\kappa x}{\sqrt{\kappa^4-5\kappa^2+6}})\phi(\frac{\kappa x}{\sqrt{2\kappa^4-7\kappa^2+6}}) \\
& + C_{12,x}\phi(\frac{\kappa x}{\sqrt{3-\kappa^2}})\phi(\frac{\kappa x}{\sqrt{\kappa^4-5\kappa^2+6}})\Phi(\frac{\kappa x}{\sqrt{2\kappa^4-7\kappa^2+6}})\}
\end{aligned}
$$

where:

$$Q = -\frac{19\sqrt{3}}{24\sqrt{2\pi}} + \frac{\sqrt{2\pi}}{\sqrt{3}}\left(-\frac{25}{24} + \frac{25}{12}[\Phi_{\Sigma_4}(0,0) + \Phi_{\Sigma_5}(0,0)]\right)$$

$$C_{1,x} = -\frac{\sqrt{2\pi(3-2\kappa^2)}}{2592(\kappa^2-2)^3}(-648\kappa^2x^2 + 1944\kappa^8 + 3888\kappa^6x^2 - 8424\kappa^6 - 7776\kappa^4x^2 + 2648\kappa^4$$

$$+ 5312\kappa^2x^2 + 28544\kappa^2 - 31392)$$

$$C_{2,x} = -\frac{\sqrt{2\pi}\kappa x}{324(3-\kappa^2)^{\frac{7}{2}}}(-162\kappa^{10}x^2 + 810\kappa^{10} + 1296\kappa^8x^2 - 6156\kappa^8 - 3888\kappa^6x^2 + 16848\kappa^6$$

$$+ 5184\kappa^4x^2 - 18021\kappa^4 - 2608\kappa^2x^2 + 2052\kappa^2 + 5772)$$

$$C_{3,x} = -\frac{\sqrt{2\pi(3-2\kappa^2)}(183\kappa^4 + 4\kappa^2x^2 - 602\kappa^2 + 495)}{162(3\kappa^2-5)^3}$$

$$C_{4,x} = \frac{\sqrt{2\pi}\kappa x(207\kappa^4 + 4\kappa^2x^2 - 678\kappa^2 + 555)}{162(5-3\kappa^2)^{\frac{7}{2}}}$$

$$C_{5,x} = -\frac{2\pi(108\kappa^8 + 288\kappa^6x^2 - 1008\kappa^6 + 64\kappa^4x^4 - 1344\kappa^4x^2 + 3432\kappa^4 + 1440\kappa^2x^2)}{16(3-\kappa^2)^{\frac{9}{2}}}$$

$$- \frac{2\pi(-5040\kappa^2 + 2700)}{16(3-\kappa^2)^{\frac{9}{2}}}$$

$$C_{6,x} = \frac{2\pi}{144(3-\kappa^2)^{\frac{9}{2}}}(972\kappa^8 + 2592\kappa^6x^2 - 9072\kappa^6 + 576\kappa^4x^4 - 12096\kappa^4x^2 + 30888\kappa^4$$

$$+ 12960\kappa^2x^2 - 45360\kappa^2 + 24300)$$

$$C_{7,x} = -\frac{\sqrt{2\pi}\kappa^4(4x^4 - 24x^2 + 12)}{16}$$

$$C_{8,x} = \frac{\sqrt{2\pi}\kappa^4(4x^4 - 24x^2 + 12)}{8}$$

$$C_{9,x} = (\{512\sqrt{2}\pi\{\{(2\kappa^2-3)^2$$

$$\times [\frac{3\sqrt{2}(174\kappa^8 + 217\kappa^6x^2 - 1379\kappa^6 - 690\kappa^4x^2 + 3975\kappa^4 + 549\kappa^2x^2 - 4977\kappa^2 + 2295)}{4\sqrt{3}(\kappa^2-3)^3\sqrt{3-2\kappa^2}(3\kappa^2-5)^3}$$

$$+ \frac{18\kappa^2x^2(3-2\kappa^2)^{\frac{3}{2}}}{\sqrt{6}(\kappa^2-3)^3(6\kappa^2-10)} + \frac{72\sqrt{3}\kappa^2x^2(17\kappa^2-27)(\frac{\kappa^2-3}{9\kappa^2-15})^{\frac{3}{2}}(\frac{\kappa^2}{2}-\frac{3}{4})}{\sqrt{6}(3-\kappa^2)^{\frac{9}{2}}\sqrt{(5-3\kappa^2)(3-2\kappa^2)}}]\}/16$$

$$- \kappa x(3-2\kappa^2)^{\frac{3}{2}}(\frac{36\kappa x(\frac{\kappa^2}{2}-\frac{3}{4})}{\sqrt{3}(\kappa^2-3)^2(6\kappa^2-10)} - \frac{9\sqrt{3}\kappa x(\frac{\kappa^2-3}{9\kappa^2-15})^{\frac{3}{2}}(17\kappa^2-27)}{2\sqrt{3}(3-\kappa^2)^{\frac{7}{2}}\sqrt{5-3\kappa^2}})/2\sqrt{2}$$

$$+ \frac{9\kappa^2x^2(3-2\kappa^2)^{\frac{3}{2}}}{4\sqrt{6}(3\kappa^4-14\kappa^2+15)}\}\}/81\sqrt{3})$$

$$C_{10,x} = \{\{512\sqrt{2}\pi\{\{(2\kappa^2-3)^2$$
$$\times\{\frac{9\kappa x\sqrt{3-2\kappa^2}(\frac{4\sqrt{3-2\kappa^2}}{\sqrt{3(5-3\kappa^2)}} - \frac{2\sqrt{3}(\frac{\kappa^2-3}{9\kappa^2-15})^{\frac{3}{2}}\sqrt{3-2\kappa^2}(-3\kappa^6-32\kappa^4x^2+23\kappa^4+48\kappa^2x^2-57\kappa^2+45)}{\sqrt{3}(3-\kappa^2)^{\frac{5}{2}}(3\kappa^2-5)}}{\sqrt{2}(\kappa^2-3)^3}$$
$$-\frac{3\sqrt{2}\kappa^3x^3(2\kappa^2-3)^2}{\sqrt{3}(\kappa^2-3)^4\sqrt{5-3\kappa^2}} - \frac{18\sqrt{2}\kappa^3x^3(2\kappa^2-3)^2}{\sqrt{3}(\kappa^2-3)^4(5-3\kappa^2)^{\frac{3}{2}}}$$
$$+\frac{\sqrt{2}\kappa x(2\kappa^2-3)(-1620\kappa^6-576\kappa^4x^2+10476\kappa^4+864\kappa^2x^2-21708\kappa^2+14580)}{6\sqrt{3}(\kappa^2-3)^4(5-3\kappa^2)^{\frac{7}{2}}}\}\}$$
$$-\{\kappa x(3-2\kappa^2)^{\frac{3}{2}}(\frac{9\sqrt{2}\kappa^2x^2(3-2\kappa^2)^{\frac{3}{2}}}{2\sqrt{6}(\kappa^2-3)^3\sqrt{5-3\kappa^3}}$$
$$-\frac{\frac{36\sqrt{3-2\kappa^2}}{\sqrt{3(5-3\kappa^2)}} - \frac{18\sqrt{3}(\frac{\kappa^2-3}{9\kappa^2-15})^{\frac{3}{2}}\sqrt{3-2\kappa^2}(-3\kappa^6-32\kappa^4x^2+23\kappa^4+48\kappa^2x^2-57\kappa^2+45)}{\sqrt{3}(3-\kappa^2)^{\frac{5}{2}}(3\kappa^2-5)}}{4(\kappa^2-3)^2}$$
$$+\frac{18\kappa^2x^2(3-2\kappa^2)^{\frac{3}{2}}}{\sqrt{2}(\kappa^2-3)^3(5-3\kappa^2)^{\frac{3}{2}}})\}/(2\sqrt{2}) + \frac{6\sqrt{2}\kappa^3x^3(\frac{\kappa^2}{2}-\frac{3}{4})}{\sqrt{3(5-3\kappa^2)}(\kappa^2-3)}$$
$$+\frac{3\sqrt{2}\kappa^3x^3(2\kappa^2-3)(\frac{\kappa^2}{2}-\frac{3}{4})(9\kappa^2-21)}{\sqrt{3}(\kappa^2-3)^2(5-3\kappa^2)^{\frac{3}{2}}}\}\}/(8\sqrt{3}) + \frac{16\pi\kappa x(2\kappa^2-3)(5\kappa^2-9)}{9(\kappa^2-3)^2(5-3\kappa^2)^{\frac{3}{2}}}\}$$
$$C_{11,x} = \{\frac{4\pi(3-2\kappa^2)^{\frac{3}{2}}}{9\kappa^4-45\kappa^2+54} + \{512\sqrt{2}\pi\{\{(2\kappa^2-3)^2$$
$$\{\frac{3\sqrt{2}(22\kappa^8+19\kappa^6x^2-191\kappa^6-69\kappa^4x^2+609\kappa^4+63\kappa^2x^2-846\kappa^2+432)}{3\sqrt{3(3-2\kappa^2)}(\kappa^2-2)^3(\kappa^2-3)^3}+$$
$$\frac{9\kappa^2x^2(3-2\kappa^2)^{\frac{3}{2}}}{2\sqrt{6}(\kappa^2-2)(\kappa^2-3)^3} + \frac{12\kappa^2x^2(\frac{\kappa^2-3}{\kappa^2-2})^{\frac{3}{2}}(\frac{\kappa^2}{2}-\frac{3}{4})(5\kappa^2-9)}{\sqrt{6(2-\kappa^2)(3-2\kappa^2)(3-\kappa^2)^{\frac{9}{2}}}}\}\}/16$$
$$-\frac{\kappa x(3-2\kappa^2)^{\frac{3}{2}}(\frac{9\kappa x(\frac{\kappa^2}{2}-\frac{3}{4})}{\sqrt{3}(\kappa^2-2)(\kappa^2-3)^2} - \frac{3\kappa x(\frac{\kappa^2-3}{\kappa^2-2})^{\frac{3}{2}}(5\kappa^2-9)}{4\sqrt{3(2-\kappa^2)}(3-\kappa^2)^{\frac{7}{2}}})}{2\sqrt{2}} + \frac{9\kappa^2x^2(3-2\kappa^2)^{\frac{3}{2}}}{8\sqrt{6}(\kappa^4-5\kappa^2+6)}\}\}/(81\sqrt{3})\}$$

$$C_{12,x} = \{\{512\sqrt{2}\pi\{\{(2\kappa^2-3)^2$$
$$\times\Big\{\frac{9\kappa x\sqrt{3-2\kappa^2}\Big(\frac{2\sqrt{3-2\kappa^2}}{\sqrt{3(2-\kappa^2)}}-\frac{2\left(\frac{\kappa^2-3}{\kappa^2-2}\right)^{\frac{3}{2}}\sqrt{3-2\kappa^2}\left(-\kappa^6-2\kappa^4x^2+8\kappa^4+3\kappa^2x^2-21\kappa^2+18\right)}{6\sqrt{3}(\kappa^2-2)(3-\kappa^2)^{\frac{5}{2}}}\Big)}{\sqrt{2}(\kappa^2-3)^3}$$
$$-\frac{3\sqrt{2}\kappa^3x^3(2\kappa^2-3)^2}{2\sqrt{3(2-\kappa^2)}(\kappa^2-3)^4}-\frac{9\sqrt{2}\kappa^3x^3(2\kappa^2-3)^2}{4\sqrt{3}(2-\kappa^2)^{\frac{3}{2}}(\kappa^2-3)^4}$$
$$+\frac{3\sqrt{2}\kappa x(2\kappa^2-3)\left(-24\kappa^6-4\kappa^4x^2+174\kappa^4+6\kappa^2x^2-414\kappa^2+324\right)}{16\sqrt{3}(2-\kappa^2)^{\frac{7}{2}}(\kappa^2-3)^4}\Big\}\}/16$$
$$-\Big\{\kappa x(3-2\kappa^2)^{\frac{3}{2}}\Big(\frac{9\sqrt{2}\kappa^2x^2(3-2\kappa^2)^{\frac{3}{2}}}{4\sqrt{6(2-\kappa^2)}(\kappa^2-3)^3}$$
$$-\frac{\frac{18\sqrt{3-2\kappa^2}}{\sqrt{3(2-\kappa^2)}}-\frac{6\left(\frac{\kappa^2-3}{\kappa^2-2}\right)^{\frac{3}{2}}\sqrt{3-2\kappa^2}\left(-\kappa^6-2\kappa^4x^2+8\kappa^4+3\kappa^2x^2-21\kappa^2+18\right)}{2\sqrt{3}(\kappa^2-2)(3-\kappa^2)^{\frac{5}{2}}}}{4(\kappa^2-3)^2}$$
$$+\frac{18\kappa^2x^2(3-2\kappa^2)^{\frac{3}{2}}}{8\sqrt{3}(2-\kappa^2)^{\frac{3}{2}}(\kappa^2-3)^3}\Big)\Big\}/(2\sqrt{2})+\frac{3\sqrt{2}\kappa^3x^3\left(\frac{\kappa^2}{2}-\frac{3}{4}\right)}{\sqrt{3(2-\kappa^2)}(\kappa^2-3)}$$
$$+\frac{9\sqrt{2}\kappa^3x^3(2\kappa^2-3)^2(2\kappa^2-5)}{16\sqrt{3}(2-\kappa^2)^{\frac{3}{2}}(\kappa^2-3)^2}\Big\}\}/(81\sqrt{3})+\frac{4\pi\kappa x(8\kappa^4-30\kappa^2+27)}{9(2-\kappa^2)^{\frac{3}{2}}(\kappa^2-3)^2}\Big\}$$
$$\Sigma_1 =: \begin{pmatrix} 4-2\kappa^2 & \sqrt{3-2\kappa^2} \\ \sqrt{3-2\kappa^2} & 1 \end{pmatrix}$$
$$\Sigma_2 =: \begin{pmatrix} \frac{9\kappa^2-15}{\kappa^2-3} & \frac{2\sqrt{3-2\kappa^2}}{\sqrt{3-\kappa^2}} \\ \frac{2\sqrt{3-2\kappa^2}}{\sqrt{3-\kappa^2}} & 1 \end{pmatrix}$$
$$\Sigma_3 =: \begin{pmatrix} \frac{3\kappa^2-6}{\kappa^2-3} & \frac{\sqrt{3-2\kappa^2}}{\sqrt{3-\kappa^2}} \\ \frac{\sqrt{3-2\kappa^2}}{\sqrt{3-\kappa^2}} & 1 \end{pmatrix}$$
$$\Sigma_4 =: \begin{pmatrix} 5 & 2 \\ 2 & 1 \end{pmatrix}$$
$$\Sigma_5 =: \begin{pmatrix} 2 & 1 \\ 1 & 1 \end{pmatrix}$$

6.3.2 Degenerate

When $\kappa^2 = \frac{N+2}{N}$, the height density is degenerate, we have the following results:

$N = 3$, $i_0 = 1$

$$
\begin{aligned}
h(x) = \frac{72\phi(x)}{\pi(36+29\sqrt{6})}\{&\frac{5\pi\sqrt{15\pi}}{18}x^3\Phi(\frac{\sqrt{5}}{2}x) - \frac{5\pi\sqrt{15\pi}}{18}x^3\Phi_{\Sigma_1}(\frac{\sqrt{30}}{6}x, \frac{\sqrt{15}}{3}x)\\
&- \frac{155\sqrt{6}\pi}{72}x^2e^{-\frac{5}{8}x^2}\sigma(x) + \frac{155\sqrt{6}\pi}{72}x^2e^{-\frac{5}{8}x^2}\\
&- \frac{5\sqrt{6}\pi}{36}x^2e^{-\frac{5}{2}x^2}\sigma(x) - \frac{5\pi\sqrt{15\pi}}{6}x\Phi(\frac{\sqrt{5}}{2}x)\\
&+ \frac{5\pi\sqrt{15\pi}}{6}x\Phi_{\Sigma_1}(\frac{\sqrt{30}}{6}x, \frac{\sqrt{15}}{3}x) + \frac{4\sqrt{6}\pi}{9}e^{-\frac{5}{8}x^2}\sigma(x)\\
&- \frac{4\sqrt{6}\pi}{9}e^{-\frac{5}{8}x^2} - \frac{4\sqrt{6}\pi}{9}e^{-\frac{5}{2}x^2}\sigma(x)\}
\end{aligned}
$$

where:

$$
\Sigma_1 =: \begin{pmatrix} \frac{2}{3} & -\frac{2\sqrt{2}}{6} \\ -\frac{2\sqrt{2}}{6} & \frac{1}{3} \end{pmatrix}
$$

$$
\sigma(x) = \begin{cases} 0 & x < 0 \\ \frac{1}{2} & x = 0 \\ 1 & x > 0 \end{cases}
$$

$N = 3$, $i_0 = 3$

$$h(x) = \frac{12\sqrt{12}\phi(x)}{29 - 6\sqrt{6}}\{(\frac{5\sqrt{30}}{12}x - \frac{5\sqrt{30}}{36}x^3)\sqrt{\pi}[1 - \Phi(\sqrt{5}x) - \Phi(\frac{\sqrt{5}}{2}x)]$$
$$+ (\frac{5\sqrt{6\pi}}{36}x^2 - \frac{4\sqrt{6\pi}}{9})\phi(\sqrt{5}x) + \frac{3\sqrt{3\pi}(2480x^2 + 512)}{1728\sqrt{2}}\phi(\frac{\sqrt{5}}{2}x)\}\mathbb{1}_{\{x\geq 0\}}$$

$N = 4$, $i_0 = 4$

$$h(x) = \frac{\phi(x)}{Q}\{c_{1,x}\phi(\sqrt{3x}) + c_{2,x}\phi(3x) + c_{3,x}\phi(x)$$
$$+ c_{4,x}(\phi(x)\Phi(2\sqrt{2}x) + \phi(x)\Phi(\sqrt{2}x)) + c_{5,x} + c_{6,x}\Phi(\sqrt{3}x)\}\mathbb{1}_{\{x\geq 0\}}$$

where:

$$Q = -\frac{19\sqrt{3}}{24\sqrt{2\pi}} + \frac{\sqrt{2\pi}}{\sqrt{3}}\{-\frac{25}{24} + \frac{25}{12}[\Phi_{\Sigma_1}(0,0) + \Phi_{\Sigma_2}(0,0)]\}$$
$$C_{1,x} = -\frac{2\sqrt{2\pi}x}{2187}(\frac{2415}{16} - \frac{627x^2}{16})$$
$$C_{2,x} = \frac{4\sqrt{6\pi}x}{81}(6x^2 + \frac{15}{4})$$
$$C_{3,x} = -\frac{2\sqrt{2}\pi}{81\sqrt{3}}(144x^4 + 108x^2 + \frac{27}{4})$$
$$C_{4,x} = \frac{2\sqrt{2}\pi}{729\sqrt{3}}(1296x^4 + 972x^2 + \frac{243}{4})$$
$$C_{5,x} = -\frac{\sqrt{2\pi}(9x^4 - 54x^2 + 27)}{16}$$
$$C_{6,x} = \frac{\sqrt{2\pi}(9x^4 - 54x^2 + 27)}{8}$$
$$\Sigma_1 =: \begin{pmatrix} 5 & 2 \\ 2 & 1 \end{pmatrix}$$
$$\Sigma_2 =: \begin{pmatrix} 2 & 1 \\ 1 & 1 \end{pmatrix}$$

6.3.3 Simulation

From the explicit formulae the last two sections given, there are only a small part of height distribution can be calculated directly without too much calculation when N is not large. This section will give the algorithm to simulate the height distribution when it can not be calculated easily.

Non Degenerate

For Non-Degenerate condition, we can simulate the height density for index=i by the following steps:

1. Simulate n GOI matrices with given N and κ for both denominator and numerator.

2. Calculate the eigenvalues of each GOI matrix and order them from small to large, store the reordered eigenvalues.

3. For a series of x, which represents the range of height density. Plug the n stored eigenvalues into the formula 6.6 one by one to get the expectation of both denominator and numerator.

When $\kappa^2 \leq 1$, the simulation approach for the GOI matrix can still be employed. However, utilizing the GOE matrix simplifies the calculation of both the denominator and numerator. The process of simulating the height density is similar to the GOI method, with the difference being the substitution of the eigenvalues of the GOE matrix into Theorem 6.1.1. The figure 6.1 shows the exact height densities of critical points of isotropic Gaussian fields

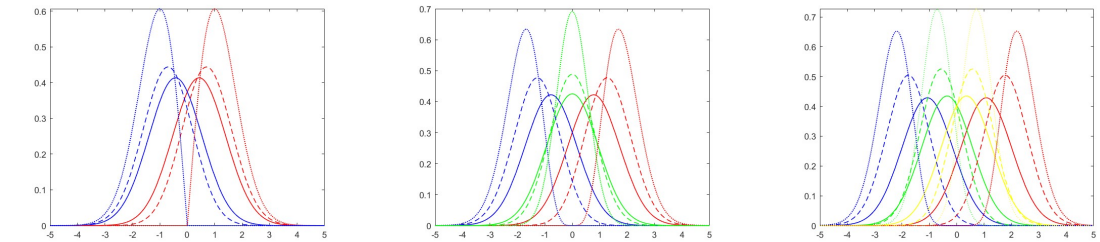

$N = 1$ $N = 2$ $N = 3$

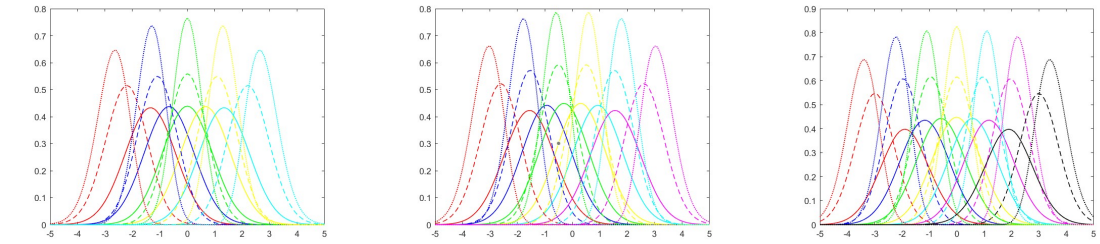

$N = 4$ $N = 5$ $N = 6$

Figure 6.1: Exact height densities of critical points of isotropic Gaussian fields on $\mathbb{R}^N$. For each figure, the solid, dashed and dotted curves are densities with $\kappa = 0.6$, $\kappa = 1$ and the boundary case $\kappa = \sqrt{(N+2)/N}$, respectively; and for a fixed κ, the densities from left to right, indicated by different colors, are $h_0(x)$, $h_1(x)$, $\ldots$, $h_N(x)$, respectively.

on $\mathbb{R}^N$.

Degenerate

The steps to simulate the Degenerate height density is similar to the Non-Degenerate one, just change the plugged in expectations for denominator and numerator.

6.4 Asymptotic Distribution on Euclidean Space

When $N \to \infty$, $(N+2)/N \to 1$, which means nearly all $\kappa^2 < 1$. When $\kappa^2 < 1$, By Lemma A.1 in the work of Cheng[14], the density (6.6) can be written as

$$f_i(x) = \frac{\phi(x)\mathbb{E}^{N+1}_{\mathrm{GOE}}\left[e^{\frac{\lambda^2_{i+1}}{2} - \frac{(\lambda_{i+1} - \kappa x/\sqrt{2})^2}{1-\kappa^2}}\right]}{\sqrt{1-\kappa^2}\,\mathbb{E}^{N+1}_{\mathrm{GOE}}\left[e^{-\frac{\lambda^2_{i+1}}{2}}\right]}. \tag{6.19}$$

So if we know the asymptotic distribution of each eigenvalue of GOE matrix, the corresponding asymptotic distribution of equation 6.19 can also be achieved.

6.4.1 The Distribution of the Eigenvalues Which are Not the Maximum

From the paper of O'Rourke, S.[29], we can get the following results with the definition:

$$G(t) = \frac{2}{\pi}\int_{-1}^{t}\sqrt{1-x^2}dx \qquad -1 \le t < 1. \tag{6.20}$$

Theorem 6.4.1. *Let $x_1 < x_2 < \cdots < x_n$ be the ordered eigenvalues from matrix drawn from the GOE, GUE, GSE. Consider $\{x_{k_i}\}_{i=1}^m$ such that $0 < k_i - k_{i+1} \sim n^{\theta_i},\ 0 < \theta_i \le 1, and\ \frac{k_i}{n} \to a_i \in (0,1)$ as $n \to \infty$. Define $s_i = s_i(k_i, n) = G^{-1}(k_i/n)$ and set*

$$X_i = \frac{x_{k_i} - s_i\sqrt{2n}}{(\frac{logn}{2\beta(1-s_i^2)n})^{\frac{1}{2}}}, \qquad i = 1, \ldots, m$$

Where $\beta = 1, 2, 4$ corresponds to the GOE, GUE, GSE. Then as $n \to \infty$,

$$P[X_1 \le \xi_1, \ldots, X_m \le \xi_m] \longrightarrow \Phi_\Lambda(\xi_1, \ldots, \xi_m)$$

Where Φ_Λ is the cdf for the m-dimensional normal distribution with covariance matrix $\Lambda_{i,j} = 1 - max\{\theta_k : i \le k \le j \le m\}$ if $i \le j$ and $\Lambda_{i,j} = 1$.

In this project, we only take one eigenvalue, so we can take $m = 1$, then Theorem 6.4.1 can be stated as follow.

Corollary 6.4.1.1. Set $t = t(k,n) = G^{-1}(k/n)$ where $k = k(n)$ is such that $k/n \to a \in (0,1)$ as $n \to \infty$. If x_k denotes eigenvalue number k in the GOE, GUE, or GSE, it holds that, as $n \to \infty$,

$$\frac{x_k - t\sqrt{2n}}{(\frac{\log n}{2\beta(1-t^2)n})^{\frac{1}{2}}} \longrightarrow N(0,1)$$

in distribution where $\beta = 1, 2, 4$ corresponds to the GOE, GUE, or GSE.

By the corollary 6.4.1.1, we can calculate the asymptotic height density by (1.5).

Theorem 6.4.2. *When $N \to \infty$ and $\kappa^2 \leq 1$, let $\mu = t\sqrt{2n}$ and $\sigma = \frac{\log n}{2(1-t^2)n}$, where t is defined before, the asymptotic height density for index$(\nabla^2 X(t)) = i_0$ can be written as a form of normal distribution:*

$$h(x) = \frac{1}{\sqrt{2\pi\alpha}} e^{-\frac{(x-\frac{\sqrt{2}\kappa\mu}{\sigma^2+1})^2}{2\alpha}}$$

Where $\alpha = \frac{\kappa^2\sigma^2-\kappa^2+\sigma^2+1}{\sigma^2+1}$, which is constant.

Proof. From (1.5) and corollary 6.4.1.1, we can write the height density as follow:

$$h(x) = \frac{\phi(x)\mathbb{E}^{N+1}_{\mathrm{GOE}}(e^{\frac{\lambda^2_{i_0+1}}{2} - \frac{(\lambda_{i_0+1} - \frac{\kappa x}{\sqrt{2}})^2}{1-\kappa^2}})}{\sqrt{1-\kappa^2}\mathbb{E}^{N+1}_{\mathrm{GOE}}(e^{-\frac{\lambda^2_{i_0+1}}{2}})} \tag{6.21}$$

The denominator is:

$$\begin{aligned}\sqrt{1-\kappa^2}\mathbb{E}^{N+1}_{\mathrm{GOE}}(e^{-\frac{\lambda^2_{i_0+1}}{2}}) =& \sqrt{1-\kappa^2}\int_{-\infty}^{\infty} e^{-\frac{\lambda^2_{i_0+1}}{2}} \frac{1}{\sqrt{2\pi}\sigma} e^{-\frac{(\lambda_{i_0+1}-\mu)^2}{2\sigma^2}} d\lambda_{i_0+1} \\ =& \frac{\sqrt{1-\kappa^2}}{\sqrt{1+\sigma^2}} e^{-\frac{\mu^2}{2(\sigma^2+1)}}\end{aligned} \tag{6.22}$$

where $\mu = t\sqrt{2n}$ and $\sigma = (\frac{\log n}{2(1-t^2)n})^{\frac{1}{2}}$, and t is the solution of $G^{-1}(k/n) = a_i$

Then the numerator is:

$$\begin{aligned}
&\phi(x)\mathbb{E}_{\mathrm{GOE}}^{N+1}(e^{\frac{\lambda_{i_0+1}^2}{2}-\frac{(\lambda_{i_0+1}-\frac{\kappa x}{\sqrt{2}})^2}{1-\kappa^2}}) \\
=&\phi(x)\int_{-\infty}^{\infty} e^{\frac{\lambda_{i_0+1}^2}{2}-\frac{(\lambda_{i_0+1}-\frac{\kappa x}{\sqrt{2}})^2}{1-\kappa^2}}\frac{1}{\sqrt{2\pi}\sigma}e^{-\frac{(\lambda_{i_0+1}-\mu)^2}{2\sigma^2}}d\lambda_{i_0+1} \\
=&\phi(x)\int_{-\infty}^{\infty} e^{\frac{\lambda_{i_0+1}^2}{2}-\frac{\lambda_{i_0+1}^2}{1-\kappa^2}+\frac{\sqrt{2}\kappa x\lambda_{i_0+1}}{1-\kappa^2}-\frac{\kappa^2x^2}{2(1-\kappa^2)}}\frac{1}{\sqrt{2\pi}\sigma}e^{-\frac{\lambda_{i_0+1}^2-2\mu\lambda_{i_0+1}+\mu^2}{2\sigma^2}}d\lambda_{i_0+1} \\
=&\phi(x)\int_{-\infty}^{\infty} \frac{1}{\sqrt{2\pi}\sigma}e^{(\frac{1}{2}-\frac{1}{1-\kappa^2}-\frac{1}{2\sigma^2})\lambda_{i_0+1}^2+(\frac{\sqrt{2}\kappa x}{1-\kappa^2}+\frac{\mu}{\sigma^2})\lambda_{i_0+1}-(\frac{\kappa^2x^2}{2(1-\kappa^2)}+\frac{\mu^2}{2\sigma^2})}d\lambda_{i_0+1}
\end{aligned} \tag{6.23}$$

Let $a = -(\frac{1}{2}-\frac{1}{1-\kappa^2}-\frac{1}{2\sigma^2})$, $b = \frac{\sqrt{2}\kappa x}{1-\kappa^2}+\frac{\mu}{\sigma^2}$ and $c = -(\frac{\kappa^2x^2}{2(1-\kappa^2)}+\frac{\mu^2}{2\sigma^2})$, then the integral can be written as:

$$\begin{aligned}
&\phi(x)\mathbb{E}_{\mathrm{GOE}}^{N+1}(e^{\frac{\lambda_{i_0+1}^2}{2}-\frac{(\lambda_{i_0+1}-\frac{\kappa x}{\sqrt{2}})^2}{1-\kappa^2}}) \\
=&\phi(x)\int_{-\infty}^{\infty} \frac{1}{\sqrt{2\pi}\sigma}e^{(\frac{1}{2}-\frac{1}{1-\kappa^2}-\frac{1}{2\sigma^2})\lambda_{i_0+1}^2+(\frac{\sqrt{2}\kappa x}{1-\kappa^2}+\frac{\mu}{\sigma^2})\lambda_{i_0+1}-(\frac{\kappa^2x^2}{2(1-\kappa^2)}+\frac{\mu^2}{2\sigma^2})}d\lambda_{i_0+1} \\
=&\phi(x)\int_{-\infty}^{\infty} \frac{1}{\sqrt{2\pi}\sigma}e^{-a\lambda_{i_0+1}^2+b\lambda_{i_0+1}+c}d\lambda_{i_0+1} \\
=&\phi(x)\int_{-\infty}^{\infty} \frac{1}{\sqrt{2\pi}\frac{1}{\sqrt{2a}}}\frac{1}{\sqrt{2a}\sigma}e^{-\frac{(\lambda_{i_0+1}-\frac{b}{2a})^2}{2(\frac{1}{\sqrt{2a}})^2}}e^{c+\frac{b^2}{4a}}d\lambda_{i_0+1} \\
=&\phi(x)\frac{1}{\sqrt{2a}\sigma}e^{c+\frac{b^2}{4a}}
\end{aligned} \tag{6.24}$$

Then we can get the height distribution:

$$\begin{aligned}
h(x) &= \frac{\phi(x)\frac{1}{\sqrt{2a}\sigma}e^{c+\frac{b^2}{4a}}}{\frac{\sqrt{1-\kappa^2}}{\sqrt{1+\sigma^2}}e^{-\frac{\mu^2}{2(\sigma^2+1)}}} \\
&= \frac{1}{\sqrt{2\pi}\sqrt{\frac{1}{2\alpha}}}e^{-\frac{(x-\frac{\sqrt{2}\kappa\mu}{\sigma^2+1})^2}{2(\sqrt{\frac{1}{2\alpha}})^2}},
\end{aligned} \tag{6.25}$$

where $\alpha = \frac{\sigma^2+1}{2(\kappa^2\sigma^2-\kappa^2+\sigma^2+1)}$, which is constant, if we let $\alpha = \frac{(\kappa^2\sigma^2-\kappa^2+\sigma^2+1)}{\sigma^2+1}$, the results in the theorem can be obtained. □

6.4.2 The Distribution of the Largest Eigenvalue of GOE Matrix

From the previously mentioned theorem, we have obtained the distribution of any eigenvalue of the GOE matrix when $a_i \in (0, 1)$. Now, we will focus on describing the distribution of the largest eigenvalue of the GOE matrix.

Tracy-Widom Distribution

For GOE matrix, the Tracy-Widom distribution can be defined as:

$$F(x) = \lim_{n\to\infty} \text{Prob}\left((\lambda_{max} - \sqrt{2n})(\sqrt{2})n^{1/6} \leq x\right)$$

Where $F(x)$ is the CDF of x.

Simulation of Tracy-Widom Distribution

With the Tracy-Widom distribution, we can obtain the height density through simulation. Since the Tracy-Widom distribution does not have an explicit form, we need to simulate it using numerical methods. The distribution can be simulated using the following steps:

1. For a given N, we can get the numerical CDF($F(x)$) of Tracy-Widom distribution.

2. Calculate the numerical PDF($f_N(x)$) with small enough step size.

3. Calculate the expectation of both denominator and numerator of the GOE formula in theorem 6.1.1 by calculating the Riemann Integral.

6.4.3 Simulation

This section will show the asymptotic distribution when N is growing large.

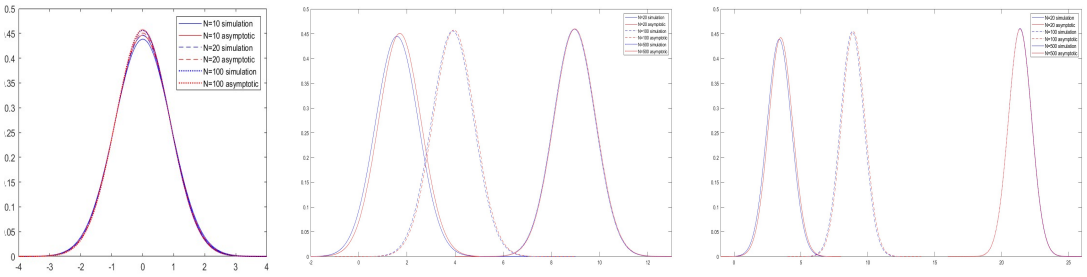

a_i = 0.5 a_i = 0.75 Maximum

Figure 6.2: The comparison between asymptotic distributions and simulations.

6.5 Explicit Distribution on Sphere

The previous section was based on $\mathbb{R}^N$, whereas this section demonstrates the analogous output of the height density on sphere.

6.5.1 Non Degenerate

When $0 < \kappa^2 - \eta^2 < (N+2)/N$, the height density is non-degenerate, we have the following implicit results:

$$F_i(u) = \frac{\int_u^\infty \phi(x)\mathbb{E}_{\mathrm{GOI}((1+\eta^2-\kappa^2)/2)}[\prod_{j=1}^N |\lambda_j - \kappa x/\sqrt{2}|\mathbb{1}_{\{\lambda_i<\kappa x/\sqrt{2}<\lambda_{i+1}\}}]dx}{\mathbb{E}_{\mathrm{GOI}((1+\eta^2)/2)}[\prod_{j=1}^N |\lambda_j|\mathbb{1}_{\{\lambda_i<0<\lambda_{i+1}\}}]} \tag{6.26}$$

Then, we can get the height distribution:

$$h_i(u) = \frac{\phi(u)\mathbb{E}_{\mathrm{GOI}((1+\eta^2-\kappa^2)/2)}[\prod_{j=1}^N |\lambda_j - \kappa u/\sqrt{2}|\mathbb{1}_{\{\lambda_i<\kappa u/\sqrt{2}<\lambda_{i+1}\}}]}{\mathbb{E}_{\mathrm{GOI}((1+\eta^2)/2)}[\prod_{j=1}^N |\lambda_j|\mathbb{1}_{\{\lambda_i<0<\lambda_{i+1}\}}]} \tag{6.27}$$

$N = 3, i_0 = 0$

$$
\begin{aligned}
h(x) = & \left\{ \frac{1}{2\sqrt{2(3+\eta^2)}} \left[\frac{3}{2} + \frac{(1+\eta^2)(2\eta^4+7\eta^2+11)}{4(3+\eta^2)} \right] + \frac{(\eta^2-1)(\eta^2+2)}{4\sqrt{2(2+\eta^2)}} \right\}^{-1} \phi(x) \\
& \times \left\{ \left[\frac{\kappa^2[(1+\eta^2-\kappa^2)^3 + 6(1+\eta^2-\kappa^2)^2 + 12(1+\eta^2-\kappa^2) + 24]}{4(3+\eta^2-\kappa^2)^2} x^2 \right.\right. \\
& \left. + \frac{2(1+\eta^2-\kappa^2)^3 + 3(1+\eta^2-\kappa^2)^2 + 6(1+\eta^2-\kappa^2)}{4(3+\eta^2-\kappa^2)} + \frac{3}{2} \right] \frac{1}{\sqrt{2(3+\eta^2-\kappa^2)}} \\
& \times e^{-\frac{\kappa^2 x^2}{2(3+\eta^2-\kappa^2)}} \Phi\left(\frac{2\kappa x}{\sqrt{(3+\eta^2-\kappa^2)(5+3\eta^2-3\kappa^2)}} \right) \\
& + \left[\frac{\kappa^2(2+\eta^2-\kappa^2)}{4} x^2 + \frac{(\eta^2-\kappa^2)(1+\eta^2-\kappa^2)}{2} - 1 \right] \frac{1}{\sqrt{2(2+\eta^2-\kappa^2)}} \\
& \times e^{-\frac{\kappa^2 x^2}{2(2+\eta^2-\kappa^2)}} \Phi\left(\frac{\kappa x}{\sqrt{(2+\eta^2-\kappa^2)(5+3\eta^2-3\kappa^2)}} \right) \\
& + \left[7 + \eta^2 - \kappa^2 + \frac{3(1+\eta^2-\kappa^2)^3 + 12(1+\eta^2-\kappa^2)^2 + 28(1+\eta^2-\kappa^2)}{2(3+\eta^2-\kappa^2)} \right] \\
& \times \frac{\kappa}{4\sqrt{\pi}(3+\eta^2-\kappa^2)\sqrt{5+3\eta^2-3\kappa^2}} x e^{-\frac{3\kappa^2 x^2}{2(5+3\eta^2-3\kappa^2)}} \\
& \left. + [\kappa^2 x^2 + 3(\eta^2-\kappa^2)] \frac{\sqrt{\pi}\kappa}{4} x \left[\Phi_{\Sigma_1}\left(0, \frac{\kappa x}{\sqrt{2}}\right) + \Phi_{\Sigma_2}\left(0, \frac{\kappa x}{\sqrt{2}}\right) \right] \right\}
\end{aligned}
\tag{6.28}
$$

Where:

$$
\Sigma_1 = \begin{pmatrix} \frac{3}{2} & -1 \\ -1 & \frac{3+\eta^2-\kappa^2}{2} \end{pmatrix}, \qquad \Sigma_2 = \begin{pmatrix} \frac{3}{2} & -\frac{1}{2} \\ -\frac{1}{2} & \frac{2+\eta^2-\kappa^2}{2} \end{pmatrix}
$$

Simulation

6.5.2 *Degenerate*

When $\kappa^2 - \eta^2 = \frac{N+2}{N}$, it represents a degenerate condition, and we can derive the following implicit formula:

$$F_i(u) = \frac{\mathbb{E}_{\mathrm{GOI}((1+\eta^2)/2)}\left[\prod_{j=1}^{N} |\lambda_j| \mathbb{1}_{\{\lambda_i<0<\lambda_{i+1}\}} \mathbb{1}_{\{\sum_{j=1}^{N} \lambda_j/N \le -\sqrt{(N+2+N\eta^2)/(2N)}u\}}\right]}{\mathbb{E}_{\mathrm{GOI}((1+\eta^2)/2)}\left[\prod_{j=1}^{N} |\lambda_j| \mathbb{1}_{\{\lambda_i<0<\lambda_{i+1}\}}\right]} \tag{6.29}$$

With the implicit form of CDF of the height distribution, we can get the corresponding PDF.

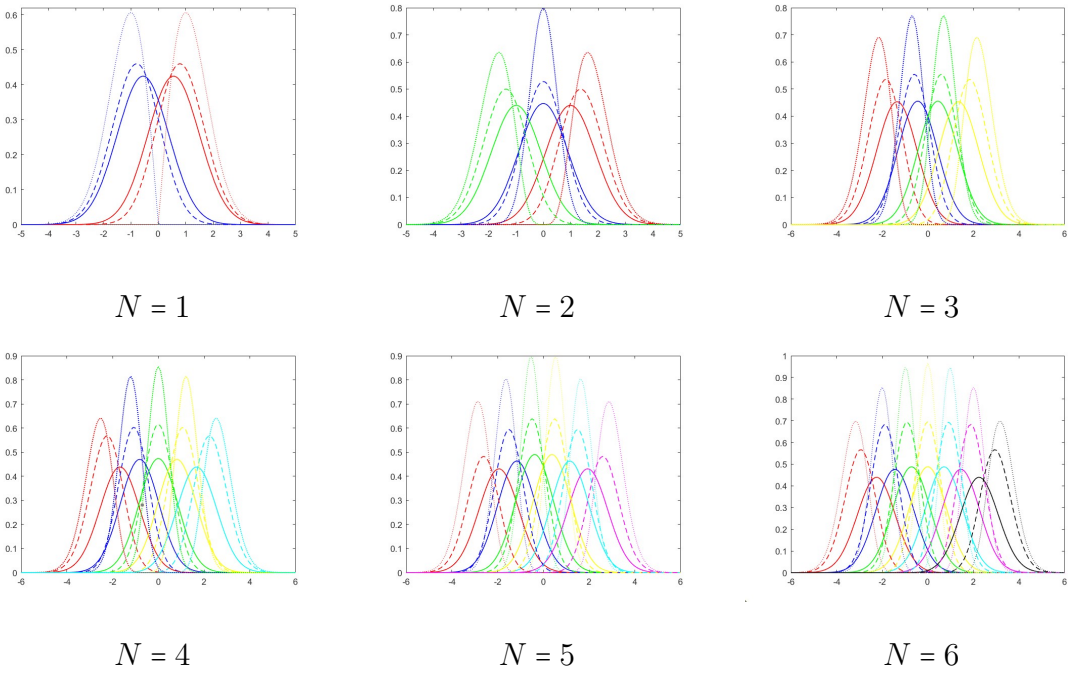

$N = 1$ $N = 2$ $N = 3$

$N = 4$ $N = 5$ $N = 6$

Figure 6.3: Exact height densities of critical points of isotropic Gaussian fields on $\mathbb{S}^N$. In each figure, the solid, dashed and dotted curves are densities with $(\kappa^2, \eta^2) = (0.64, 0.16)$, $(\kappa^2, \eta^2) = (1.5, 0.5)$ and the boundary case $(\kappa^2, \eta^2) = (2, 1 - 2/N)$, respectively; and for a fixed pair (κ^2, η^2), the densities from left to right, indicated by different colors, are $h_0(x)$, $h_1(x)$, $\ldots$, $h_N(x)$, respectively.

6.6 Asymptotic Distribution on Sphere

From the work of Cheng and Schwartzman [14], we know the implicit height distribution can be written as:

$$\begin{aligned} F_i(u) &= \frac{\mathbb{E}[\mu_i(X,u)]}{\mathbb{E}[\mu_i(X)]} \\ &= \frac{\sqrt{1+\eta^2}\int_u^\infty \phi(x)\mathbb{E}^{N+1}_{\mathrm{GOE}}\left\{\exp\left[\frac{\lambda_{i+1}^2}{2} - \frac{(\lambda_{i+1}-\kappa x/\sqrt{2})^2}{1+\eta^2-\kappa^2}\right]\right\}dx}{\sqrt{1+\eta^2-\kappa^2}\mathbb{E}^{N+1}_{\mathrm{GOE}}\left\{\exp\left[\frac{\lambda_{i+1}^2}{2} - \frac{\lambda_{i+1}^2}{1+\eta^2}\right]\right\}} \end{aligned} \tag{6.30}$$

Then the density can be expressed as:

$$h_i(x) = \frac{\sqrt{1+\eta^2}\phi(x)\mathbb{E}^{N+1}_{\mathrm{GOE}}\left\{\exp\left[\frac{\lambda_{i+1}^2}{2} - \frac{(\lambda_{i+1}-\kappa x/\sqrt{2})^2}{1+\eta^2-\kappa^2}\right]\right\}dx}{\sqrt{1+\eta^2-\kappa^2}\mathbb{E}^{N+1}_{\mathrm{GOE}}\left\{\exp\left[\frac{\lambda_{i+1}^2}{2} - \frac{\lambda_{i+1}^2}{1+\eta^2}\right]\right\}} \tag{6.31}$$

Theorem 6.6.1. *The asymptotic peak height distribution on sphere is:*

$$h(x) = \frac{1}{\sqrt{2\pi\beta}} e^{-\frac{(x-\frac{\sqrt{2}\kappa\mu}{1+\eta^2+\sigma^2-\eta^2\sigma^2})^2}{2\beta}} \tag{6.32}$$

Where $\beta = \frac{1+\sigma^2-\kappa^2+\eta^2+\kappa^2\sigma^2-\eta^2\sigma^2}{1+\eta^2+\sigma^2-\eta^2\sigma^2}$

Proof. From (6.2) and corollary 6.4.1.1 The denominator is:

$$\begin{aligned} &\sqrt{1+\eta^2-\kappa^2}\mathbb{E}^{N+1}_{\mathrm{GOE}}(e^{\frac{\lambda_{i+1}^2}{2}-\frac{\lambda_{i+1}^2}{1+\eta^2}}) \\ =&\sqrt{1+\eta^2-\kappa^2}\int_{-\infty}^{\infty} e^{\frac{\lambda_{i+1}^2}{2}-\frac{\lambda_{i+1}^2}{1+\eta^2}}\frac{1}{\sqrt{2\pi}\sigma}e^{-\frac{(\lambda_{i+1}-\mu)^2}{2\sigma^2}}d\lambda_{i+1} \\ =&\sqrt{1+\eta^2-\kappa^2}\int_{-\infty}^{\infty}\frac{1}{\sqrt{2\pi}\sigma}e^{\frac{(\sigma^2+\eta^2\sigma^2-2\sigma^2-1-\eta^2)\lambda_{i+1}^2+(2\mu+2\mu\eta^2)\lambda_{i+1}-(\mu^2+\mu^2\eta^2)}{2(1+\eta^2)\sigma^2}}d\lambda_{i+1} \\ =&\sqrt{\frac{(\eta^2+1)(1+\eta^2-\kappa^2)}{\sigma^2+\eta^2-\sigma^2\eta^2+1}}e^{\frac{\mu^2(\eta^2-1)}{2(-\eta^2\sigma^2+\eta^2+\sigma^2+1)}} \end{aligned} \tag{6.33}$$

Then the numerator is:

$$\begin{aligned} &\phi(x)\mathbb{E}^{N+1}_{\mathrm{GOE}}(e^{\frac{\lambda_{i+1}^2}{2}-\frac{(\lambda_{i+1}-\kappa x/\sqrt{2})^2}{1+\eta^2-\kappa^2}}) \\ =&\int_{-\infty}^{\infty}\frac{1}{\sqrt{2\pi}}e^{-\frac{x^2}{2}}e^{\frac{\lambda_{i+1}^2}{2}-\frac{(\lambda_{i+1}-\kappa x/\sqrt{2})^2}{1+\eta^2-\kappa^2}}\frac{1}{\sqrt{2\pi}\sigma}e^{-\frac{(\lambda_{i+1}-\mu)^2}{2\sigma^2}}d\lambda_{i+1} \end{aligned} \tag{6.34}$$

Do some calculation, we can get:

$$\begin{aligned}
&\sqrt{1+\eta^2}\phi(x)\mathbb{E}_{\mathrm{GOE}}^{N+1}(e^{\frac{\lambda_{i+1}^2}{2}-\frac{(\lambda_{i+1}-\kappa x/\sqrt{2})^2}{1+\eta^2-\kappa^2}}) \\
=&\frac{1}{\sqrt{2\pi}}\sqrt{\frac{(1+\eta^2)(\eta^2-\kappa^2+1)}{\sigma^2+\eta^2-\kappa^2-\sigma^2\eta^2+\sigma^2\kappa^2+1}}e^{-\frac{-\eta^2\mu^2+\kappa^2\mu^2-\kappa^2\sigma^2x^2+\kappa^2x^2-2\sqrt{2}\kappa\mu x+\mu^2+\sigma^2x^2+x^2}{-2\eta^2\sigma^2+2\eta^2+2\kappa^2\sigma^2-2\kappa^2+2\sigma^2+2}} \\
=&\frac{1}{\sqrt{2\pi}}\sqrt{\frac{(1+\eta^2)(\eta^2-\kappa^2+1)}{\alpha}}e^{-\frac{-\eta^2\sigma^2+\eta^2+\sigma^2+1}{2\alpha}x^2+\frac{\sqrt{2}\kappa\mu}{\alpha}x-\frac{-\eta^2\mu^2+\kappa^2\mu^2+\mu^2}{2\alpha}}
\end{aligned} \tag{6.35}$$

Where $\alpha = -\eta^2\sigma^2 + \eta^2 + \kappa^2\sigma^2 - \kappa^2 + \sigma^2 + 1$, then we can get the height distribution as the form:

$$h(x) = \frac{1}{\sqrt{2\pi\beta}}e^{-\frac{(x-\frac{\sqrt{2}\kappa\mu}{1+\eta^2+\sigma^2-\eta^2\sigma^2})^2}{2\beta}} \tag{6.36}$$

Where $\beta = \frac{1+\sigma^2-\kappa^2+\eta^2+\kappa^2\sigma^2-\eta^2\sigma^2}{1+\eta^2+\sigma^2-\eta^2\sigma^2}$ □

6.6.1 Simulation

This section demonstrates the performance of the asymptotic distribution in terms of its similarity to the simulated height density.

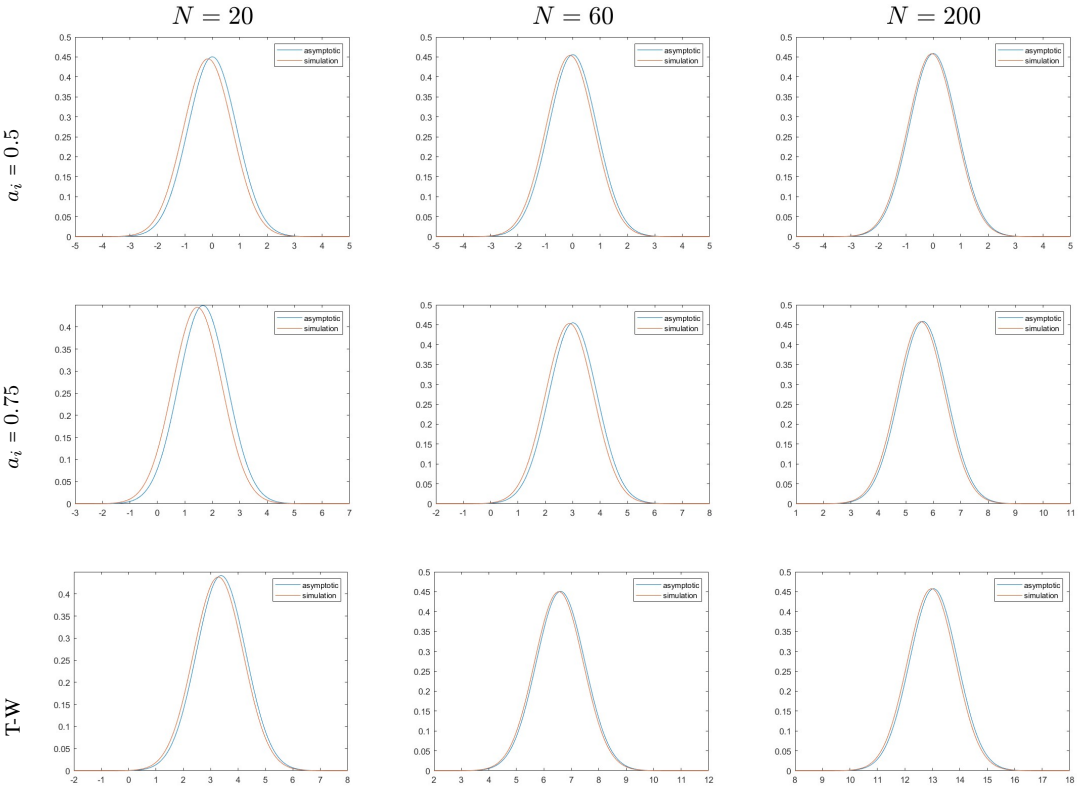

Figure 6.4: The comparison between asymptotic distributions and simulations when $N = 20, 60, 200$, $a_i = 0.5, 0.75$ and maximum eigenvalue with $\kappa^2 = 0.64$, $\eta^2 = 0.16$

.

REFERENCES

[1] Adler, R., J. Taylor and K. Worsley, "Applications of random fields and geometry: Foundations and case studies.", In preparation (2012).

[2] Adler, R. J. and J. E. Taylor, "Random fields and geometry", New York. MR2319516 (2007).

[3] Annibale, A., A. Cavagna, I. Giardina and G. Parisi, "Supersymmetric complexity in the sherrington–kirkpatrick model.", Phys. Rev. E (3) 68 061103, 5. MR2060973 (2003).

[4] Balogh, A., H. Hudson, K. Petrovay and R. von Steiger, "Introduction to the solar activity cycle: Overview of causes and consequences.", The Solar Activity Cycle. Space Sciences Series of ISSI, vol 53. Springer (2015).

[5] Bardeen, J., J. Bond, N. Kaiser and A. Szalay, "The statistics of peaks of gaussian random fields.", Astrophys. J. 304 15–61. (1985).

[6] Bray, A. and D. Dean, "Statistics of critical points of gaussian fields on large-dimensional spaces.", Rev. Lett. 98 150201. (2007).

[7] Bulut, A. A. K. S., T. F. P. Shin, H. Jasso, L. Yan and A. Elgamal, "Real-time nondestructive structural health monitoring using support vector machines and wavelets.", Advanced Sensor Technologies for Nondestructive Evaluation and Structural Health Monitoring", vol. 5770, pp. 180–189 (2005).

[8] Cavagna, I., A.and Giardina and G. Parisi, "Stationary points of the thouless–anderson–palmer free energy.", Phys. Rev. B 57 251. (1997).

[9] Cheng, D., "Peak height distributions of certain nonisotropic gaussian random fields.", arXiv:2307.01974. (2023).

[10] Cheng, D., V. Cammarota, Y. Fantaye, D. Marinucci and A. Schwartzman, "Multiple testing of local maxima for detection of peaks on the (celestial) sphere", Bernoulli 26 (1) 31 - 60. (2020).

[11] Cheng, D., Z. He and A. Schwartzman, "Multiple testing of local extrema for detection of change points", Electronic Journal of Statistics 14, 2, 3705–3729 (2020).

[12] Cheng, D. and A. Schwartzman, "Distribution of the height of local maxima of gaussian random fields", Extremes 18, 213–240 (2015).

[13] Cheng, D. and A. Schwartzman, "Multiple testing of local maxima for detection of peaks in random fields", The Annals of Statistics 45, 2, 529–556 (2017).

[14] Cheng, D. and A. Schwartzman, "Expected number and height distribution of critical points of smooth isotropic gaussian random fields", Bernoulli 24, 4B, 3422–3446 (2018).

[15] Cheng, D., A. Schwartzman and Y. Zhao, "Regional and generalized peak height distributions for random fields", Preprint (2023).

[16] Cramér, H. and M. Leadbetter, "Stationary and related stochastic processes. sample function properties and their applications.", New York: Wiley. MR0217860 (1967).

[17] Crisanti, A., L. Leuzzi, G. Parisi and T. Rizzo, "Spin-glass complexity.", Phys. Rev. Lett. 92 127203. (2004).

[18] Fyodorov, Y., "Complexity of random energy landscapes, glass transition, and absolute value of the spectral determinant of random matrices.", Phys. Rev. Lett. 92 240601. (2004).

[19] Halperin, B. and M. Lax, "Impurity-band tails in the high-density limit. i. minimum counting methods.", Phys. Rev. 148 722–740. (1966).

[20] Hann, C. E., I. Singh-Levett, B. L. Deam, J. B. Mander and J. G. Chase, "Real-time system identification of a nonlinear four-story steel frame structure at application to structural health monitoring", IEEE Sensors Journal 9, 11, 1339– 1346 (2009).

[21] Khan, F., A. Ghaffar, N. Khan and S. H. Cho, "An overview of signal processing techniques for remote health monitoring using impulse radio uwb transceiver", Sensors 20, 9, 2479 (2020).

[22] Kharinov, M., "Image segmentation using optimal and hierarchical piecewiseconstant approximations", Pattern recognition and image analysis 24, 3, 409–417 (2014).

[23] Larson, D. and B. Wandelt, "The hot and cold spots in thewilkinson microwave anisotropy probe data are not hot and cold enough.", Astrophys. J. 613 85–88. (2004).

[24] Liao, S. X. and M. Pawlak, "On image analysis by moments", IEEE Transactions on Pattern analysis and machine intelligence 18, 3, 254–266 (1996).

[25] Lindgren, G., "Local maxima of gaussian fields.", Ark. Mat. 10, 195–218 (1972).

[26] Lindgren, G., "Wave characteristics distributions for gaussian waves – wave-length, amplitude and steepness.", Ocean Engng. 9 411–432. (1982).

[27] Longuet-Higgins, M., "Reflection and refraction at a random moving surface. ii. number of specular points in a gaussian surface.", J. Opt. Soc. Amer. 50 845–850. MR0113490 (1960).

[28] Nichols, T. and S. Hayasaka, "Controlling the familywise error rate in functional neuroimaging: A comparative review.", Methods Med. Res. 12 419–446. MR2005445 (2003).

[29] O'Rourke, S., "Gaussian fluctuations of eigenvalues in wigner random matrices.", Journal of Statistical Physics volume 138, 1045–1066. (2010).

[30] Rice, S., "Mathematical analysis of random noise.", Bell System Tech. J. 24 46–156. MR0011918 (1945).

[31] Schwartzman, A., Y. Gavrilov and R. J. Adler, “Multiple testing of local maxima for detection of peaks in 1d”, Annals of statistics 39, 6, 3290 (2011).

[32] SMITH, S. M. and T. E. NICHOLS, “Threshold-free cluster enhancement: Addressing problems of smoothing, threshold dependence and localisation in cluster inference.”, Neuroimage 44 83–98. (2009).

[33] Taylor, J. and K. Worsley, “Detecting sparse signals in random fields, with an application to brain mapping.”, Amer. Statist. Assoc. 102 913–928. MR2354405 (2007).

[34] Worsley, K., S. Marrett, P. Neelin and A. Evans, “Searching scale space for activation in pet images.”, Human Brain Mapping 4 74–90. (1996).

[35] Worsley, K., J. Taylor, F. Tomaiuolo and J. Lerch, “Unified univariate and multivariate random field theory.”, Neuroimage 23 189–195. (2004).

[36] WORSLEY, K. J., S. MARRETT, P. NEELIN, A. C. VANDAL, K. J. FRISTON and A. C. EVANS, “A unified statistical approach for determining significant signals in images of cerebral activation.”, Human Brain Mapping 4 58–73. (1996b).

[37] WORSLEY, K. J., J. E. TAYLOR, F. TOMAIUOLO and J. LERCH, “Unified univariate and multivariate random field theory.”, Neuroimage 23 S189–195. (2004).